AN ANALYSIS OF CHANGES IN STREAM TEMPERATURE DUE TO FOREST HARVEST PRACTICES USING DHSVM-RBM

A Thesis

presented to

the Faculty of California Polytechnic State University

San Luis Obispo

In Partial Fulfillment

of the Requirements for the Degree

Master of Science in Forestry Sciences

by

Julia Ridgeway

June 2019

COMMITTEE MEMBERSHIP

TITLE:	An analysis of changes in stream temperature due to forest harvest practices using DHSVM-RBM
AUTHOR:	Julia Ridgeway
DATE SUBMITTED:	June 2019

COMMITTEE CHAIR:	Christopher Surfleet, Ph.D. Professor Natural Resources Management and Environmental Sciences
COMMITTEE MEMBER:	Bwalya Malama, Ph.D. Associate Professor Natural Resources Management and Environmental Sciences
COMMITTEE MEMBER:	Misgana Muleta, Ph.D. Associate Professor Civil Engineering

ABSTRACT

An analysis of changes in stream temperature due to forest harvest practices using DHSVM-RBM

Julia Ridgeway

Forest harvesting has been shown to cause various changes in water quantity and water quality parameters, highlighting the need for comprehensive forest practice rules. Studies show a myriad of impacts to ecosystems as a result of watershed level changes, such as forest harvesting. Being able to better understand the impact that forest harvesting can have on stream temperature is especially critical in locations where federally threatened or endangered fish species are located. The overall goal of this research project is to assess responses in stream temperature to various riparian and forest harvest treatments in a maritime, mountainous environment. The results of this study aim to inform decision makers with additional information pertaining to the effects of forest harvest on water temperature. Modeling is done as a part of the third Caspar Creek Paired Experimental Watershed study. Located in Mendocino County, the site provides a place for California researchers and decision makers to learn about the cumulative watershed effects of forest management operations on peak flows, sediment production, anadromous fish, macro-invertebrate communities, nutrient cycling and more.

Historic data was used to calibrate the Distributed Hydrology Soil Vegetation Model (DHSVM) and River Basin Model (RBM) to measured stream temperatures in the South Fork of Caspar Creek (SFC) for hydrologic years 2010-2016. Critical summer time periods, when temperatures are highest and flows are low, are the primary concern for this work. The key modeling scenarios evaluated were (1) varying percentages of Watercourse and Lake Protection Zone canopy cover, (2) the 2018-

2019 SFC forest harvest and (3) an experimental design converting dominant riparian vegetation along 300-yard stream reaches.

Modeling results showed that stream temperatures begin to rise above third-growth conditions when canopy cover is reduced to 25 and 0% retention levels. Larger increases in Maximum Weekly Maximum Temperature (MWMT) value, compared to Maximum Weekly Average Temperature (MWAT) values, were seen across all scenarios. There was essentially no difference between altering buffer areas along only class I streams, compared to along all stream classes. At the 0% canopy retention, MWMT values consistently rose above recommended thermal limits for Coho salmon *(Oncorhynchus kisutch)* and state regulations prohibiting more than a 5°F increase in waters. Clearcutting the entire watershed produced less of an effect than simulations clearing on only the riparian area, suggesting that groundwater inflows act to mitigate stream temperature rises in the SFC. The 2018-2019 harvest showed a relatively consistent increase in MWAT values (avg. 0.11°C) and more varied increases in MWMT values (avg. 0.32°C). Simulations converting dominant riparian vegetation by clearing could not be considered conclusive due to sensitivity analyses suggesting potentially unrealistic tracking of downstream temperatures. Additional sensitivity analyses suggest that tree height and the monthly extinction coefficient (a function of LAI) are most influential on stream temperature changes in SFC. This is consistent with other modeling studies and suggests stream temperature management focus on tall, dense buffers as opposed to wider buffer widths.

ACKNOWLEDGMENTS

I would like to thank my graduate committee, Dr. Christopher Surfleet, Dr. Bwalaya Malama and Dr. Misgana Muleta, for their input and direction on this project; with a special note to my adviser, Dr. Surfleet, for his considerable work, guidance, support and expression of gratitude for the beautiful area that we have had the pleasure to research. Thank you to Dr. John Yearsley and Dr. Ning Sunn for their open communication and assistance with modeling questions. Thank you to the California Department of Forestry and Fire Protection (CalFire) for funding and supporting this research; the Pacific Southwest Research Station (PSW) for site specific and technical support; and the California Department of Fish and Wildlife (CDFW) for willing to share their data sets. And above all, to the many people who have tirelessly worked to maintain Caspar Creek as one of the most extensive paired watershed studies in the world, especially those with boots on the ground collecting the data that made this modeling work possible.

Finally, thank you to both the California Polytechnic State University Aerospace and Computer Sciences departments for the use of computer hardware and assistance, with a special note to Andrew Adriance for his computer programming work. To my own department, Natural Resources Management and Environmental Sciences, for supporting and inspiring me to continue on with my academic career. To Tyler Davis for his field work assistance and friendship over these past two years. And lastly, thank you to my friends and family for their undying love, support and encouragement for me to pursue my passions.

Sincerely,
Julia Ridgeway

TABLE OF CONTENTS

LIST OF TABLES

LIST OF FIGURES

Chapter 1

Introduction

1.1 Background & Problem Statement

The California Forest Practice Rules (FPR) attempt to mitigate the impacts that forest harvesting can have on forested ecosystems. This study aims to link policy to environmental outcome, by examining stream temperature responses to various components of the most up-to-date California FPRs.

Many studies have evaluated various human and non-human activities that result in changes to stream temperature. More specifically, there is extensive literature attempting to analyze the impact that forest harvest practices have on stream temperature (Lynch and Corbett, 1990; Patric, 1980; Wilkerson et al., 2006; Johnson and Jones, 2000; Moore et al., 2005; Beschta et al., 1987; Brown and Krygier, 1970). However, only a few select studies use highly detailed, distributed models to analyze the impacts of forest harvest on stream temperature in Maritime environments.

1.2 Statement of Overall Research Goal

The overall research goal of this project is to better understand the impacts that changes in riparian shading and forest harvest have on stream temperature in a coastal watershed.

1.3 Research Objectives

- Calibrate the Distributed Hydrology Soil Vegetation Model (DHSVM) and the River Basin Model (RBM) to measurements of flow and stream temperature in the South Fork Caspar Creek (SFC).
- Determine the impact of the size and structure of California Forest Practice Rules "Watercourse and Lake Protection Zones (WLPZs)" on stream temperatures.
- Determine the impact of a modern forest harvest scenario on stream temperature.
- Determine the impact of a theoretical riparian vegetation conversion on stream temperature.

1.4 Importance of the Project

The logging industry has long been a productive business for California, since it became an official state in 1850 (Morgan et al., 2012). However, forest harvesting has been shown to cause changes to water movement, quantity and quality not only in California, but across the world (Kura et al., 2012; Cole and Newton, 2013; Waterloo et al., 2007; Stednick, 1996). Being able to better understand the impact that forest

harvesting can have on stream temperatures is essential to protecting the habitat for aquatic species that are sensitive to changes.

Caspar Creek is home to endangered and threatened Coho Salmon *(Oncorhynchus kisutch*) and Steelhead trout *(Oncorhynchus mykiss)*. Low flows occurring during peak summer temperatures have the potential to create additional stress and deleterious habitat for salmonid species. California FPRs have been put in place to attempt to mitigate impacts such as these. However it is important to link policy to environmental outcome. Therefore, the results of this study aim to provide policy makers additional information to create conscientious, feasible regulations.

1.5 General Approach

The Distributed Hydrology Soil Vegetation Model (DHSVM) and River Basin Model (RBM) were used to simulate various riparian and upslope vegetation scenarios. Many of these scenarios simulate past and present California FPRs. Scenarios include varying the size and structure of WLPZ canopies, simulating the actual 2018-2019 harvest completed at the study site and an experimental design scenario. We will use DHSVM-RBM to determine which forest harvesting scenarios show marked changes in stream temperature. Both models were calibrated with data collected at South Fork Caspar Creek (SFC). A High-Performance Computing cluster run by the College of Engineering at California Polytechnic State University, San Luis Obispo was used to calibrate and run the model scenarios.

1.6 Scope

1.6.1 Location

The study area evaluated was the South Fork within the Caspar Creek Experimental Watershed, located on the Jackson Demonstration State Forest near Fort Bragg, California (Figure 3.1 and 3.2). The research watershed is located in the northern part of the California Coast Ranges and has a total area of 2,167 ha. A detailed description of the study site is located in the Caspar Creek overview (Section 2.6) of this report.

1.6.2 Date and Timing

Data collection has been on going in Caspar Creek since its establishment in 1961. This study will focus only on the South Fork of Caspar Creek using data collected between 2009 and 2016; specially analysis of stream temperatures was for the 2011-2016 hydrologic years. The majority of data used in this study came from the experimental watershed itself. However, for those variables not collected on site, or to fill gaps in Caspar collected datasets, other sources included the California Irrigation Management Information System (CIMIS), a Meso-West meteorological station and the National Centers for Environmental Information (NCEI) Arcata Airport station.

1.6.3 Equipment

This report utilizes the open-source Distributed Hydrology Soil Vegetation Model (DHSVM), in conjunction with the River Basin Model (RBM) to simulate watershed hydrology and estimate stream temperatures. To speed up simulations, model scripts were optimized by Adriance (2018) to run in parallel with distributed comput-

ing options available on California Polytechnic State University's High-Performance Computing cluster managed by the College of Engineering.

Chapter 2

Literature Review

2.1 Introduction

This literature review focuses on elements related to California Forest Practice Rules (FPR), the importance of stream temperature in forest environments, the effect that forest harvesting has on stream temperature, hydrologic and stream temperature computer modeling, the Distributed Hydrology Soil Vegetation Model (DHSVM), the River Basin Model (RBM) and the Caspar Creek Paired Experimental Watershed Study.

2.2 Evolution of the California Forest Practice Rules

California's FPRs have evolved throughout the last half century, changing to keep up with social pressures and interests of the public, landowners, regulators and stakeholders. Clar (1959, 1969) chronicled California state forestry, noting that it was not until the State Board of Forestry, the first of its kind in the United States, was established in 1885 that regulatory laws for forest harvesting were enacted. The four key issues that lead to forest legislation were (1) the accelerated need for timber

with the gold rush, (2) susceptibility of California to wildfire due to climate, (3) advanced perception that vegetative cover could aid in watershed protection and (4) the conventional idea of reforesting harvested areas and afforesting treeless brush and grasslands to create more timber (Clar, 1957). Some early efforts to manage pest outbreaks took place, and the creation of work camps to address high unemployment rates from the Great Depression started to spur legislation. However, overall the primary focus of legislation was on fire prevention and slash disposal (Arvola, 1976).

In 1927 the Legislature created the Department of Natural Resources (Chapter 128) four divisions: forestry, mines and mining, parks, and fish and game (Clar, 1957). In 1943 Governor Earl Warren signed into act Chapter 172 of the 1943 Legislative Session, the "minimum-diameter law", which was essentially the first step to what would become the California Forest Practice Act (Arvola, 1976; Clar, 1957). These statutes also established a legislative Forestry Study Committee, who developed an extensive proposal for forestry legislation that were accepted in 1945. Again, initially these rules were focused on fire protection and reforestation.

Until the 1970's, Forest Practice Rules (FPRs) were also heavily influenced by landowner-based district practice committees, since most forest harvesting was taking place on private land, outside of public view. However, by the end of the 1960's public interest in outdoor recreation and conservation, as well as decreasing salmon populations, resulted in public outcry and scrutiny of California's logging industry (Mount, 1995). This is why in 1971 the original California Forest Practice Act (1945), was declared void in *Bayside Timber Company v. Board of Supervisors of San Mateo County.* Following this the 1973 Z'berg-Nejedly Forest Practices Act was passed. This new act established the FPRs and created a politically-appointed Board of Forestry to oversee the implementation of said rules. The California Department of Forestry and Fire Protection (CalFire) is now the lead agency responsible for approving logging plans and enforcing FPRs under the direction of the board.

In 1998 the state agreed to organize an independent panel of scientists to complete a comprehensive review of the FPRs ability to protect salmonid species. A formal report by Ligon et al. (1999) was completed, concluding that the FPRs were not protecting salmon and Steelhead populations from cumulative watershed effects, both temporally and spatially. Recommendations were to improve enforcement and regulations regarding on-site operations and road maintenance, that would reduce sediment production, improve stream habitat and guarantee unrestricted passage for migration.

Studies during the early 2000's continued with this movement, highlighting a need to review the impact of forest practices on water quality. These reports ultimately concluded that the THP method was insufficient at: addressing effects on watersheds, due to being too subjective at accessing current resource conditions and the potential for additional impacts (The Univeristy of California Committee on Cumulative Watershed Effects, 2001); protecting water quality and endangered species (Kersten, 2002); or allowing enough time for review and estimation of the risk and resources associated with proper examination (Humboldt Watersheds Independent Scientific Review Pannel, 2003). Subsequently, the state published the *Recovery Strategy for California Coho Salmon*, which required a forest practice monitoring group be set up. Since then, the Board of Forestry has worked to improve riparian areas through the implementation of Watercourse and Lake Protection Zones (WLPZs) and other impact mitigation measures.

Cafferata and Reid (2013) acknowledged that little had changed in the methods used by Registered Professional Foresters (RPFs) to assess resources and potential cumulative impacts of forest harvesting, stating that Timber Harvest Plans (THPs) are inadequate as effective assessment methods, but acknowledging that research is being done to address this issue. Klein et al. (2012) found that Best Management Practices (BMPs) can help to reduce erosion, but they are not always implemented

properly and can therefore result in severe degradation to water quality if too large of an area is harvested over too short a time period. Later, Brandow and Cafferata (2014) evaluated the California FPR Implementation and Effectiveness Program from 2008 to 2013 and concluded that implementation rates are high and FPRs are effective in preventing sedimentation and retaining high levels of post harvest WLPZ canopy.

Overall, as our understanding and science have progressed, FPRs have continued to be modified over the years. Some key changes to the FPRs are included in Figure 2.1. However, because the primary variable analyzed in this study is the structure of WLPZ areas, only a detailed discussion of the regulations pertaining to this specific aspect of the FPRs follows.

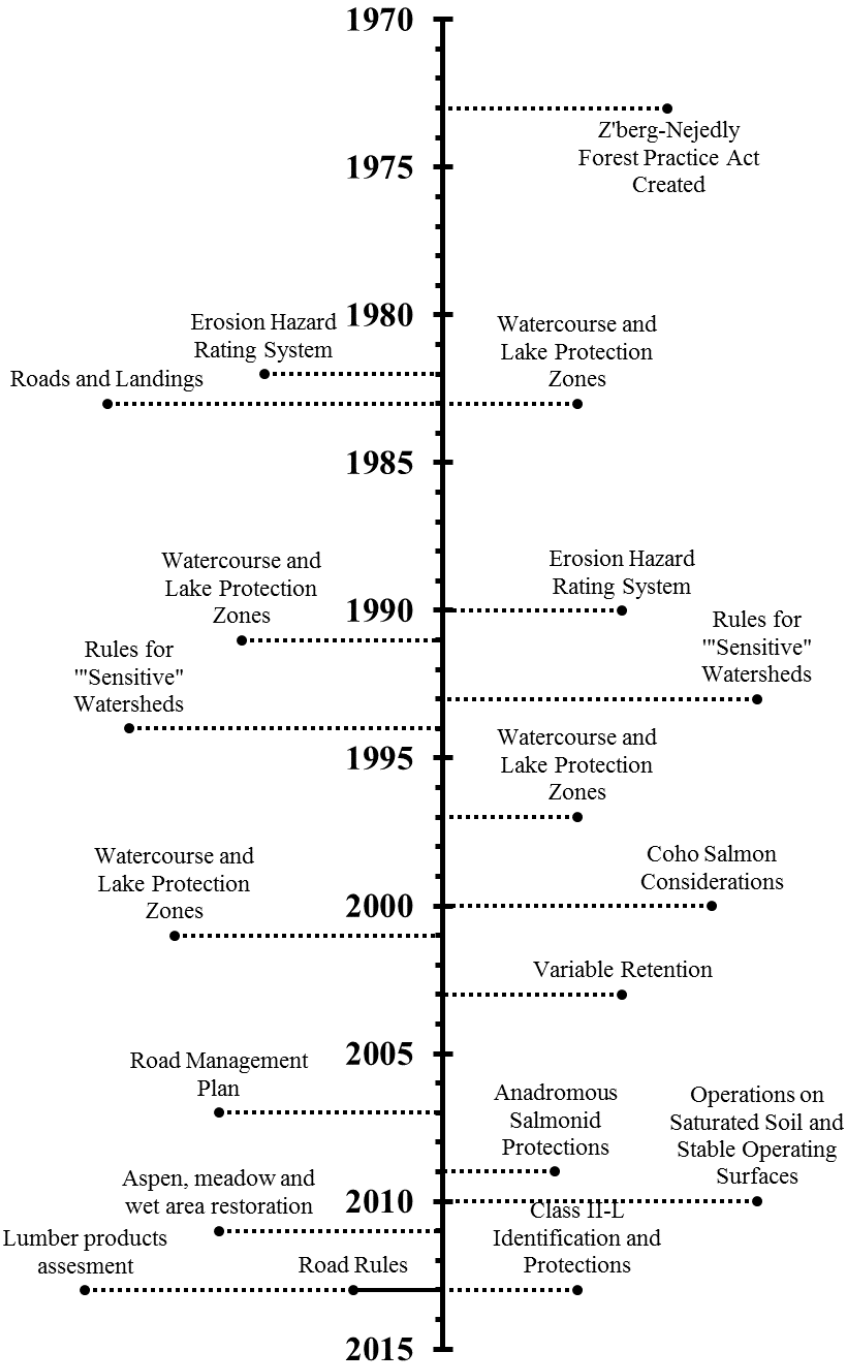

Figure 2.1: **Timeline of Forest Practice Rules.** Timeline of key changes made to forest management regulations in California (Thompson and Dicus, 2005; Gentry, 2016).

2.2.1 Watercourse and Lake Protection Zones (WLPZ)

Buffer strips, also referred to as Watercourse and Lake Protection Zones (WLPZs), first began to be required along fish bearing streams in California in 1973 (Cafferata, 1990). CalFire states that the two primary functions of WLPZs are to provide shade for water temperature and longterm inputs for large woody debris. Additional functions include filtering inputs of fine sediments, maintenance of microclimates for temperature and humidity, and the input of energy in the form of organic debris that supports other biota (Ligon et al., 1999).

Figure 2.2: **Example WLPZ.** WLPZ buffer from the NFC study (IVE tributary lower left, MUN upper right). Figure excerpted from Cafferata and Reid (2013); taken in March 1990.

Under the FPRs, streams are divided into four classes based on beneficial uses. Class I streams are either domestic water sources and/or where fish are always or seasonally present. Class II streams are those that fish are always or seasonally present offsite within 1,000 feet downstream and/or aquatic habitat for non-fish aquatic species (including vegetation). Class III streams are streams with no aquatic life present, but where the watercourse acts as a link between Class I & II streams. Lastly, Class IV streams are human-made watercourses, which are usually downstream of those classified as other uses. WLPZ width is determined based on the designated stream class and adjacent hillslope gradient. Table 2.1 outlines the 2019 width requirements based on corresponding stream class and slope.

Table 2.1: **WLPZ Widths.** WLPZ width based on stream class and slope (California Department of Forestry and Fire Protection, 2019). "Discretionary" defers decisions to the Registered Professional Foresters (RPFs) or CalFire.

Stream Class	**<30% Slope**	**30-50% Slope**	**>50% Slope**
Class I	75'	100'	150'
Class II	50'	75'	100'
Class III	Discretionary	Discretionary	Discretionary
Class IV	N/A	N/A	N/A

For areas where anadromous fish are present, California uses a three zone setup within WLPZs. The core zone is meant to promote bank stability, wood recruitment by bank erosion and canopy retention. Therefore no harvesting is allowed in this zone. The inner zone has a no-harvest prescription and the primary objective is to provide large wood, shading and ecological diversity. Lastly, logging is allowed in the outer zone, which is meant to protect the inner two zones, such as for wind protection and microclimate control. The size of the three zones are based on geographic location and are outlined in Table 2.2.

Table 2.2: **WLPZ Zone Widths.** Width of each zone within a WLPZ, based on geographic location of the stream (California Department of Forestry and Fire Protection, 2019).

Geographic Location	**WLPZ Width**	**Core**	**Inner**	**Outer**
Non-anadromy zone	100'	30'	40'	30'
Anadromous Fish Present	150'	30'	70'	50'
Flood prone area	150-200+'	30'	A:70-120' B: End of FA	End of FA+50'

Additional rules for areas with anadromous fish by each stream class include:

- Class I streams: Post-harvest canopy must be composed of both conifer and hardwood species and have at least 25% overstory conifer canopy. For the Coast and Southern Districts, the inner zone must maintain 80% of the overstory canopy, while the Northern Forest District requires 70%. For this inner zone,

the 13 largest trees per acre (TPA) must be kept. Forest harvest operations are allowed in the outer zone as long as 50% of the overstory canopy cover is retained.

- Class II streams: the inner zone requires 60% overstory canopy retention and has as a TPA requirement of 7. The outer zone requires 50% retention of the overstory canopy cover.

- Class III and IV streams: there is no distinction of core, inner and outer zones. However, a 20 foot buffer along streams with slopes >30% and a 30 foot buffer along streams with slopes <30% , where all trees must be retained, is required. Trees that fall outside of these buffers are subject to "normal" harvesting practices.

2.3 Water Temperature

Like with the environmental awakening that lead to the creation of the FPRs, public awareness of anthropogenic degradation in rivers and streams increased during the 1970's. Since then, water temperature has been regulated across the United States by the Federal *Water Pollution Control Act*, also known as the *Clean Water Act*, in Sections 316a and 316b. For California, the State Water Board set up nine Regional Water Quality Control Boards to address localized differences in climate, topography, geology and hydrology. Water quality standards are set by regional Basin Plans, as well as statewide Plans and Policies. In cold water systems, like Caspar Creek, the primary regulation overseeing stream temperature protection is that:

> "At no time or place shall the temperature of any COLD water be increased by more than 5°F (2.78°C) above natural receiving water temperature" (North Coast Regional Water Quality Control Board, 2011).

Processes that may raise stream temperatures can be broken down into "first", "second" and "third-order" controls, as described by Dugdale et al. (2017). First order controls include climatic and hydrological processes that dictate headwater temperatures and control rates of downstream warming or cooling due to radiative, latent (evaporation), sensible and advective (groundwater, hyporpheic and transient storage) heat exchanges. Second and third order controls are those that alter the degree to which first order processes can affect stream temperature. Second order controls occur at the whole-river scale, such as riparian forests and steep topography, while third order controls act on the reach scale, such as channel morphology and topology. Dugdale et al. (2017) acknowledges that although the effect of individual processes on stream temperature have been well studied, the way they amalgamate with one another is still being researched.

Literature reviews pertaining to all aspects of stream temperatures include Smith (1972), Ward (1985), Caissie (2006) and Webb et al. (2008). This literature review will focus only on the importance of stream temperature in regards to fish species, as well as studies analyzing the impacts of forest harvest on stream temperature, spotlighting those from the Pacific Northwest.

2.3.1 Importance

Water temperature is widely recognized as being a primary driver of various factors and processes in freshwater systems, including: dissolved oxygen levels (Rajwa-Kuligiewicz et al., 2015), microbial decomposition of detritus (Ferreira and Chauvet, 2011), primary production and invertebrate grazing rates (Ahlgren, 1987; Chapra, 1997; Rutherford et al., 2000) and biota growth rates (Hogg and Williams, 1996). Aside from ecosystem and organism functioning, water temperature is also important to maintaining clean drinking water supplies (Kundzewicz et al., 2007) and the pro-

duction of energy (Strzepek et al., 2015). Yet most often, scientists and management officials are concerned with the lethal stress water temperatures can have on cold water species, such as mayflies, stoneflies and certain fish species (Quinn et al., 1994; Eliason et al., 2011). For this reason, and that Caspar Creek is home to threatened Steelhead trout *(Oncorhynchus mykiss)* and endangered Coho Salmon *(Oncorhynchus kisutch*), this section will primarily focus on the importance stream temperature plays in regards to fish.

Freshwater fish species are of particular concern due to their importance as indicators of ecosystem health and shrinking populations. Fish are poikilotherms, meaning that their body temperature directly relates to the external environment that they live in, giving them little control over body temperature. As a result, metabolism is greatly affected by water temperature and thus the need for food increases with water temperature. If food is available and dissolved oxygen is sufficient a fish will grow. However, if food is limited or other stresses exist (low dissolved oxygen, pollution, etc.) then the fish will not grow to its potential, within physiological limits. With higher stream temperatures, oxygen demand will increase in fish species while there is decreased dissolved oxygen. Therefore, different seasons, weather and time of day cause oxygen concentrations to change. It has been suggested that growth stops when water temperatures exceed 18 to 20.3°C (Welsh et al., 2004; Armour, 1991). Beyond such limits, even if food is available water temperature can be stressful enough to become lethal to the fish (Ligon et al., 1999).

When discussing thresholds for water temperature, there are two types of lethal water temperatures- chronic sublethal temperatures and acute lethal temperatures. Acute lethal temperatures are short term, intense temperatures that result in "fish kills". These are typically easier to study than chronic sublethal temperatures, however sublethal temperatures can block migration, reduce growth and activity, create disease issues and inhibit smoltification (Elliot, 1981). In essence, the effects of water

temperature are cumulative and positively correlated to the duration and severity of the exposure (Ligon et al., 1999).

Eaton et al. (1995) determined the estimated maximum stream temperature tolerances using field surveys for various fish species (Table 2.3). For Coho salmon, they was also reported that alternate literature found the maximum growth tolerance to be 15°C and the EPA (1976) water quality criteria for growth and survival was between 18 and 24°C. Other studies reported that physiological stress and blockages to migration for Coho salmon occur from 19 to 23°C, and 21 to 24°C for Steelhead trout (McCullough et al., 2001). The lower range of annual maximum stream temperature was 22.3°C for Steelhead presence in a study conducted in southern California (Sloat and Osterback, 2013). On the Mattole River, just north of Caspar Creek, juvenile Coho were not present in streams where the Maximum Weekly Average Temperature (MWAT) exceeded 16.7°C or the Maximum Weekly Maximum Temperature (MWMT) exceeded 18.0°C (Welsh et al., 2004). Differences in these studies point to the wide discrepancy in determining a single value to protect fish species.

Table 2.3: **Maximum Fish Temperature Tolerances.** 95^{th} percentile weekly mean temperatures for the highest 5% of Fish/Temperature pairs based on temporal and spatial field data (Eaton et al., 1995).

Species	**°C**	**Standard Error**
chum salmon	19.8	0.18
pink salmon	21.0	1.01
brook trout	22.3	0.40
mountain whitefish	23.2	0.66
cutthroat trout	23.2	0.43
coho salmon	23.4	0.23
chinook salmon	24.0	0.12
rainbow trout	24.0	0.14
brown trout	24.1	24.1
smallmouth bass	29.5	0.21

Potential increases in water temperature as a result of land cover change, water management and/or climate change pose a threat to biodiversity and aquatic ecosystems (Hester and Doyle, 2011). Studies have shown an increase in water temperatures throughout North America and Europe as a result of water diversion for irrigation and water supply, water confinement, thermal discharge and land use change such as logging, farming and urbanization (Kaushal et al., 2010; Foreman et al., 2001; Morrison et al., 2002; Webb and Nobilis, 1995, 2007). A 2018 Intergovernmental Panel on Climate Change Report, states that increases in mean air temperatures and the probability of drought, precipitation deficits and extreme low flow events in the Western United States should be expected, all of which would negatively impact the availability of cold freshwater (Hoegh-Guldber et al., 2018). Furthermore, it has been shown that climate change is likely to exacerbate these issues and further increase water temperature (Van Vliet et al., 2011; Meyer et al., 1999) or be magnified when paired with changes in hydrologic regimes (Mantua et al., 2010).

A major issue with truly understanding the effect of water temperature on fish species is due to the symbiotic nature between factors such as food availability, previous exposure to stress, genetic adaptation, age and size (Ligon et al., 1999). Eliason et al. (2011) suggests the use of site-specific approaches to determine appropriate thermal regulations for different streams, because of cardio-respiratory physiology differences at the population levels in Fraser River sockeye salmon. Better understanding the impacts that forest harvesting can have on water temperatures, will aid in conservation approaches that aim to protect these and other freshwater organisms.

2.3.2 Impacts from Forest Harvesting

The connection between forest harvesting and hydrology is argued to be one of the longest-studied aspects of interactions between land cover/land use and hydrology

(Buttle, 2011). However, because the primary concern for forest management in California was initially fire protection, little effort was given to watershed projects during the late 1800's and early 1900's (Clar, 1957). Since then, various studies have been completed to analyze the impacts of forest harvesting on hydrology for forests in California (Keppeler and Ziemer, 1990; Klein et al., 2012; Cafferata and Reid, 2013; Jones et al., 2013). Although forest management techniques can affect watershed hydrology in a plethora of ways (Figure 2.3), this review will only focus on the effects forest harvesting has on stream temperature for studies specifically done in the Pacific Northwest area.

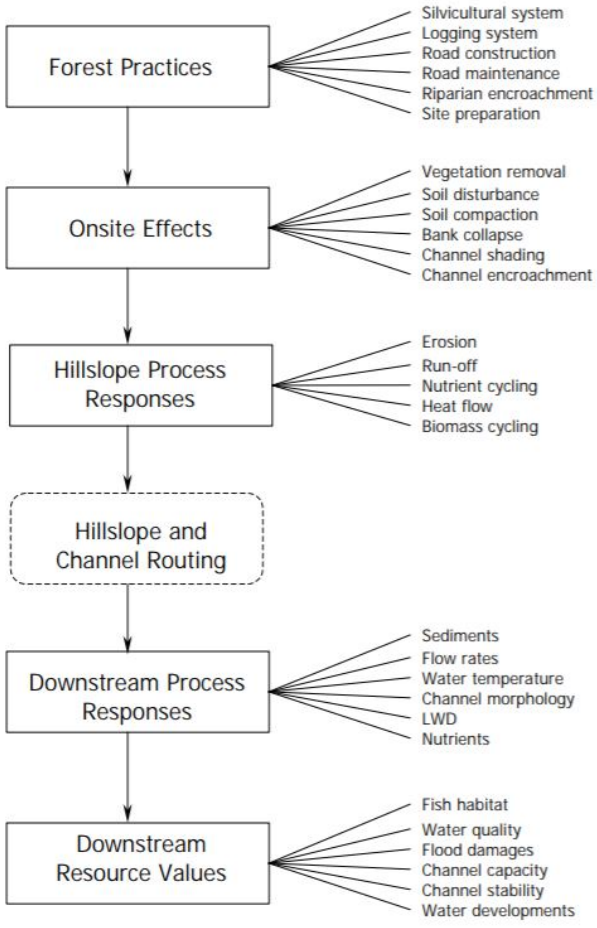

Figure 2.3: **Effects of Forest Practices on Hydrologic Processes.** Flow chart depicting the effect of forest practices on watershed hydrology. Excerpted from Ligon et al. (1999).

Even with decades of research throughout the Pacific Northwest, there is still much debate regarding the thermal impact of forest harvesting (Moore et al., 2005). It is commonly accepted that the removal of shade canopy increases stream temperatures (Carroll et al., 2004; Lynch and Corbett, 1990; Patric, 1980; Wilkerson et al., 2006; Johnson and Jones, 2000; Moore et al., 2005; Beschta et al., 1987; Brown and Krygier, 1970) and the general consensus in temperate, rain-dominated ecosystems, is that harvesting without incorporating a riparian buffer significantly increases summer water temperatures, especially maximum values and diurnal range (Moore et al., 2005).

Studies to evaluate how changes in water temperature persist downstream are one such phenomenon under debate in regards to forest harvest effects on stream temperatures. Story et al. (2003) studied two reaches and found that for one stream, cooling did not occur until downstream groundwater inflows were introduced (150 m). However at a second reach, temperatures were more stable because of continuous groundwater inputs. These results spotlight the influence of hydrology on temperature patterns.

The primary debate regarding impacts to forest harvesting on stream temperatures, however, is the size and structure needed for riparian buffers to adequately mitigate any changes in water temperature. Parkyn et al. (2003) concluded that canopy closure, long buffer lengths and the protection of small tributaries and headwaters are necessary to reduce water temperatures and in turn rehabilitate invertebrate communities. Adding that stream restoration is most successful when a continuous buffer width is used from the headwaters down through the watershed. However, various studies suggest conflicting findings as to the actual width necessary for adequate protection.

For example, Sweeney and Newbold (2014) conducted a review of the effectiveness of streamside forest buffers on various factors. Concluding that, for temperatures, buffer widths greater than or equal to 20 m keep stream temperatures within 2°C, compared to a fully forested watershed. Additionally concluding that full protection from measurable temperature increases can only be assured by a buffer width of greater than or equal to 30 m. On the other hand, Gomi et al. (2006) concluded that 30 m buffers were effective at minimizing post-harvest stream warming, but added that the 10 m buffer also appeared to minimize warming but with confounding results due to short-term data collection. A study done in British Columbia however recorded increases of 4-6°C five years following harvest, regardless of using 20 or 30 m buffers.

Orientation of the stream (E-W vs N-S) is also widely recognized as playing an important role in the effectiveness of riparian buffers (Gomi et al., 2006; Larson and Larson, 1996; DeWalle, 2010). Gomi et al. (2006) found that streams exhibiting a N-S orientation are well shaded from late morning to early afternoon, even at only a 10 m width. DeWalle (2010) found that for E-W streams, no additional shading was provided by buffers larger than 6-7 m, whereas for N-S streams optimum buffers were approximately 18-20 m, although notably less defined. However, it is noted that wider buffers may be sought to provide for benefits other than shade.

Various other factors such as depth and velocity of flow, hydrologic regime (spatial and temporal variations in the water budget), groundwater and headwater lake inputs, forest roads, drainage size, geology and weather also all play a role in the effectiveness of buffer widths (Moore et al., 2005). Overall, it is difficult for regulators to be confident in setting one-size fits all guideline to streams over large spatial areas.

2.4 Hydrologic Modeling

Various types of hydrologic models exist, which can be broken down by two classification systems. First, hydrolgic models can be either deterministic or stochastic (Dwarakish and Ganasri, 2015). Deterministic models are physically based, run by parameters in equations that predict physical processes. Stochastic models are at least partially random, using probability distributions to make predictions. From there, deterministic models can either be lumped, semi-distributed or distributed. Lumped models use spatially averaged characteristics and are generally applied to a specific point. Semi-distributed models divide the watershed into units based on variables such as land cover, soil type or slope. Lastly, distributed models use a gridded format, defining model variables as functions of spacial dimensions.

Additionally, hydrologic models have been developed based on their hydrological processes, classifying them as conceptual, empirical or fully physical models. Empirical models build relationships between input and output on hydro-meteorological data, but are limited in that they do not consider physical processes such as subsurface flow and infiltration. Conceptual models simplify complex processes, with portions of the model described by empirical functions based on observations. Lastly, fully physical models use only physical equations to explicitly represent the spatial variability of land surface characteristics and climatic parameters.

The Variable Infiltration Capacity (VIC) model and Distributed Hydrology Soil Vegetation Model (DHSVM), are two widely used, physically-based distributed hydrologic models. Both share the same physically based energy balance snow model (Wenger et al., 2010), however, VIC is a semi-distributed macroscale hydrologic model, whereas DHSVM is a fully distributed model intended to be used on smaller scale watersheds. Originally developed by Liang et al. (1994) at the University of Washington, VIC has been applied to many major river basins around the world

to study various topics including drought (Cayan et al., 2010), flooding (Das et al., 2011), declining snowpacks (Mote et al., 2005), climate change (Beyene et al., 2010) and hydropower (Christensen et al., 2004). However, because VIC simulations are intended for larger scale use, having shown fine-scale biases that become less important at broader scales (Yearsley, 2012; Wenger et al., 2010), DHSVM was used for this study. Additional factors in decision making included previous user history and that Wenger et al. (2010) noted VIC had particular difficulty in predicting summer high and low flows, which was the primary goal of the stream temperature modeling.

2.4.1 DHSVM

DHSVM-RBM numerically represents, with high spatial resolution, the effects of local weather, topography, soil type, and vegetation on hydrologic processes within watersheds. The model was developed in the early 1990's (Wigmosta et al., 1994) and then worked on at the Pacific Northwest National Laboratory (PNNL) and the University of Washington by a variety of people under the direction of Dennis P. Lettenmaier. Since then, the model has been evaluated to be a successful tool in simulating various different forested watersheds (Whitaker et al., 2003; Thyer et al., 2004), hydrologic changes relating to climate change (Elsner et al., 2010; Brennan, 2015), glacial recession (Naz et al., 2014), forest harvesting (Storck et al., 1998; Kura et al., 2012), fire (Stonesifer, 2007; Surfleet et al., 2014), and roads (Surfleet et al., 2011; La Marche and Lettenmaier, 2001; Bowling and Lettenmaier, 2001).

A brief description of DHSVM is provided. Further detailed information can be found in Wigmosta et al. (1994); Wigmosta and Perkins (2001), Storck et al. (1998) or Nijssen and Lettenmaier (1999). DHSVM was originally developed for use in forested, mountainous terrain (Wigmosta et al., 1994) and then extended for use in maritime climates (Storck et al., 1995). The model calculates the spatial distribu-

tion of soil moisture, snow, evapotranspiration, and runoff in hourly or longer time increments for individual grid cells, or pixels, based on the digital elevation model of the watershed. Meteorological inputs required for each time increment of the model are precipitation, relative humidity, air temperature, wind speed, shortwave radiation and longwave radiation. A one-dimensional water balance is calculated for each grid point based on effects from vegetation, climate, soil hydraulic properties and topography. The model uses a two layer canopy representation to calculate interception and evapotranspiration of vegetation, a two-layer energy balance model for snow accumulation and snowmelt, a multilayer unsaturated soil model based on Darcy's Law and a saturated subsurface flow model. Once the water balance calculations are complete, each grid cell exchanges water with adjacent grid cells, which results in a three-dimensional redistribution of surface and subsurface water across the watershed. Streamflow in channel segments is generated by channel interception of surface and sub-surface flows in the grid cell it is located (Wigmosta and Perkins, 2001).

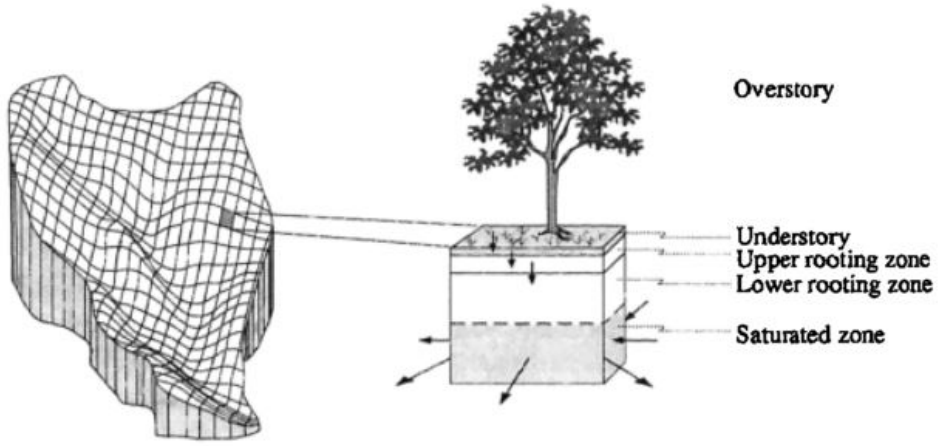

Figure 2.4: **Model Representation of DHSVM.** Drainage basin setup, where the digital elevation model modifies incoming solar radiation, precipitation, air temperature and downslope water movement within the basin. Grid cells have the ability to exchange saturated subsurface flow and for each cell one-dimension soil moisture and energy balance equations are solved. Figure from Wigmosta et al. (1994).

Storck et al. (1998) applied DHSVM to assess the hydrologic effects of forest harvesting in the Pacific Northwest for three different scenarios. For rain-on-snow events they estimated a 31% and 10% increase in peak runoff between mature vegetation and a clearcut scenario for two separate years. For spring snowmelt they estimated only a 3% decrease in peak spring streamflow events if mature vegetation was used, compared to current vegetation, and up to a 30% increase if a maximum possible harvest vegetation was simulated. Lastly, utilizing DHSVM's road runoff algorithm showed increases in peak runoff of around 16% for the five largest events.

Bowling et al. (2000) also used DHSVM to study the effects of logging in the Washington area, finding that trends were dominated by climate fluctuations. Looking at catchment pair differences, they found that peak flow changes increased following treatments, but decreased with an increasing return interval of about 10-years. However, because of the small number of catchment pairs available to study, they could not reach a definitive conclusion. Using a second, alternative approach they also detected increasing trends in the peak flow series.

Notably, Cuo et al. (2008) implemented a series of modifications to simulate the effects of impervious surfaces in order to model partially urbanized watersheds. Evaluating Springbrook Creek in King County, Washington researchers were able to use physically realistic values of the fraction of impervious surfaces. The fraction of impervious runoff routed to detention and detention drainage parameters resulted in a good match with measured flows. The modeled results were consistent with well accepted findings that urbanization increases peak flow magnitudes and decreases peak flow lag time. However, less commonly accepted findings showed substantial increase in mean annual streamflow, annual minimum low flows and increases in all seasons. The dry summer season increase, occurred when reduced evaporative demand due to vegetation removal compensated for reduced infiltration (Cuo et al., 2008).

2.5 Stream Temperature Modeling

Section 316 of the Clean Water Act specifically identifies thermal discharge as a pollutant, creating a need for models that estimate potential impacts with changes to land use/land cover and climate. Earliest research for stream temperature studies used simplistic relationships between air temperature and elevation (Walker and Lawson, 1977; Stefan and Preud'homme, 1993). Today, various stream temperature models exist for a variety of spatial and temporal resolutions.

Stream temperature models can be divided into two major types: physics based (sometimes refereed to as 'deterministic', 'mechanistic' or 'process based') and statistical. Physical models are built on mathematical equations governing physical processes, whereas statistical models rely heavily on air temperature data inputs coupled with statistical relationships. Statistical models, such as those used by Risley et al. (2003), Mohseni et al. (1998) and Donato (2002), are best used in large scale operations, where high data requirements make physical models impractical. However, statistical models are limited in that they cannot determine specific energy transfer mechanisms responsible for stream temperature patterns (Dugdale et al., 2017) and they use past information, therefore limiting the ability to predict future impacts if variables changed. Given that DHSVM-RBM is a physically based stream temperature model, the majority of this review focuses on these types of models. Benyahya et al. (2007) provides a detailed review of statistical water temperature models, if needed.

Physical stream temperature models typically use concepts regarding energy balance for heat fluxes and mass balances of water. Creating models that couple water quality and gridded systems for simulated flows makes sense, because of the synergistic relationship between water quality and stream discharge (Yearsley, 2012). These models often require significant data inputs, including meteorological data, stream

geometry, land use and hydrology to simulate land use change, altered hydrologic regimes, introduction of water impoundment structures and projected climate change. They are useful in providing process-based insights to drivers of stream temperature, information for metrics to use in larger statistical models and for forecasting temperature responses to scenarios where statistical models may not be usable (Dugdale et al., 2017). One-dimensional physically based models simulate rivers and stream that are well-mixed, whereas for more complex environments (those that include lakes and estuaries) models may require the use of higher order dimensions.

Heat exchanges (additions and losses of heat to the river) occur in two locations within a natural river system: the air-water interface and the streambed-water interface. Additional fluxes can also occur if thermal effluent and water extractions are occurring on a river system. Solar radiation, net long-wave radiation, evaporation and convective heat transfer affect the air-water interface. Geothermal heating through conduction, advection from groundwater and hyporheic flows are the primary functions that affect the streambed-water interface (Caissie, 2006). Heat inputs to a river system include incoming short and long-wave radiation, condensation, chemical and biological processes and friction with the streambed and streambanks. Losses include reflected solar radiation and evaporation, while transfers occur through channel discharge, hyporheic exchanges, groundwater up and down-welling, tributary inflows and precipitation (Hannah and Garner, 2015).

The Soil and Water Assessment Tool (SWAT), developed by Dr. Jeff Arnold is a similar, widely applied hydrological model that can be paired, like DHSVM-RBM, to a stream temperature model (Neitsch et al., 2011). The SWAT model is often coupled with the work of Ficklin et al. (2012) to predict stream temperatures based on the temperature and amount of local water contribution in the subbasin, the temperature and inflow volume from upstream subbasins and the heat transfer at the air-wave interface during the streamflow travel time in the subbasin (Brennan, 2015).

Other physically based temperature models include the Reduced Parameter Stream Temperature Model (Cheng and Wiley, 2016) and that developed by Roth et al. (2010), which uses a one-dimensional temperature model coupled with distributed temperature sensing technology.

2.5.1 RBM

The River Basin Model (RBM) is a one-dimensional stream-temperature model that solves time-dependent equations for the conservation of thermal energy in a moving stream using a mixed Eulerian-Lagrangian, or semi-Lagrangian, numerical scheme (Yearsley, 2009). Eularian models calculate change in water temperature as a function of time (t) and use a reference system that is fixed in space through which water flows (Eq. 2.1). Lagrangian models calculate the difference in water temperature as a function of space using a reference system that moves with the water (Eq. 2.2) (Hannah and Garner, 2015).

$$\frac{dT_w}{dt} = \frac{Q_{n(i,t)}}{\rho C D_{(i,t)}} \tag{2.1}$$

$$\frac{dT_w}{dx} = \frac{W_{(i)}[Q_{n(i,t)}]}{C * F_{(i,t)}} \tag{2.2}$$

Where, ρ is the density of water, D is the river depth, C is the specific heat capacity of water, Q_n is the total energy available to heat or cool the water, W is the width of the stream surface and F is the river discharge.

RBM was originally created as a tool to develop Total Maximum Daily Load (TMDL) regulations in the Columbia River System. The model was then modified to use output from VIC, a large-scale hydrologic model, and DHSVM, a regional scale hydrologic model. It was then further adapted to incorporate a riparian shading module (Sun et al., 2015).

RBM uses stream depth and an effective reach speed to solve one-dimensional, time-dependent thermal energy budget equations. It assumes that an exchange of energy across the air-water interface and advected energy from tributaries and point sources capture the important changes in rivers dominated by advection (Yearsley, 2012). The disaggregated meteorological forcing files supplied by the hydrologic simulations, in our case DHSVM, provide the data required to estimate the flux of thermal energy at the air-water interface for each grid cell (Yearsley, 2012). Output from RBM includes hydraulic parameters, stream speed and thermal energy fluxes at the air-water interface (per grid cell).

DHSVM-RBM calculates direct solar radiation received at the stream surface through calculating the attenuation of the solar 'beam' as it travels through the tree canopy. Then, the fraction of the diffuse radiation received by the stream is quantified separately, by means of an algorithm that computes the reach's sky view factor, a coefficient that represents the fraction of the hemisphere that is unblocked by tree cover/topography. DHSVM-RBM also applies shading correction to longwave fluxes. This setup is depicted in Figure 3.4, included later in the report.

Like the majority of other stream temperature models, DHSVM-RBM computes evaporation rates using Dalton's equation, wind speed, actual vapour pressure and saturation vapour pressure. Similarly, DHSVM-RBM also incorporates bed heat fluxes into the energy balance computation. DHSVM-RBM is unique in that the hydrologic model component allows for computation of groundwater inflows and the Lagrangian structure allows inflow from different courses (tributaries and groundwater) at each cell (Dugdale et al., 2017).

The RBM thermal energy budget model is based on the nonlinear discrete-time dynamic system from Schweppe (1973) and Beck (1987). It uses the Taylor series expansion and assumes that the uncertain processes have Gaussian distributions with

zero mean and that the differences between the nominal solutions and the true states are small enough that terms higher than first-order in the Taylor series expansion can be neglected (Yearsley, 2012). RBM solves the thermal energy budget equation with a semi-Lagrangian numerical method to simulate nominal water temperatures by tracking individual water parcels along their flow characteristics and storing the simulated results at discrete points on a fixed grid (Yearsley, 2009).The initial headwater conditions of RBM are estimated using the Mohseni et al. (1998) nonlinear regression model or estimates of soil temperature.

Manson et al. (2001) demonstrated that Semi-Lagrangian methods are scalable in space and time and are stable and accurate at large time steps in numerical solutions of transport when advection dominates. The change in water temperature for the particle during a time step is estimated using the speed of the particle, water depth, net exchange across the air-water interface (energy budget) and advected heat sources (tributary inputs). The model assumes that the water body is well mixed vertically and laterally, meaning density effects due to temperature gradients are neglected. Because of this, the temperature model can be uncoupled from the model simulating flow velocity and water depth, meaning these values can be simulated with other models (Yearsley, 2009). Sinokrot and Stefan (1994) concluded that although the flux of thermal energy from the stream bottom is a surface-area related phenomenon, it is generally small and can be assumed negligible.

Yearsley (2009) first tested RBM using two river systems in the Pacific Northwest. The first river system tested, Clearwater River, is located in Northern Central Idaho and has a drainage area of 24,800 km^2, with a mean annual discharge of 420 m^3/second. The Dworshak Dam and Reservoir built in 1972 has altered the historic water temperature regime and required releases for migrating salmonid species results in significant changes in flow and water temperature regimes for the entire river system. Observations of water flow and temperature during these releases allow for an

assessment of how well the methods of RBM are able to simulate water temperatures when sharp fronts associate with rapid changes in flow and temperature occurred. The study demonstrated the assumption that neglecting the dispersion of the front when simulating water temperature is reasonable.

The second river system tested, the Columbia River, was used to demonstrate applications to large-scale questions as a preliminary analysis of the impact of climate change on water temperatures. The Columbia River Basin has a drainage area of more than 670,800 km^2 and is located in British Columbia, Canada and parts of Idaho, Oregon, Washington and Wyoming. The system has an annual average stream flow of 6,540 m^3/second recorded at the mouth. The upstream river system has been highly developed by dams and reservoirs, causing many segments of the river to exceed water temperature criteria protecting cold water species (Yearsley, 2001).

In the case of the Columbia and Snake river simulations, differences between predicted and measured values were said to be due primarily to what can be characterized as parameter estimation, rather than to the inaccuracies in the numerical scheme. Uncertainty in parameter estimation include weather data from distant locations used to characterize heat fluxes, estimating hydraulic variables using simplified stream hydrodynamics and uncertainty in the formulation of energy budget terms (Yearsley, 2009).

DHSVM-RBM was then updated to incorporate a riparian shading feature to analyze the impacts of near-stream vegetation to water temperature (Sun et al., 2015). DHSVM-RBM was said to reasonably replicate streamflow at fine temporal and spatial scales in an initial small, urban watershed. The same conclusion was stated when extended to the regional scale for the Puget Sound area (Cao et al., 2016). For these two studies the primary findings were that streamside vegetation has a much larger effect on stream temperature than basin-wide land cover change

during summer periods; that basin-wide land cover and riparian vegetation have minor effects of stream temperatures during winter high flows; and that the effects of riparian vegetation during summer months is comparable to that of climate change.

Other studies using RBM thus far have included:

- Perry et al. (2011) used RBM to address potential impacts to water temperatures following dam removal under various climate change scenarios.
- Van Vliet et al. (2012a) adapted RBM to be used at large spatial and temporal scales, then applying it to a variety of different questions, including: the effect of climate change on global river flows and water temperatures (Van Vliet et al., 2013, 2015); impacts of drought and climate change on water resources and electricity supply (Van Vliet et al., 2016; Vliet et al., 2013); and the impacts of cooling water use in the energy sector (Van Vliet, 2012; Van Vliet et al., 2012b).
- Brennan (2015) compared RBM to Ficklin and Barnhart (2014)'s SWAT and Mohseni et al. (1998)'s Nonlinear Regression model, rating VIC-RBM the highest in performance.
- Raptis et al. (2016) and Raptis and Pfister (2016) looked at worldwide thermal pollution patterns and power-related freshwater thermal emissions.
- Dugdale et al. (2017) reviewed various process-based models, outlining some the similarities and differences between DHSVM-RBM and other water temperature models.
- Tobin et al. (2018) evaluated the vulnerability and resilience of various different power generation methods with global warming, using VIC-RBM for the thermo-power generation portion.

- Niemeyer et al. (2018) integrated RBM with a two-layer stratified reservoir module in order to account for the effects of reservoir stratification on downstream water temperatures.

- Truitt (2018) studied the effects of climate change on the Nooksack River basin.

2.6 Caspar Creek Paired Experimental Watershed

Paired watershed studies allow scientists to evaluate components of ecosystems, while essentially holding meteorological factors in an area constant. Effectiveness studies using paired watersheds in the Western United States include: the Alsea and Trask River Watersheds in the Oregon Coast Range, Hinkle Creek in the Oregon Cascades, Mica Creek Experimental Watershed in northern Idaho and the Caspar Creek Paired Experimental Watershed Study in Mendocino, California.

2.6.1 History

The Caspar Creek Paired Experimental Watershed was established in 1961 to study how forest harvesting could affect streamflow and suspended sediment concentration (SSC). Since then, the site has completed two experiments and is now on the third. The first experiment (1962-1985) was conducted before modern California FPRs were in place and the second experiment (1985-2016) was conducted using clear cut logging and WLPZ requirements prior to the anadromous salmon rules. The third study (present) seeks to quantify the influence of forest stand density reduction on watershed processes, while utilizing current California FPRs (Wagenbrenner, 2018). The study aims to further the understanding of how contemporary forest management affects water movement and storage, peak flows, water quality and sediment production in the South Fork of Caspar Creek.

Napolitano et al. (1989) discussed the history of logging in Caspar Creek, which began in 1860 by business partners William H. Kelly and William T. Rundle. The duo purchased 5,000 acres and built a sawmill at the mouth of the creek. Four years later the company was taken over by Jacob Green Jackson, who had three crib dams built on the North, South and main stems of Caspar Creek for log driving operations. Concurrently, skid roads built as straight and level as possible for oxen, and later bulls, were built to transport cut logs. In these early days, burning of slash in the late summer or early fall was done to ease skidding along sloped roads (Sullenberger, 1980). The operation was then updated to railroad use in 1877 and then again to steam donkey engines in the early 1890's (Wurm, 1986). Both watersheds were clearcut and burned in the late 1880's, with logging in Caspar Creek completed in 1904 (Napolitano et al., 1989). Therefore, it is believed that before the first experiment began, in 1962, the South Fork second-growth forest was estimated to be about 85 years old (Rice et al., 1979).

In 1961 the site was agreed to be a cooperative watershed management research site by the USDA Forest Service's Pacific Southwest Research Station (PSW), with formal cooperation of the State of California's Division of Forestry (now CalFire) (Ziemer, 1998). Additional entities involved in Caspar Creek over the years have included the California Department of Water Resources, State of California Department of Fish and Wildlife and various research universities. Having signed a joint 100-year Memorandum of Understanding, continuing research until 2099, the site will persist as a commitment by state and federal agencies to evaluate the impacts of forest management on watershed related issues for many years to come (Cafferata and Reid, 2013).

The first experiment, starting in 1962, was a classic paired watershed study, which used the North Fork as a control and the South Fork as a treatment. The South Fork had 4.9 miles of roads constructed and about 65% of the stand volume selectively

cut and tractor yarded. Of the 4.9 miles of roads, 2.4 of the main haul roads and 1.3 of the spur roads were within 200 feet of streams. After disturbance, the South Fork became more dependent on stream power, resulting in increases in suspended sediment concentration (SSC) discharges. Whereas the control was highly dependent on supply for sediment transport. Based on SSC increases, it was inferred that road construction and logging appeared to have raised average turbidity levels above those permitted by Regional Water Quality Regulations (Rice et al., 1979).

The second experiment, using the North Fork as a treatment and the contemporary FPRs of the time, evaluated the effects of clearcutting sub-watersheds on downstream flow and SSC. Logging occurred between 1989-1992 and used clearcutting blocks ranging from 9 to 60 ha and occupying 35-100% of the individual subwatersheds. Skyline cable yarding techniques were the primary method of use, with road/landing construction and tractor logging kept to ridgetop and upper slope locations (Henry, 1998). Roads constructed high on hillslopes typically have less impact on watercourses (Cafferata and Reid, 2013). The North Fork Caspar Creek study showed that clear-cutting 50% of the watershed using buffer strips prescribed by contemporary FPRs led to a smaller increase in water temperature and that temperatures remained within the range considered suitable for Coho and Steelhead (Nakamoto, 1998).

Results from the first two experiments at Caspar Creek have added to scientific knowledge regarding cumulative watershed effects, logging-related sediment production and impacts on anadromous fish and benthic macro-invertebrate communities. Additional findings include changes in fog drip and interception loss with harvest, nutrient cycling impacts associated with clearcutting, changes in peak flows and impacts on subsurface flow. These studies have also aided in making improvements to managing headwater channels, designing buffer strips and developing water quality monitoring efforts. Some of the key findings produced during the first and second

study are included in the appendix of this report, and are said to now be used world wide (Cafferata and Reid, 2013).

The goal of the third experiment is to quantify the influence of forest stand density reduction on watershed processes using current California FPRs. For this third phase, forest management treatments were planned to lower stand density to 20-90% of pre-existing density in approximately 70% of SFC. Harvesting took place between 2018-2019 and resulted in harvesting between 25-75% of basal area in various sub-watersheds, with some sub-watersheds kept as controls (Figure 3.9). Specific projects for the third study include those on watershed resilience and recovery, plant-soil-water dynamics, bioassessment, hydrologic modeling (this report), sediment fingerprinting, fine sediments and erosion consequences of legacy road rehabilitation. For a complete outline of the entire third study refer to Dymond (2016).

Chapter 3

Methodology

3.1 Study Area

The study was located in the South Fork of Caspar Creek (SFC) within the Caspar Creek Experimental Watersheds (39°21'N, 123°44'W) on the Jackson Demonstration State Forest (JDSF) in Mendocino County, California. The Caspar Creek watersheds are approximately 15 km southeast of Fort Bragg, California (Wagenbrenner, 2018) and encompass a drainage area of 2,167 ha, with the North and South Forks comprising of 473 and 424 ha, respectively. The climate is characterized as Mediterranean with cool, dry summers and mild, wet winters; with periods of coastal fog throughout the entire year. A westerly flow of moist air typically results in low-intensity rainfall and prolonged cloudy periods, with snow occurring rarely (Henry, 1998). Mean annual rainfall recorded in the South Fork from 2010-2016 was 1,108 mm, with 93% occurring between October and April. Less than 50% of rainfall results in streamflow, with the residual lost to either evapotranspiration or groundwater (Carr et al., 2014). Mean annual air temperature between 2010-2016 in December was 4.7°C and in July was 15.6°C (Wagenbrenner, 2018).

The SFC forest is comprised of third-growth coast redwood (*Sequoia sempervirens*), Douglas-fir (*Pseudotsuga menziesii*), grand fir (*Abies grandis*) and western hemlock (*Tsuga heterophylla*), there are minor components of Tanoak (*Lithocarpus densiflorus*), red alder (*Alnus rubra*) and bishop pine (*pinus muricata*) (Henry, 1998). Elevations range between 37 and 320 m, with average slopes ranging from 26-59% (Table 3.1). The geology at Caspar Creek consists of Franciscacn Sandstone bedrock overlain by 1 to 4 m of well-drained clay-loam ultisols and alfisols (Wagenbrenner, 2018; Henry, 1998; Carr et al., 2014). The dominant soil subgroups are Mollic hapludalf, Ultic haludalf and Typic hapluhumult (Dymond, 2016). Watershed characteristics for each of the eleven subbasins of SFC are broken down in Table 3.1. Subsurface pipeflow dynamics have been formally studied in the North Fork Caspar Creek, where it was concluded that pipe discharges are predominantly a quickflow process and pipes were said to be at depths up to 2 m within trenched swales and at the head of gullied channels in small headwater drainages (Ziemer and Alright, 1987).

Table 3.1: **Physical Characteristics of SFC Sub-Watersheds.** Station ID, area (ha), elevation range (m), average slope (%) and dominant soil subgroup(s) for each of the sub-watersheds in the South Fork of Caspar Creek. Excerpted from Wagenbrenner (2018).

Watershed Name	Station ID	Area (ha)	Elevation Range (m)	Average Slope (%)	Dominant Soil Subgroup(s)
South Fork Caspar	SFC	424	46-329	59.6	Ultic hapludalf
Ogilvie	OGI	18	58-174	26.3	Mollic/Ultic hapludalf
Porter	POR	32	61-186	34.2	Ultic hapludalf
Quetelet	QUE	394	48-329	49.8	Mollic/Ultic hapludalf
Richards	RIC	49	73-198	41.6	Mollic/Ultic hapludalf
Sequoyah	SEQ	17	79-207	37.9	Ultic hapludalf
Treat	TRE	14	98-244	46.5	Mollic/Ultic hapludalf
Uqildisi	UQL	13	122-323	48.5	Typic haplohumult
Williams	WIL	26	146-323	50.5	Typic haplohumult
Yocum	YOC	53	146-329	47.5	Typic haplohumult
Ziemer	ZIE	25	213-329	43.0	Typic haplohumult

There are currently five active stream temperature stations (set to hourly intervals) and eleven stream flow stations at each sub-watershed outlet (set to 10-min intervals) (Figure 3.1 and 3.2). Water temperatures readings taken by CDFW between May 2010 and October 2017 at four locations throughout the South Fork av-

eraged 12.0°C, with an ultimate low of 7.42°C and high of 17.5°C. The flow regime of the South Fork is typical of small forested watersheds, with flows low relative to maximum discharges most of the time and most of the flow volume, especially the sediment load, occurs during short periods of high discharge (Rice et al., 1979).

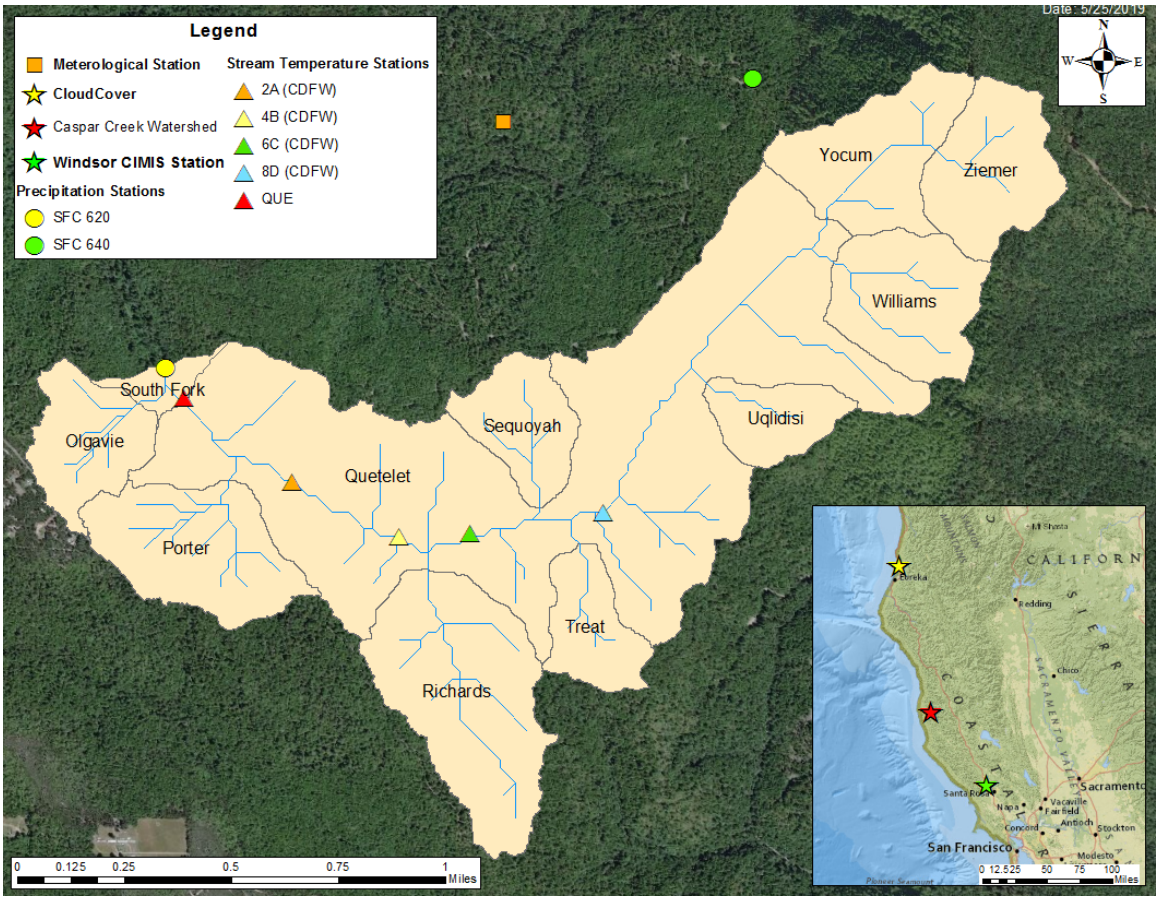

Figure 3.1: **SFC Map.** Map depicting SFC sub-watersheds, stream temperature stations and precipitation stations. Where SFC is in relation to the Windsor CIMIS station and Arcata Airport station are also included.

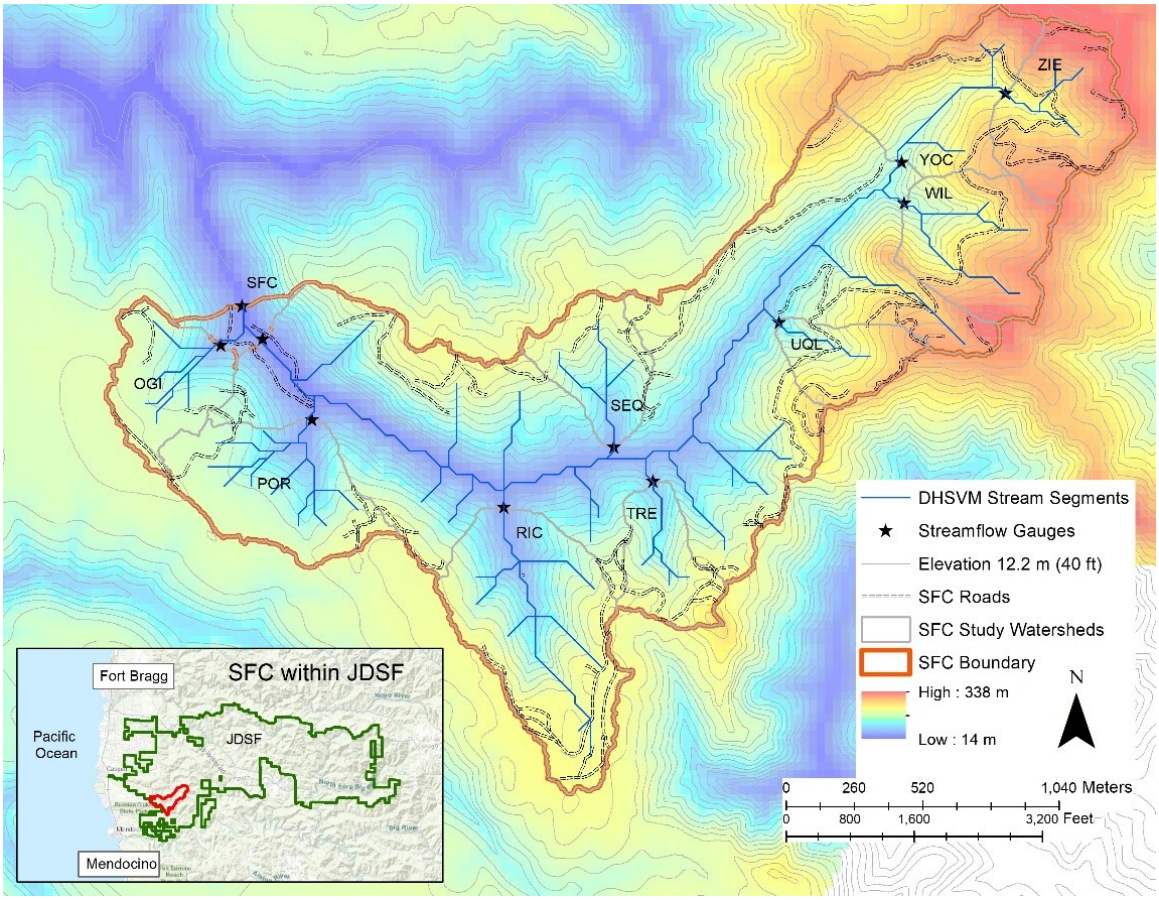

Figure 3.2: **SFC Road Locations Map.** Map of the South Fork Caspar Creek, including stream segments, roads and location within Jackson Demonstration State Forest.

3.2 DHSVM Background

3.2.1 DHSVM Inputs

For input, DHSVM requires (1) spatial information about the watershed in the form of binary grids created from ArcInfo coverages of elevation, soil type, soil depth, and vegetation type, and (2) connecting arcs (spatially aligned lines) for the stream network and road network. A 30-m DEM for SFC was projected from LIDAR data with a resolution of 2 m provided by the United States Forest Service Pacific South-

west Research Station. A pixel size of 30 m was chosen because it would be large enough to encompass the stream channel and road widths found in SFC (a constraint of DHSVM) and is an efficient scale for model precision for small watersheds. A uniform vegetation representing a third growth coast redwood and fir forest was used in DHSVM. An average tree height of 45 m and leaf area index (LAI) of 7 was used based on forest stand data from JDSF (Webb, 2019).

DHSVM allows partitioning of sub-surface media or soil into different layers based on differing physical and hydraulic parameters. A sub-surface media depth of 5 m was used across SFC, based on soil core depths created for sub-surface water studies (Keepeler, 2019). In the 5 m sub-surface media a soil depth of 1.8 m was used based on maximum depth of soil in the watershed (Staff, 2019). This depth was similar to hydrologic modelling done in the North Fork of Caspar Creek, which used a 1.5 m soil depth (Carr et al., 2014). The 1.8 - 5.0 m depth was considered weathered bedrock, below 5 m we assume to be bedrock. The a priori soil parameters used in DHSVM were derived from soil hydraulic properties measured in the nearby North Fork of Caspar Creek (Carr et al., 2014) and are located in the calibration section of this report (Table 3.6).

The stream network for SFC for use in DHSVM was generated by the "createstreamnetwork" Python script (Duan, 2017) using a 10,000 m^2 contributing area for runoff generation. This script assigns stream dimensions, based on user inputs, and establishes the spatial proximity and routing order of surface water for DHSVM calculations. A variety of contributing areas were experimented with to develop the stream network for DHSVM. The 10,000 m^2 contributing area provided the best simulation of stream segment maps used by the Jackson Demonstration State Forest.

Meteorological Forcing Files

DHSVM requires meteorological inputs at hourly or 3-hourly timesteps for air temperature (°C), wind speed (m/s), relative humidity (%), incoming short and long-wave radiation (W/m^2) and precipitation. As advised by the model developers, DHSVM-RBM was run at a 3-hour timestep from August 2009 to September 2016.

Figure 3.3: **South Fork Caspar Creek Meteorological Station.** Taken December 11, 2017.

DHSVM-RBM also allows for multiple meteorological stations to be used based on location within the watershed. One meteorological station *MET1* (39°21', 00" N, -123°44' 20" W) and two precipitation stations *SFC620* (39°20' 29", -123°45' 13") and *sfc640* (39°21' 05", -123°43' 41") are located in the experimental watershed (Figure 3.1). The locations of the two precipitation stations were used as meteorological stations in DHSVM to most accurately represent the spatial variation of rainfall throughout the watershed.

Most of the meteorological variables needed to run the model (air temperature, wind speed and relative humidity) were collected at the South Fork meteorological station (Figure 3.3) in 15 minute intervals. This data was converted to 3 hour readings by taking the average of the 15 minute readings every

3 hours. Although PAR (photosynthetically available radiation) data is also collected at the meteorological station, actual incoming shortwave radiation collected by the California Irrigation Management Information System (CIMIS) *Windsor Station #103*, approximately 100 miles away from the research site (Figure 3.1), was used to more accurately estimate the amount of shortwave radiation reaching the site (California Department of Water Resources, 2019).

Incoming long-wave solar radiation is often computed from a general equation following the form of the Stefan-Boltzmann equation (Eq. 3.1). However, various parameterizations to estimate clear versus cloudy sky values exist (Flerchinger et al., 2009). Based on the findings of Flerchinger et al. (2009) and Wu et al. (2012), the Prata (1996) algorithm (Eq. 3.2) coupled with the Unsworth and Monteith (1975) cloud cover correction (Eq. 3.3) were chosen. Because cloud cover is not recorded at Caspar Creek, hourly estimations from the National Centers for Environmental Information (2018) *Arcata Airport Station* (40°58' 41", 124°6' 32") (Figure 3.1) were matched to recommended optimum values of K_{clr} and K_{cld} for the Prata-Unsworth Montheirth combination (Table 3.2).

$$ILR = \epsilon_{eff}\sigma T_{eff}^4 \tag{3.1}$$

Where ϵ_{eff} and T_{eff} (K) are the effective emissivity and temperature of the atmosphere above the site and σ is the Stefan-Boltzmann constant.

$$\epsilon_{clr} = 1 - (1 + w)exp(-(1.2 + 3w)^{\frac{1}{2}}) \tag{3.2}$$

Where ϵ_{clr} is the clear-sky emissivity, $w = 465(\frac{e_o}{T_o})$, T_o is the near-surface air temperature (K) and e_o is the vapor pressure (kPa) calculated as $\frac{6.11*10^{\frac{7.5T_d}{237.3+T_d}}}{10}$, where T_d is the dew point temperature.

$$\epsilon_a = (1 - 0.84c)\epsilon_{clr} + 0.84c \tag{3.3}$$

Where c is the fraction of cloud cover and ϵ_a is the effective atmospheric emissivity.

Table 3.2: **Cloud Cover Values.** C-values for long-wave radiation calculations based on recommended values from Flerchinger et al. (2009) for a Prata-Unsworth Montheirth algorithm combination.

Arcata Cloud Cover	**Corresponding C-Value**
Clear	0.7
Scattered	0.533
Broken	0.366
Overcast	0.2

The last meteorological input required by DHSVM-RBM is precipitation. This is measured at Caspar Creek in 0.01 inch increments. To summarize this data into a 3-hourly format, timestamps were rounded to the closest hour, summed for equivalent 3-hour timesteps and converted to meters, the required input for DHSVM.

Of the 62,832 total hours between August 1st, 2009 and September 30th, 2016 2,038 hours were missing for the Caspar collected data (3.2%). In order to have continuous readings in the met files, gaps lasting less than 48 hours were filled by taking the average of adjacent readings or directly from corresponding hours (i.e. 9:00 am and 9:00 am) within a 5 day time period. When direct readings were substituted, data was chosen based on having similar precipitation patterns to the missing periods. Four larger gaps (82, 351, 450 and 934 hours) were filled using data from the MESO-West McGuires (MCGC1) Station, located approximately 7 miles further inland than Caspar and residing at 627 feet of elevation (39° 21' 8", -123° 35' 46") (Iowa Environmental Mesonet (IEM), 2019). For the CIMIS shortwave solar radiation data, 40 recordings were missing (0.06%). These gaps were filled by either taking the average of the surrounding two hours or copied from the corresponding hour from the day before or the day after the missing value. Lastly, for the Arcata Airport cloud cover used in calculating incoming long-wave radiation, 18,377 hours were listed as obstructed

or left blank (29.2%). These gaps were filled by either matching the two surrounding hours, if the same (i.e. clear and clear), or linearly interpolated if different (i.e. between clear and broken).

3.3 RBM Background

The one-dimensional RBM stream-temperature model (Yearsley, 2009, 2012; Sun et al., 2015) was used to simulate historical stream temperatures in the South Fork of Caspar Creek. RBM solves time dependent equations for the conservation of thermal energy between the air-water interface using a semi-Lagranagian method (Yearsley, 2009, 2012). Water inflow and outflow for each stream segment, as well as energy budget components, are produced as outputs from DHSVM for RBM. These outputs, and parameters dictating initial upstream temperatures (Mohseni Parameters) and stream speed and depth (Leopold Parameters), are used to complete the calculations. Downstream water temperatures are estimated using solar radiation, net longwave radiation, sensible heat flux, latent heat flux, groundwater and advected heat from adjacent tributary segments. The water parcels are tracked through the river basin to determine results for points throughout the stream network.

The newest version of RBM allows vegetation height, buffer width, a monthly extinction coefficient, percent overhanging vegetation, canopy bank distance and channel width to be manipulated for each stream segment. Part A in Figure 3.4 shows a 3-D view of the riparian shading setup RBM uses to calculate the shadow length of the buffer canopy at each time step using solar altitude (ϕ), azimuth (θ_{sun}), stream azimuth ($\theta_{streams}$), bank height (H_{bank}) and vegetation height (H_{tree}). Part B depicts an example cross section where I_1 is the length of stream that receives direct radiation, I_2 is the length of the stream that receives radiation attenuated by the canopy and I_3 is the portion of the stream that is fully shaded (Sun et al., 2015).

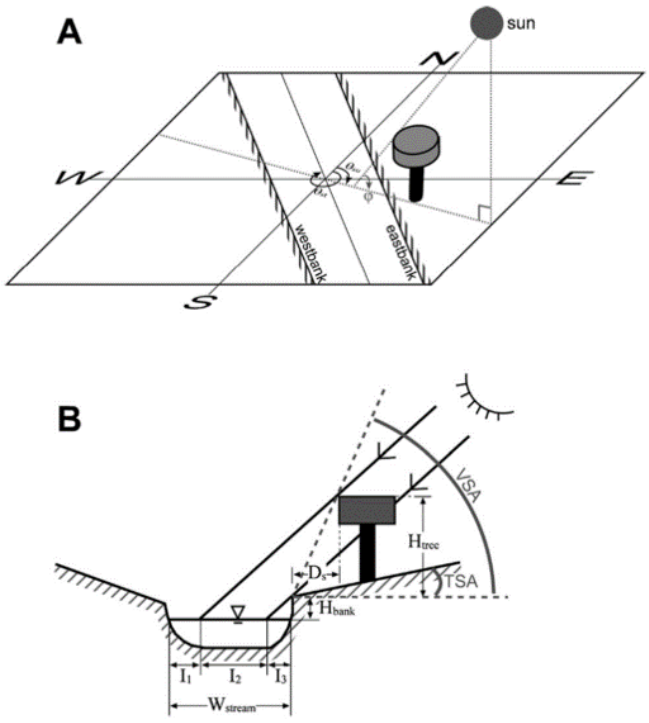

Figure 3.4: **RBM Riparian Shading.** Diagram of how riparian shading over stream surfaces occurs in RBM. Excerpted from (Sun et al., 2015).

3.3.1 RBM Inputs

RBM uses the output forcing files created by DHSVM, which include air temperature (°C), net shortwave and long wave radiation (Wattts m^{-2}), vapor pressure (pascals), wind speed (m s^{-1}) and stream inflow and outflow (m^3 s^{-1}) calculated for each stream segment at each timestep. Additional Mohseni and Leopold parameters used to estimate initial headwater temperatures and establish hydraulic characteristics, respectively, are also required as input.

Mohseni Parameters

RBM requires estimates of initial headwater temperatures. Yearsley (2012) tested two methods to provide these estimates, daily soil temperature and the Mohseni et al. (1998) nonlinear regression model relating air and stream temperature, and found no improvements to model results using soil temperature. For this reason we used the Mohseni et al. (1998) method. The Mohseni nonlinear regression analysis model is as follows

$$T_s = \mu + \frac{\alpha - \mu}{1 + e^{\gamma(\beta - T_{smooth})}} \tag{3.4}$$

Where T_s is the simulated stream temperature, μ is the estimated minimum stream temperature, T_{smooth} is the smoothed air temperature, α is the maximum actual stream temperature, γ is a measure of the steepest slope of the function, β is the air temperature at the inflection point and γ is a function of the slope $tan\theta$ at said point of inflection.

$$\gamma = \frac{4 \tan \theta}{\alpha - \mu} \tag{3.5}$$

$$T_{smooth} = \lambda * T_{air}(t) + (1 - \lambda) * T_{air}(t - 1) \tag{3.6}$$

For T_{smooth}, the value of λ is determined by the highest possible correlation coefficient between smoothed air temperature and measured water temperature.

For this project, these parameters were calculated using stream temperature and micro-climate data collected between 2010 and 2016 by the California Department of Fish and Wildlife (CDFW). These stations were used, as opposed to the primary Caspar station (QUE), because of the close proximity between air and stream temperature gauges. They are located above the Porter and Quetelet sub-watersheds (2A), below the Richards sub-watershed (4B), below the Sequoyah sub-watershed (6C) and above the Treat and below the Uqlidisi sub-watersheds (8D) (Figure 3.1). An initial

evaluation using *JMP Pro 13* of all air and water temperature values can be seen in (Figure 3.5).

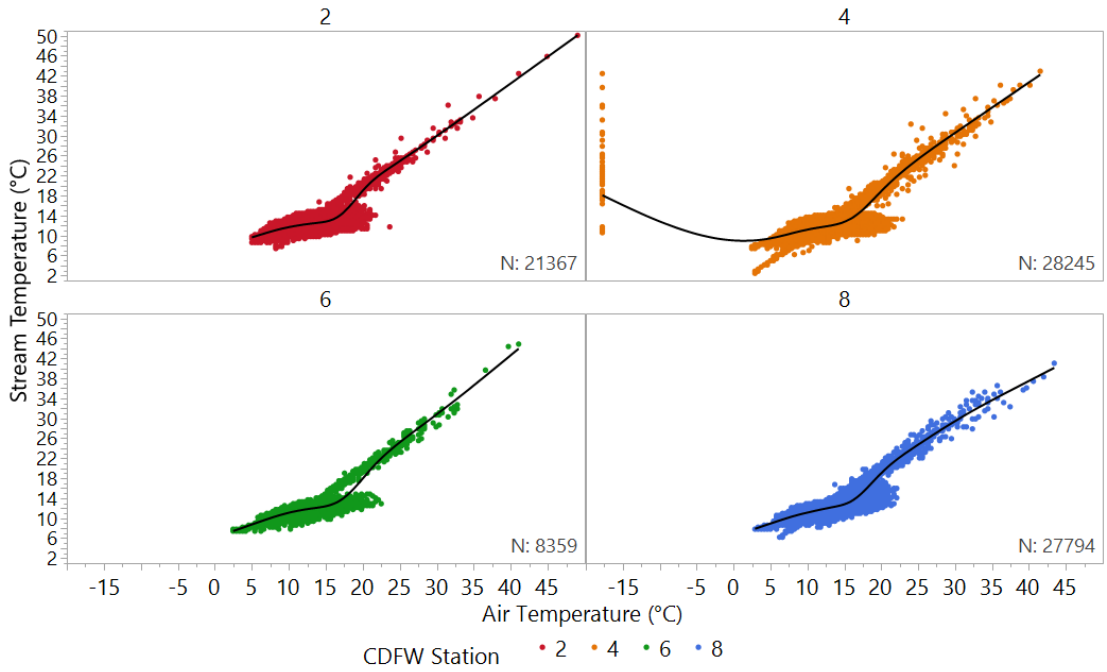

Figure 3.5: **Development of Mohseni Parameters - Outliers Included.** Air temperature (°C) vs. stream temperature (°C), with outliers included, to calculate Mohseni headwater parameters.

Values with a Mahalanobis distance greater than 2.448 for each station were considered outliers, according to the *Outlier Analysis* feature in *JMP Pro 13*. In total, 4,026 of the 85,765 points possible (4.69%) were then excluded from further analysis as outliers. The smoother element, a cubic spline that shows a smooth curve through the data, and a lambda value of 33.3 was used for all four graphs (Figure 3.6) to determine the air temperature (°C) at the steepest slope following the inflection point (β) and the angle of trend line at that point (θ).

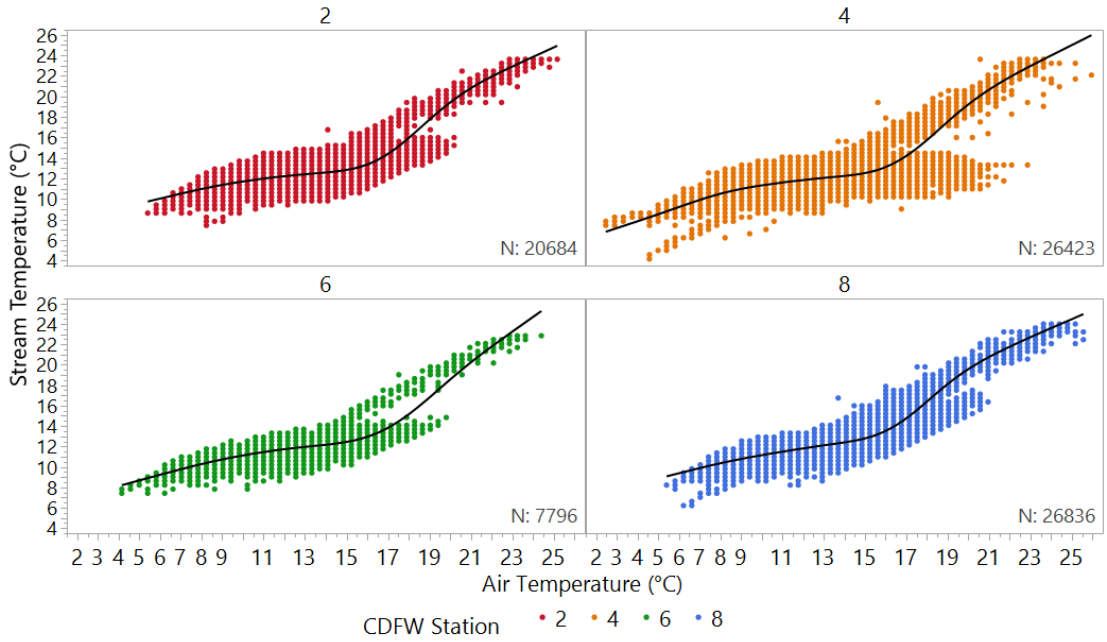

Figure 3.6: **Development of Mohseni Parameters - Outliers Excluded.** Air temperature (°C) vs. stream temperature (°C), with outliers excluded, used to establish Mohseni headwater parameters.

These values were then used in equations 3.4, 3.5 and 3.6 to estimate parameters used by RBM for initial headwater stream temperatures. These parameters are presented in Table 3.3, as well as the final parameter set used in RBM. Final parameters were determined by incrementally adjusting the Mohseni and Leopold variables to find those that resulted in stream temperature estimates closest to measured readings at the outlet of the mainstem (QUE).

Table 3.3: **Mohseni Parameters.** Mohseni variables produced using CDFW data.

CDFW Station	α (°C)	θ (°C)	γ	β (°C)	μ (°C)	λ
2A	23.63	22.75	0.234	18.5	7.43	0.99
4B	23.63	22.50	0.1145	18.00	4.15	0.90
6C	22.86	22.50	0.145	19.00	7.43	1.10
8D	24.01	22.75	0.213	17.5	6.22	1.20
Best Fit Parameters for QUE	13.50	NA	0.20	10.5	4.0	0.04

Leopold Parameters

RBM uses coefficients relating velocity and depth to river discharge to establish hydraulic characteristics based on the works of Leopold and Maddock (1953). These coefficients can be set for each stream segment or generalized to the entire watershed. Equations 3.7 and 3.8 are the power equations used to relate depth and velocity to discharge. Where D is depth, v is velocity, Q is discharge and a, b, c and d are empirical constants determined from discharge rating curves. RBM also allows minimum stream speeds to be set, to account for the potential for abnormally low stream speeds because these equations are constant in time.

$$D = aQ^b \tag{3.7}$$

$$v = cQ^d \tag{3.8}$$

The data needed to establish these relationships has not been established at SFC. Empirical equations to predict stream width and depth exist (Allen et al., 1994; Ames et al., 2009); however, these equations were determined to be too uncertain due to the different hydrologic conditions where they were developed (i.e. snow). Therefore, historical stage and discharge readings, as well as known weir dimensions, were used to back out estimates of these parameters.

A 2 m Lidar DEM of the watershed was used to estimate a natural cross section of the channel. From this, the width (ft) and average depth (ft), determined using 1 foot intervals, was used to surmise the cross sectional area (ft^2) of eight individual cross-sections (Figure 3.7).

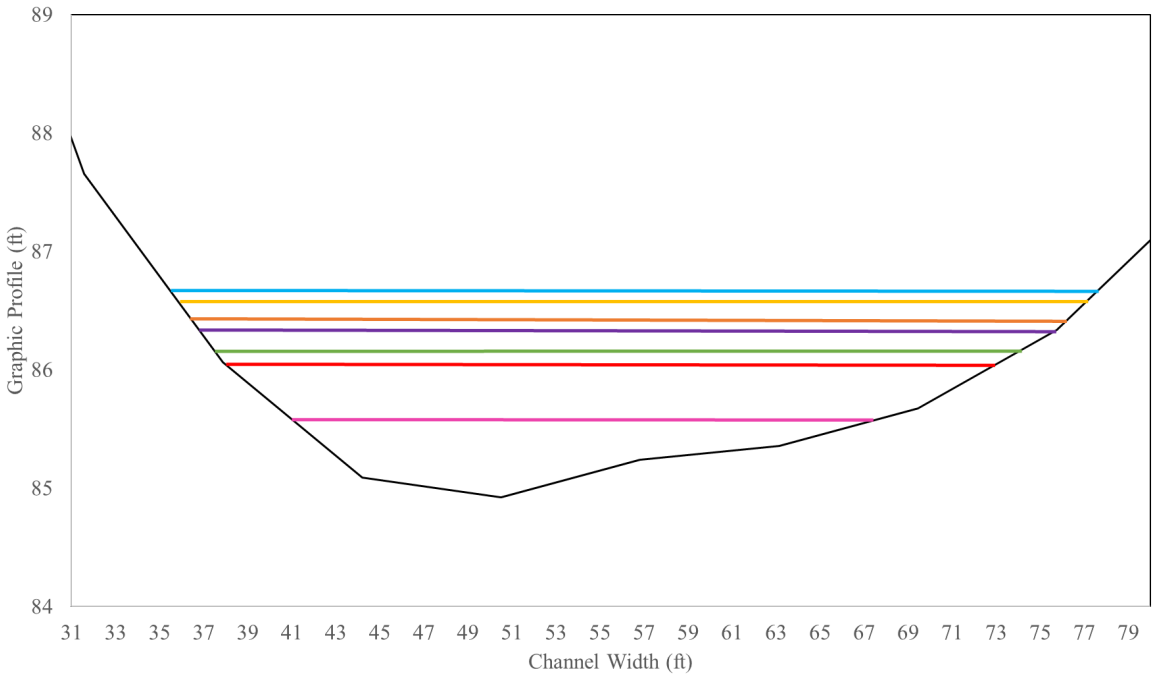

Figure 3.7: **Leopold Parameters - Cross Section.** Cross section just upstream of the SFC weir, using a 2-meter resolution DEM, to estimate natural channel width and depth estimations.

Only cross sections with areas where flow would be large enough to enact the use of the broad crested weir, instead of the v-notch weir, were selected for accuracy purposes. A historically determined weir stage to cross sectional area relationship, based on the broad crested weir dimensions, was then used to estimate a stage reading for each of the eight cross-sections. Historical SFC 10-minute flow data collected from 1996 to 2016 was matched with the corresponding historical average discharge for each cross section. Lastly, velocity was back calculated by dividing the discharge by the cross sectional area. Resulting depth and velocity to stream discharge relationships with best fit power equations can be seen in Figures 3.8a and 3.8b. The final Leopold parameters used for RBM calibration are in Table 3.4.

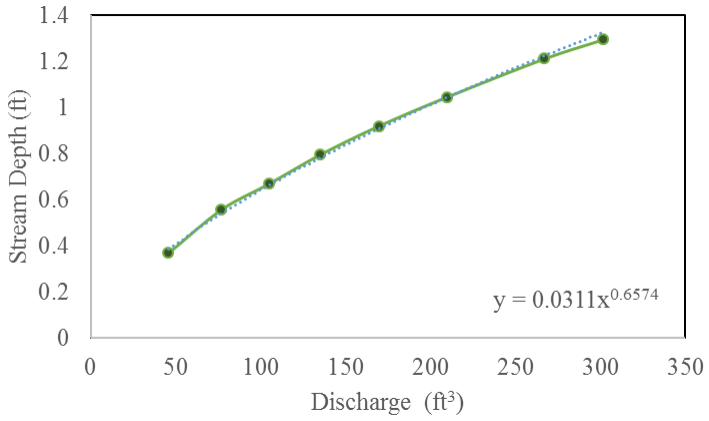

(a)

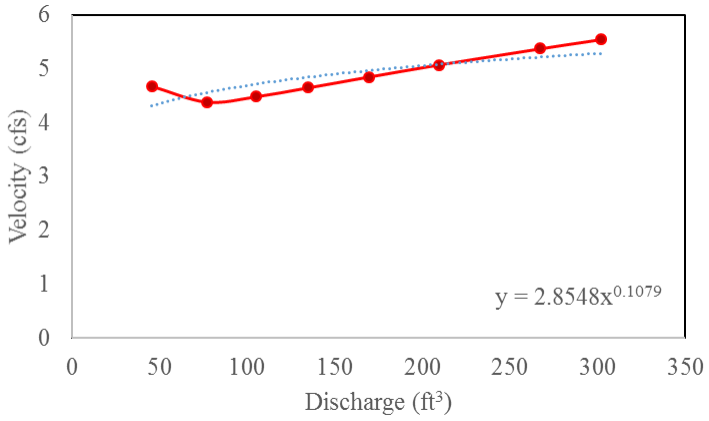

(b)

Figure 3.8: **Leopold Parameters - Relationships.** (a) Depth to stream discharge and (b) velocity to stream discharge relationship calculated for the South Fork of Caspar Creek.

Table 3.4: **Leopold Parameters.** Final Leopold parameters used for calibration and temperature simulations.

	Coefficient	**Exponent**	**Minimum**
Velocity (ft^3/sec)	2.85	0.11	0.25
Depth (ft)	0.03	0.66	0.50

Expected ranges for the exponent terms b and d reported by Chapra (1997) range from 0.1-0.6 for depth (b) and 0.3-0.7 for velocity (d). Our exponent terms fall slightly

above and below these ranges, highlighting a potential source of error. No expected ranges are reported for the coefficient terms.

Riparian Shading

As mentioned, RBM allows various riparian characteristics to be altered for each stream segment, including: tree height (m), buffer width (m), monthly extinction coefficient (similar to LAI), overhang coefficient (the percentage of tree height that overhangs the stream), canopy bank distance (m) and channel width (m). Riparian characteristics used in the initial pre-harvest simulation are in Table 3.5. Buffer widths were chosen based on California FPRs. However, RBM does not allow for the creation of core, inner and outer zones as prescribed by the California FPRs, therefore presenting a limitation to the study. Tree height was estimated by Caspar personnel from Lidar data within the 150 foot Class I WLPZ. An average monthly extinction coefficient for *Pseudotsuga menziesii* was taken from the work of Thomas and Winner (2011) and the overhang coefficient was based on the mean percent canopy density for SFC (California Department of Fish and Wildlife, 2006). The monthly extinction coefficient can be adjusted month to month, however these values were kept constant, like in the works of Truitt (2018), to represent a coniferous dominated forest.

Table 3.5: **Initial Riparian Characteristics.** Riparian characteristics used for initial, third-growth conditions

	Class I	**Class II**	**Class III**
Buffer Width (ft)	100	85	25
Channel Width (m)	4	2	1
Tree Height (m)	50.6	50.6	50.6
Monthly Extinction Coefficient	0.525	0.525	0.525
Overhang Coefficient	0.90	0.90	0.90
Canopy Bank Distance (m)	1	1	1

3.4 Model Calibration

3.4.1 RBM

For most coastal western US areas, stream temperatures are generally highest during summer, coinciding with when flows are lowest and energy inputs are highest (clear skys). Therefore, similar to the works of Sun et al. (2015), the period of May 1st to September 30th was evaluated to capture this critical time period for aquatic species. In order to gauge model fit, the Nash-Sutcliffe Efficiency (NSE) (Eq. 3.9) was used to assess the goodness of fit and the root mean square error (RMSE) (Eq. 3.10) was used to assess the quality of the fit. When NSE values are equal to 1.0, simulated values perfectly match measured values. When NSE values are ≤ 0 the simulated values are worse than the measured mean. Lower RMSE values indicate a better fit.

$$NSE = 1 - \frac{\sum_{t=1}^{n}(T_{s_t} - T_{a_t})^2}{\sum_{t=1}^{n}(\bar{T_a} - T_{a_t})^2} \tag{3.9}$$

$$RMSE = \sqrt{\frac{\sum_{t=1}^{n}(T_{s_t} - T_{a_t})^2}{n-4}} \tag{3.10}$$

Where, T_{s_t} is the simulated stream temperature at time t, T_{a_t} is the actual stream temperature at time t and $\bar{T_a}$ is the average of the actual stream temperatures recorded.

RBM was calibrated to measured stream temperatures collected at the primary stream temperature station (QUE) located at the outlet of SFC (Figure 3.1). Modifiable parameters include the Mohseni, Leopold and smoothing coefficients. After allowing a year and a half of model spin up time, the first three summers (2011-2013) were evaluated as a calibration period and the later three summers (2014-2016) as a verification period. The 3-hour output was aggregated and the maximum of the

7-day average temperatures (MWAT) and maximum of the 7-day maximum temperatures (MWMT) were calculated to compare to measured values. Cao et al. (2016) addresses that although the use of a 3-hour timestep has the potential to limit RBMs ability to capture daily maxima, it does not do so significantly enough to recommend against using RBM output to calculate the MWMT. Additionally, the MWAT and MWMT are used by the EPA and many other government agencies to identify viable water temperatures for aquatic species, making their use in these results more widely applicable to decision makers.

3.4.2 DHSVM

Calibration of DHSVM was based on fit to measured streamflow at the outlet of SFC and RIC watersheds (Figure 3.2). A 3 hour time step was used for DHSVM simulations. DHSVM was run from 2010 to 2016 HY with the 2010 HY used as a spin-up period to equilibrate the initial water balance. DHSVM was calibrated for the 2011 to 2013 HY and verified for the 2014 to 2016 HY. HY at Caspar Creek runs from August 1 to July 31.

The model was calibrated by adjusting four sensitive soil hydraulic parameters: (1) lateral hydraulic conductivity, (2) exponent of decay (an exponent of the natural logarithm describing the decrease in hydraulic conductivity by depth of soil), (3) porosity of the soil matrix, and (4) vertical hydraulic conductivity. These four parameters, and the range of values for each parameter selected, were based on preliminary model trials that demonstrated competence at achieving model fit to measured streamflow.

Statistical fit of the simulated to measured streamflow time series was evaluated using again the Nash Sutcliffe Efficiency (NSE) (Eq. 3.9), as well as the Relative Efficiency (EREL) (Eq. 3.11). The NSE is a common measure of goodness-of-fit for

hydrologic models that uses squared values making them sensitive to high streamflow events. The EREL value modifies the NSE as relative deviations, adjusting model fit based on size of event, thus better reflecting fit of the entire series and reducing the influence of the absolute differences during high flows (Surfleet et al., 2012). As a result, EREL values are more sensitive to systematic over- or under-prediction, in particular during low flow conditions (Krause et al., 2005), with higher values indicating higher model fit. Calibration was based on achieving high values of EREL metrics (>0.9), while maintaining reasonable NSE values (>0.6). The primary stream temperature analysis in this study was summer stream temperatures during lowflow periods. The EREL is a better metric for smaller streamflows then NSE.

$$E_{rel} = 1 - \frac{\sum_{i=1}^{n} (\frac{O_i - P_i}{O_i})^2}{\sum_{t=1}^{n} (\frac{O_i - \bar{O}}{\bar{O}})^2} \tag{3.11}$$

With O observed and P predicted values.

Table 3.6: **DHSVM Variables.** A priori and calibrated parameters for SFC 2011-2016 HY. A priori parameters are in parenthesis. HC= hydraulic conductivity.

Depth(m)	**Porosity**	**Vertical HC (m/s)**	**Exponent of Decay**	**Horizontal HC (m/s)**
0 - 1.8	(0.5) 0.46	($2.2\text{x}10^{-5}$) $1.9\text{x}10^{-4}$	3.9	($2.2\text{x}10^{-5}$) $9.0\text{x}10^{-3}$
1.8 - 5.0	(0.1) 0.09	($2.2\text{x}10^{-5}$) $1.9\text{x}10^{-4}$	3.9	($2.2\text{x}10^{-6}$) $1.0\text{x}10^{-6}$

3.5 Modeling Scenarios

Computer modeling allows scenarios that may otherwise be un-feasible or pose too high of a risk to the environment to be analyzed. Scenarios developed for this

report were guided based on input from an advisory committee including California Department of Forestry and Fire Protection and US Forest Service Caspar Creek staff. The simulations run are broken into three sections- canopy reductions, the harvest scenario and an experimental riparian reach design.

3.5.1 Canopy Reduction

The first set of scenarios decreased tree height, the monthly extinction coefficient (similar to LAI) and canopy overhang to 80, 65, 50, 25 and 0% of the initial conditions along all stream classes. Two extreme scenarios, clear cutting the entire watershed (including the buffer areas) and treating the watershed as if it had been preserved for old growth were also simulated. Table 3.7 outlines the riparian characteristics used for each canopy scenario. For all scenarios the buffer width and channel width remained at the initial conditions based on stream class (Table 3.5).

The simulation of clearcutting the entire South Fork of Caspar Creek or in an old growth forest condition will influence streamflow that could influence stream temperatures. For this reason, in addition to modification of riparian vegetation for the old growth or clearcut watershed the upslope vegetation inputs in DHSVM were also modified. The LAI and height of vegetation were adjusted in DHSVM for the scenarios. The old growth scenarios used an upslope height of 60 m and LAI of 14. The tree height and LAI reflect a compromised value considering both coast redwood and fir trees within the stands based on Berrill and O'Hara (2007); Thomas and Winner (2011); Iberle (2016). For the clearcut watershed scenario a 1 m vegetation height and LAI of 1 was used to represent understory vegetation remaining following tree clearing.

Table 3.7: **Canopy Reduction Riparian Characteristics.** Riparian characteristics for each scenario evaluated- tree height (m), monthly extinction coefficient, overhang coefficient and canopy bank distance (m).

Scenario	**Tree Height (m)**	**Monthly Extinction Coefficient**	**Overhang Coefficient (%)**	**Canopy Bank Distance (m)**
Initial, Third Growth	50.60	0.53	0.90	1.00
80% retention	40.48	0.42	0.72	1.00
65% retention	32.89	0.34	0.59	1.00
50% retention	25.30	0.26	0.45	1.00
25% retention	12.65	0.13	0.23	1.00
0% retention	0.00	0.00	0.00	1.00
Conversion	0.00	0.00	0.00	0.00
Watershed Clearcut	0.00	0.00	0.00	0.00
Watershed Old Growth	91.44	0.62	0.90	1.00

3.5.2 SFC Phase Three Harvest Scenario

A scenario representing the Phase Three SFC experiment harvest was simulated (Dymond, 2016). In this scenario each subwatershed was reduced to the appropriate harvest level completed during the actual 2018-2019 SFC harvest. Again, a limitation to the study was that RBM cannot differentiate between core, inner and outer zones within the buffer areas as stipulated in FPRs. Therefore, in an attempt to best simulate buffer area reductions used during the actual harvest, buffer size and reduction rate were based on stream class. Class I streams received a 100' buffer and retained 80% canopy vegetation. Class II streams received an 85' buffer and retained 50% canopy vegetation. Lastly, because California FPRs allow Class III retention rates to be determined at the discretion of the primary forester, a 25' buffer and 0% canopy vegetation for class III streams was used to simulate the most extreme case possible. Figure 3.9 illustrates these values.

The upslope vegetation inputs for DHSVM were adjusted to reflect the percent

basal area reductions (Figure 3.9). The over story LAI was changed to reflect the reduced post-harvest over story (Table 3.8). A relationship between stand density index (SDI) and LAI was developed at the Jackson Demonstration State Forest (Berrill and O'Hara, 2007). Forest inventory data related basal area with SDI (Webb, 2019) allowing LAI to be interpreted for target basal areas in the South Fork Harvest.

Table 3.8: **Sub-Watershed Harvest Scenario LAI Values.** Leaf Area Index used in DHSVM simulations of the Phase Three Harvest of the South Fork of Caspar Creek. Information adapted from Jackson Demonstration State Forest (Webb, 2019).

Sub-watershed	**Pre Harvest LAI**	**Post Harvest LAI**
Olgavie	7.0	4.0
Porter	7.2	5.5
Treat	8.1	5.4
Uqlidisi	6.7	3.2
Ziemer	8.1	2.1
Sequoyah	7.9	3.0
Matrix around watersheds	7.0	3.5
Richard (no harvest)	7.0	7.0
Williams (no harvest)	7.0	7.0
Yocum (no harvest)	7.0	7.0

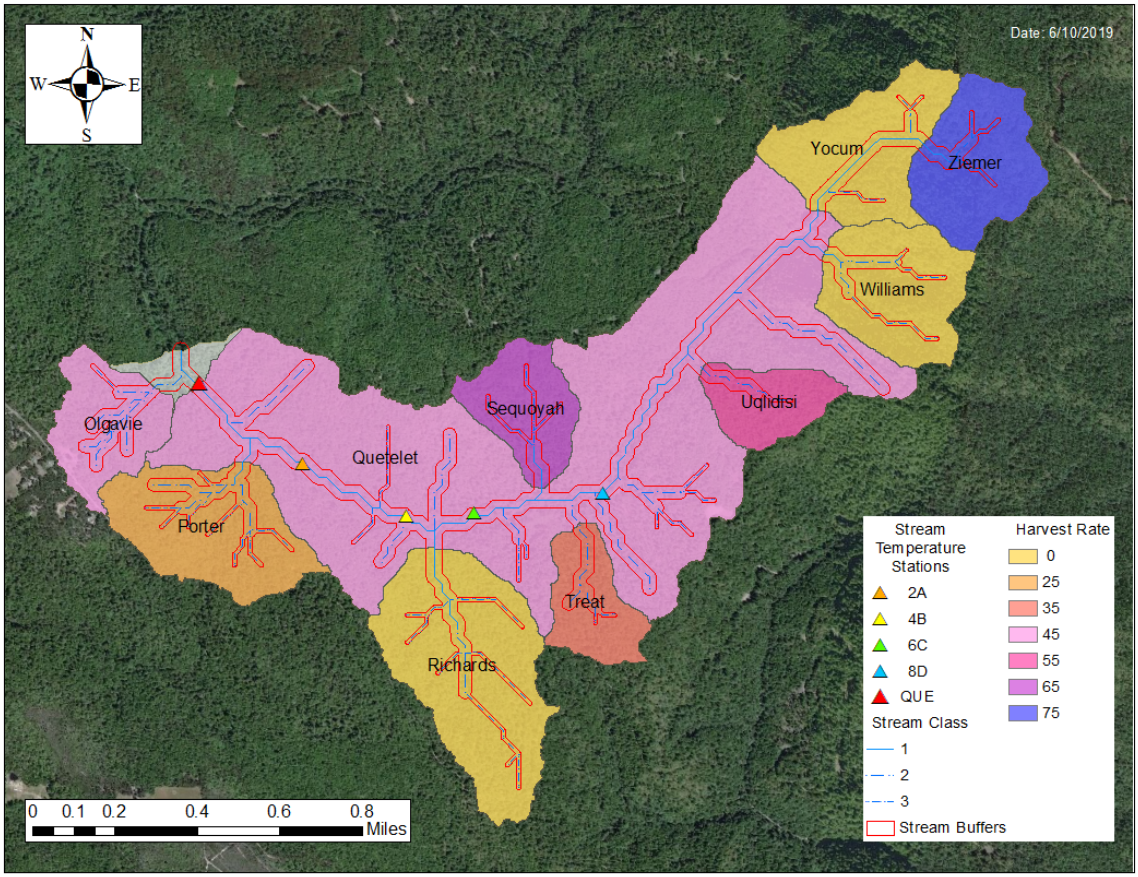

Figure 3.9: **Harvest Map.** Map of the percent reduction in basal area used for each sub-watershed in the harvest simulation.

3.5.3 Riparian Vegetation Conversion

The last scenario modeled was to investigate the impact of clearing riparian vegetatio in isolated stream reaches for conversion from one dominating vegetative species to another. Agencies such as the Washington State Department of Natural Resources outline riparian management strategies like this scenario that attempt to restore conifer dominated riparian areas (Bigley and Deisenhofer, 2006). There has been success at releasing suppressed conifers in riparian areas using patch cutting and thinning in Oregon (Maas-Hebner et al., 2005; Emmingham et al., 2000). Additionally, a study in Lassen National Forest sought to restore aspen stands for habitat and

ecosystem services (Jones et al., 2013). Therefore, we sought to model the effect of completely clearing approximately 300-yard reaches to evaluate the potential effect these extreme riparian modification designs have on water temperature. Figure 3.10 illustrates the two reaches along the main stem of SFC. Reach 1 is approximately 303 yards in length and reach 2 is approximately 352 yards. The tree height, monthly extinction coefficient, overhang and canopy bank distance were set to zero. Temperature differences between the segments directly upstream and below the reach were evaluated.

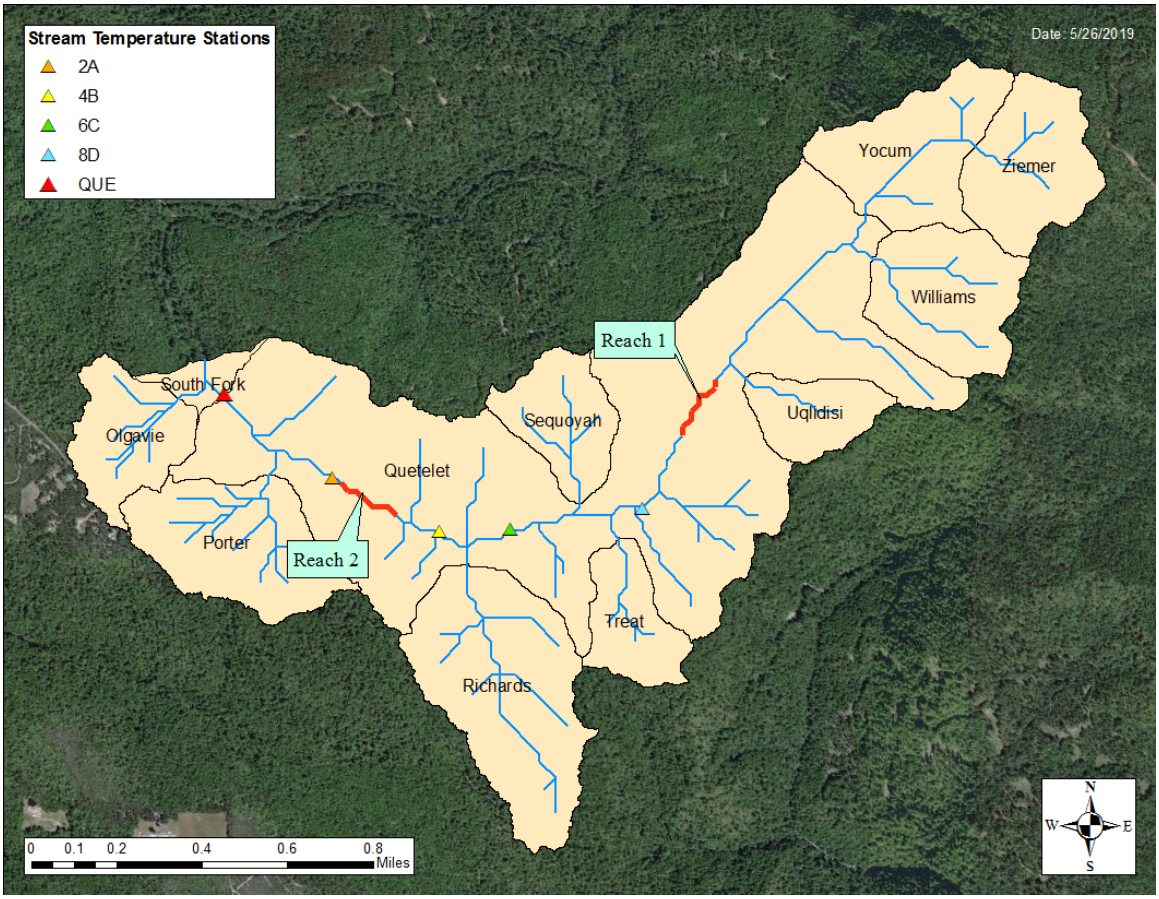

Figure 3.10: **Riparian Vegetation Conversion Map.** Map of the reaches used to evaluate riparian clearing for conversion of dominating vegetative species.

3.6 Sensitivity Analysis

To assess RBMs sensitivity and uncertainty three different analyses were completed. The first, evaluated RBM's sensitivity to each of the modifiable riparian characteristics. To do this, each variable was incrementally reduced and/or increased, while all other riparian characteristics were held at their initial, third-growth values. Table 3.9 outlines the modifications used for each variable.

The second valuation discerns RBMs sensitivity to the air temperature and relative humidity inputs used in the initial DHSVM meteorological files. For this, Caspar collected air temperature and relative humidity values were replaced with those from CIMIS station #103, located in Blithe, California (Figure 3.11).

Figure 3.11: **Blithe, CA Comparison Map.** Where Blithe, CA is located in relation to the Caspar Creek watershed.

This station was chosen because of the consistently high heat and dry conditions Blithe experiences, with an average annual air temperature of 21.5°C and relative humidity of 52% from 2011-2016. Of the 62,832 total hours, 357 hours (0.57%) for air temperature and 344 hours (0.54%) for relative humidity values had to be filled in using linear interpolation or direct readings from the hour before.

The third sensitivity analysis gauges RBMs ability to predict water temperatures at upstream segments. To do this, measured stream temperatures from the CDFW

stations located at various points along the main stem were used (Figure 3.1) . Without altering the calibration parameters used in all other analyses, MWAT and MWMT estimations at the stream segment closest to each CDFW station were evaluated.

Table 3.9: **Sensitivity Analysis Parameters.** Increases and decreases used to assess the sensitivity RBM exhibits to each adjustable riparian characteristic.

Riparian Variable	**Reductions**	**Increases**
Tree Height	50%, 0%	-
Monthly Extinction Coefficient	50%, 0%	-
Overhang Coefficient	50%, 0%	-
Buffer Width	50%, 25%	-
Canopy Bank Distance	0.1 m	5 m, 9 m
Channel Width	50%	x2, x4

Chapter 4

Results

4.1 DHSVM

The NSE and EREL metrics for DHSVM simulated streamflow for the calibration and verification time periods are shown in Table 4.1. Additionally, hydrograph comparisons illustrating DHSVM simulated to SFC measured streamflow are included in Figure 4.1. These values are within those of other studies using DHSVM, such as Cao et al. (2016) where NSE values ranged from 0.54 - 0.82 for daily streamflow and Wenger et al. (2010) where the median NSE for simulations of daily flows at 55 US Geological Survey stations was 0.43.

Table 4.1: **DHSVM Statistical Fit.** Statistical fit for calibration and verification periods for DHSVM simulated streamflow 2011-2016 to measured streamflow for SFC and RIC watersheds. Metrics are Nash Sutcliffe Efficiency (NSE) and Relative Efficiency (EREL).

Period	**SFC**		**RIC**	
	NSE	**EREL**	**NSE**	**EREL**
Calibration 2011-2013 HY	0.79	0.93	0.65	0.95
Verification 2014-2016 HY	0.79	0.80	0.68	0.94

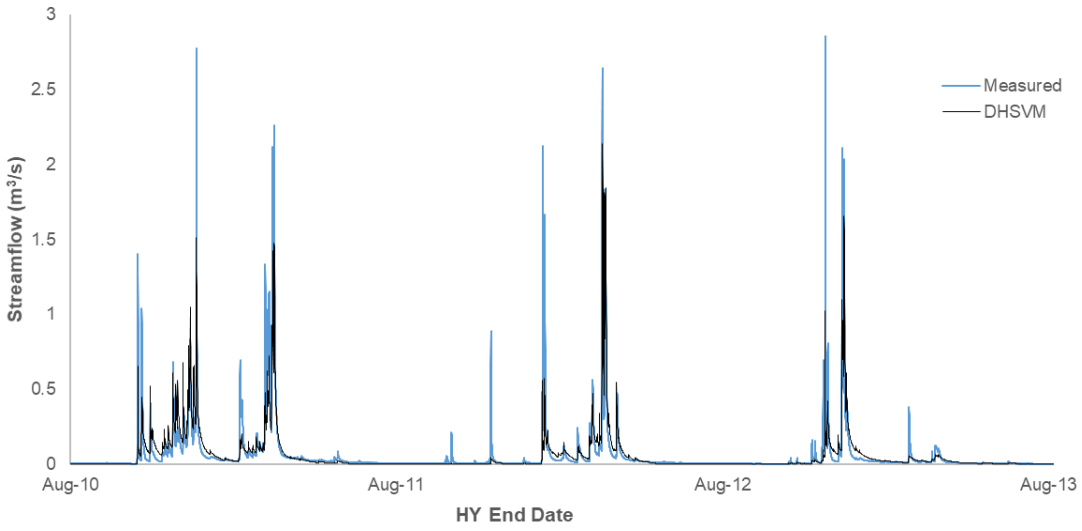

(a) Calibration Period

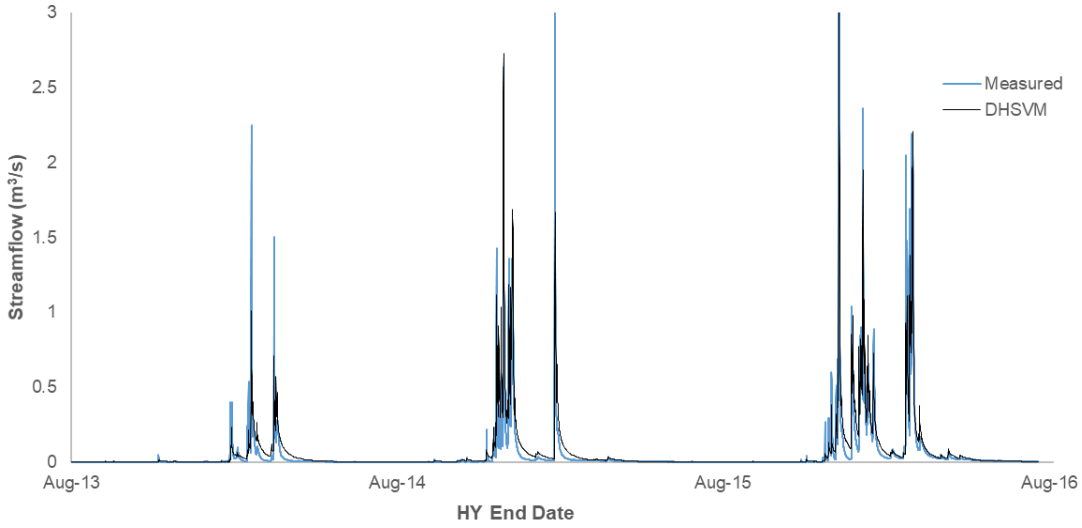

(b) Verification Period

Figure 4.1: **DHSVM Calibration.** Comparison between DHSVM simulated and measured streamflow for SFC (a) calibration period, 2011-2013 HY, and (b) verification period, 2014-2016 HY.

4.2 RBM

Although larger discrepancies between measured and simulated values occurred during winter simulations, RBM was able to capture the time period of concern (May-September) well. NSE values for RBM during the summer period were slightly lower than those of DHSVM flow results. Overall 3-hour simulations resulted in NSE values of 0.50 and 0.61 for the calibration and verification periods, respectively. When aggregated, MWAT NSE values increased (0.69, 0.65 for calibration and verification periods), while MWMT values increased during the calibration period, but decreased for the verification period (0.73 and 0.34, respectively). RMSE values ranged between 0.682 and 1.01°C between the three different categories. Comparing measured and simulated MWAT results for each year, simulations for 2015 were the closest to measured values, slightly under-predicting MWAT values (-0.18) and no difference between measured and simulated MWMT values. Simulations for 2011 were farthest away from measured results, with a 1.04°C difference between MWAT values and 0.82°C difference between MWMT values.

With the 3-hr aggregated output it can be seen that RBM was not able to fully capture the diurnal fluctuations for Caspar Creek, indicating that daily maximum and minimum temperatures were not accurately reproduced (Figure 4.2). For all three calibration summaries, it can be seen that a greater deviation between simulated and measured values tended to occur during the winter temperatures. However, this is in part because the model was specifically calibrated for the May to September time periods. For the MWMT results, RBM underestimated the initial peak summer temperatures during the verification period, appearing to estimate the peak summer temperatures better later in the season. RBM did a better job at correctly predicting these phases when evaluating MWAT values, again highlighting the inability to fully capture daily fluctuations completely.

Figures 4.2a, 4.2b and 4.2c exhibit the best fit model to measured stream temperatures at the QUE station for the entire modeled time frame, with a zoom in of May through September 2013 to provide a detailed view. NSE and RMSE values are included within each figure. Tables 4.2 and 4.3 display the calculated MWAT and MWMT values for measured and simulated results between May and September 2011-2016.

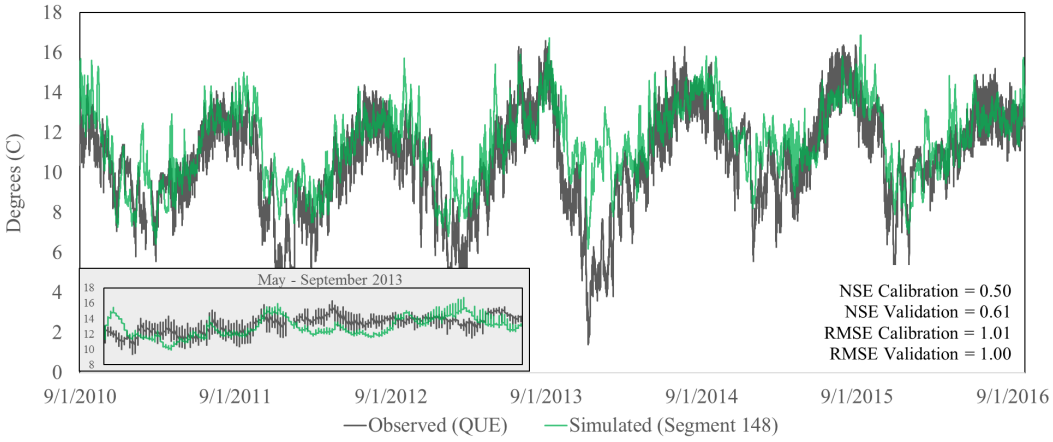

(a) 3-hr interval

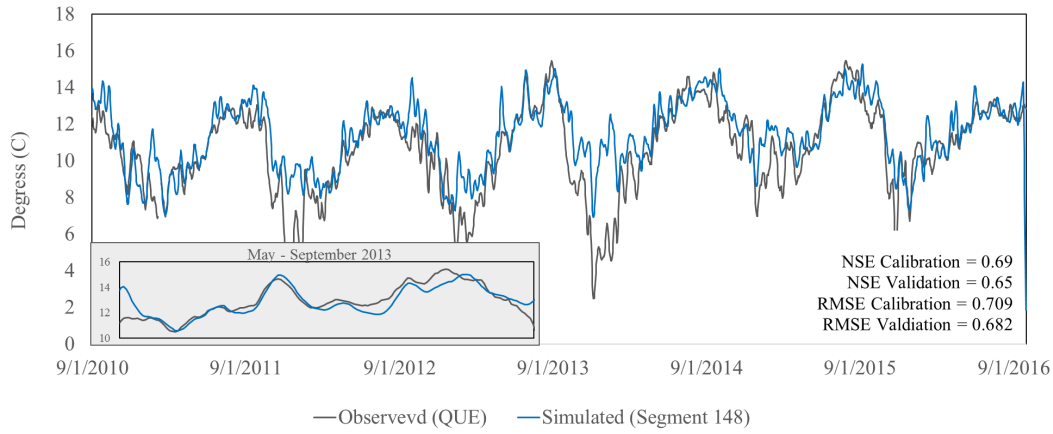

(b) MWAT

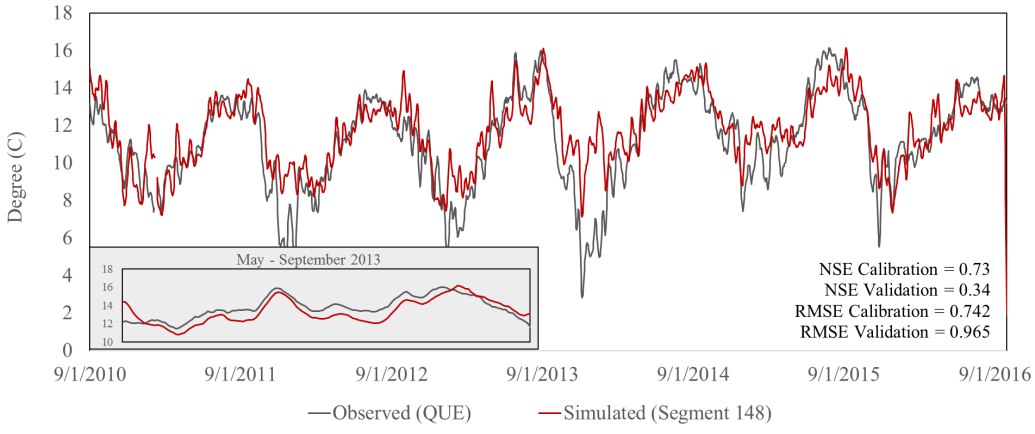

(c) MWMT

Figure 4.2: **RBM Calibration.** (a) Measured and simulated stream temperatures at a 3-hour timestep for the outlet of SFC. Resulting MWAT (b) and MWMT (c) values for measured and simulated stream temperatures.

Table 4.2: **MWAT Results.** MWAT values calculated from measured and simulated water temperatures from May-September 2011-2016.

	2011	**2012**	**2013**	**2014**	**2015**	**2016**
Measured MWAT	13.09	12.93	15.46	14.83	15.46	13.38
Simulated MWAT	14.14	13.27	15.03	14.58	15.28	14.31
Difference	1.04	0.34	-0.43	-0.25	-0.18	0.93

Table 4.3: **MWMT Results.** MWMT values calculated from measured and simulated water temperatures from May-September 2011-2016.

	2011	**2012**	**2013**	**2014**	**2015**	**2016**
Measured MWMT	13.67	13.93	16.00	15.51	16.14	14.59
Simulated MWMT	14.49	13.65	16.14	15.13	16.14	14.66
Difference	0.82	-0.28	0.14	-0.39	0.00	0.08

4.3 Modeling Scenarios

4.3.1 Canopy Reduction

Buffer area vegetation were reduced along only Class I streams (Figure 4.3) and then again along all three streams classes (Figure 4.4). The maximum MWAT and MWMT results for each year were calculated and plotted. Solid lines are used to represent when canopy cover was reduced within the buffer area, but third-growth vegetation conditions were held throughout the rest of the watershed. Dotted lines are used for scenarios where both the watershed and buffer area vegetation were modified to the designated amount.

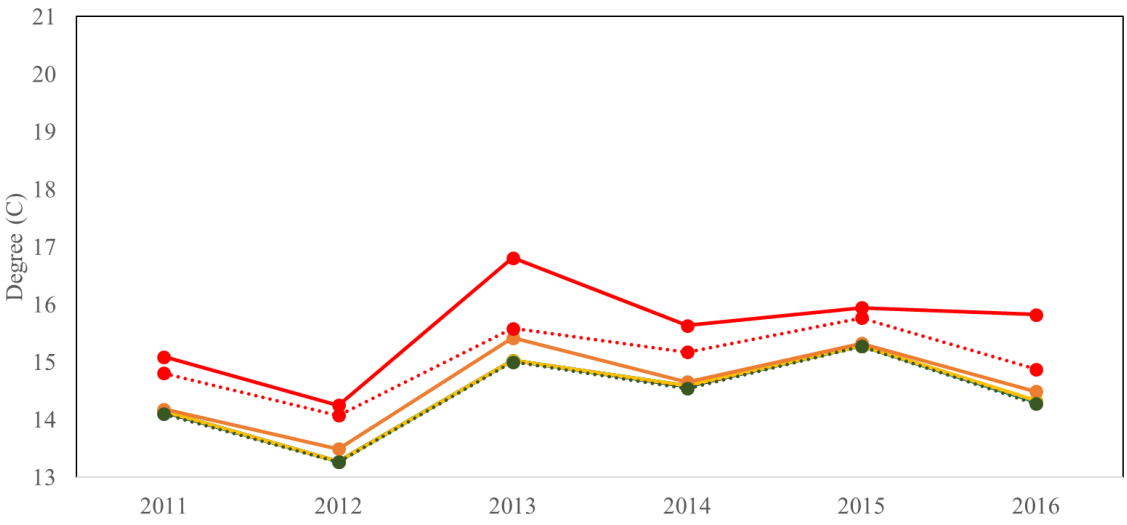

(a) MWAT

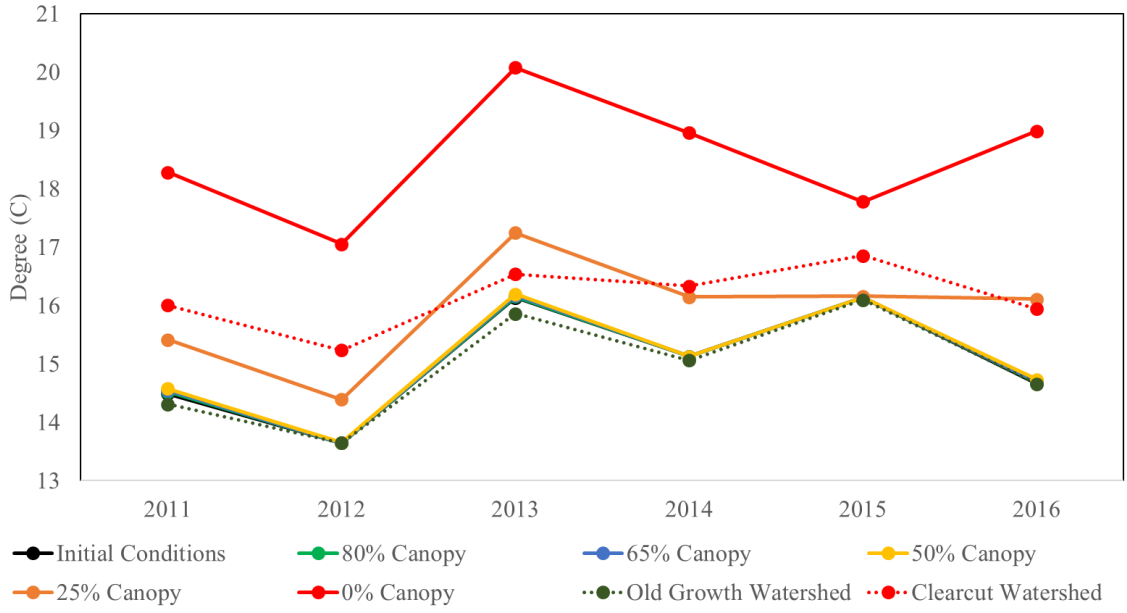

(b) MWMT

Figure 4.3: **Canopy Reduction - Class I Streams Only.** (a) Simulated MWAT and (b) MWMT temperature results for the SFC mainstem outlet, when reducing canopy cover in only class I streams. Solid lines use pre-harvest, third-growth vegetation conditions across the watershed, with varying canopy cover in the buffer areas. Dashed lines alter both the watershed and buffer area vegetation.

When altering only class I streams (Figure 4.3) a noticeable change in temperature is not seen until riparian conditions are reduced to 25% of the initial, third-growth conditions. At this reduction level the change in MWAT values above initial, third-growth conditions range from 0.04 to 0.40°C and average 0.16°C across the six years evaluated. At 0% riparian cover, which simulates clear cutting all class I streams, the increase in MWAT values range from 0.67 to 1.79°C, with an average increase of 1.16°C. There is a wider range of increases in temperature above initial conditions when evaluating MWMT results for the 25% retention level, with a range of 0.02 to 1.45°C and an average of 0.88°C above initial conditions. At the 0% retention level, the increase in MWMT values range from 1.64 to 4.33°C and average 3.49°C.

There was a larger increase in MWAT and MWMT temperatures when all stream segments had canopy reductions (Figure 4.4). Again, no significant changes were detected until the 25% and 0% scenarios occurred. At the 25% retention level, MWAT increases range from 0.07 to 0.44°C and average 0.19°C, while MWMT increases range from 0.07 to 1.61°C and average 1.03°C. For the 0% reduction scenario, MWAT increases range from 0.93 to 2.03°C and average 1.42°C, whereas MWMT increases range from 2.40 to 4.92°C and average 4.14°C.

Because the old growth and clearcut scenarios affect the entire watershed, the results for these scenarios in Figure 4.3 and Figure 4.4 are the same. For the clearcut scenario, MWAT values were 0.49 to 0.80°C above initial, third growth values and averaged a 0.61°C increase. MWMT increases ranged from 0.40 to 1.59°C and averaged 1.12°C above initial conditions. For the old growth scenario, MWAT values decreased below initial condition values between 0.01 to 0.04°C, with an average decrease of 0.02°C. MWMT values decreased between 0.01 to 0.27°C, averaging a 0.10°C decrease.

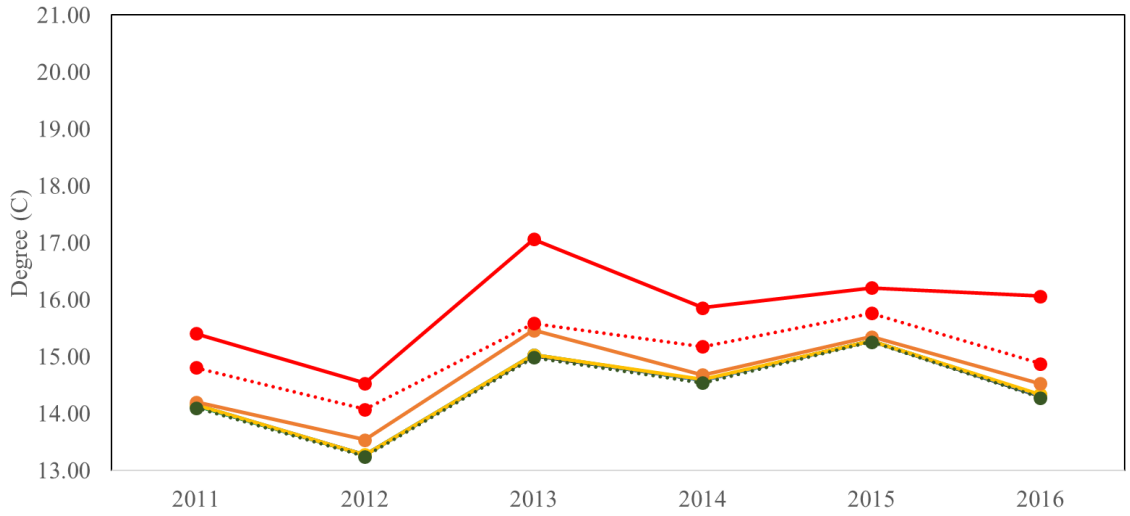

(a) MWAT

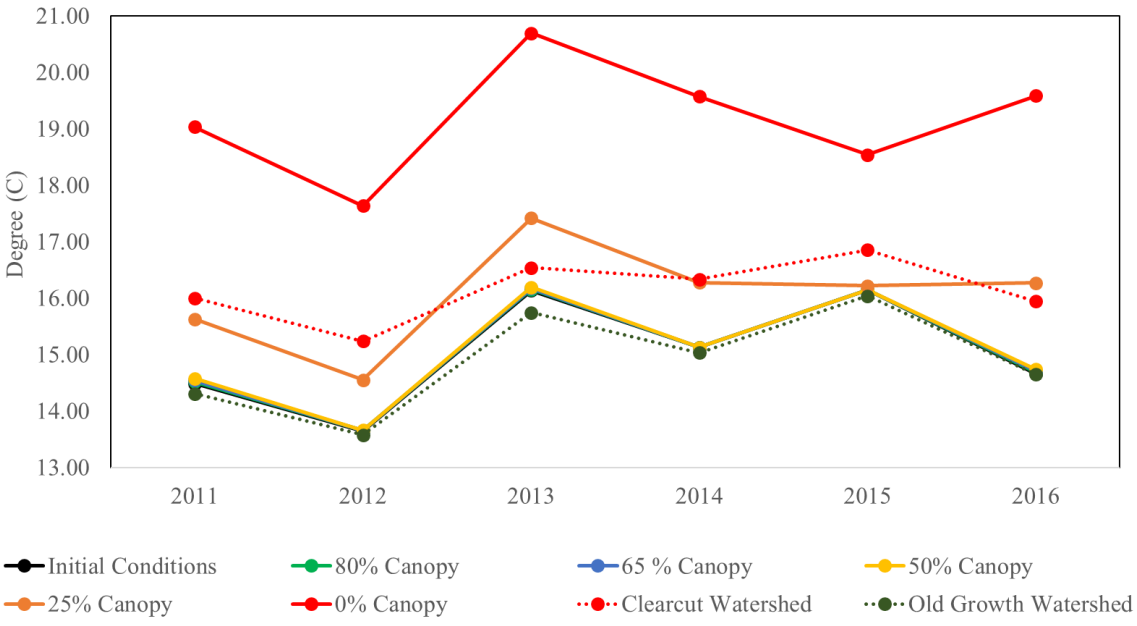

(b) MWMT

Figure 4.4: **Canopy Reduction - All Stream Classes.** (a) Simulated MWAT and (b) MWMT temperature results for the SFC mainstem outlet, when reducing canopy cover in all stream classes. Solid lines use pre-harvest, third-growth vegetation conditions across the watershed, with varying canopy cover in the buffer areas. Dashed lines alter both the watershed and buffer area vegetation.

Because the values for altering only class I segments and altering all class segments were similar, only the average change in MWAT and MWMT temperatures for each reduction scenario when modifying all stream segments was graphed (Figure 4.5). The largest difference occurred when the buffer was reduced to 0% canopy, but third-growth conditions were left in the rest of the watershed.

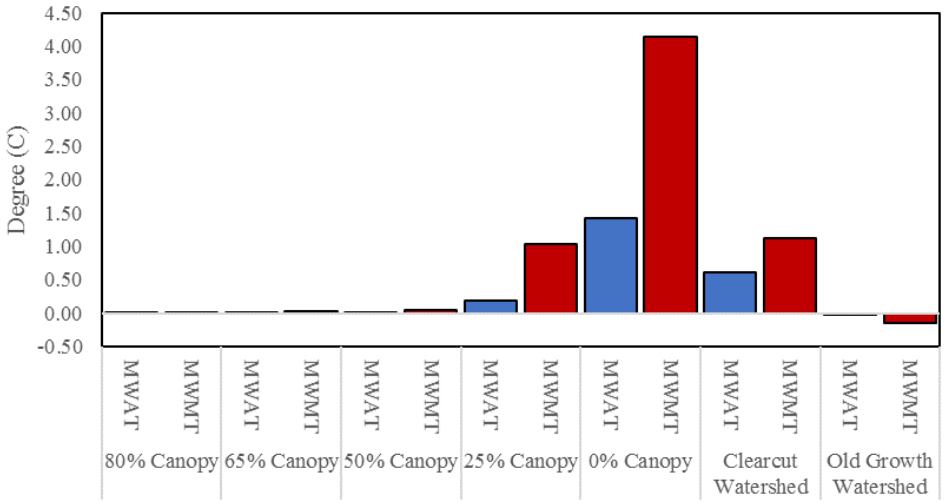

Figure 4.5: **Canopy Reduction - Change in Temperature.** Average MWAT and MWMT temperature (°C) differences between each canopy reduction scenario, when all stream classes are reduced and initial, third-growth conditions are used.

4.3.2 SFC Phase Three Harvest Scenario

For the Phase Three harvest scenario the difference between yearly MWAT and MWMT values for pre and post harvest conditions were calculated (Figure 4.6). On average, there was a 0.11°C increase in MWAT values and a 0.32°C increase in MWMT values. From year to year, MWMT values varied more than MWAT values (MWMT: 0.14-0.53°C; MWAT: 0.10-0.12°C). The larger difference for HY 2013 is believed to be a result of the spikes in both observed and simulated stream temperatures and that average air temperatures measured between May and September were the third largest (14.2°C) in 2013, while precipitation was the second lowest (36.4' in the HY).

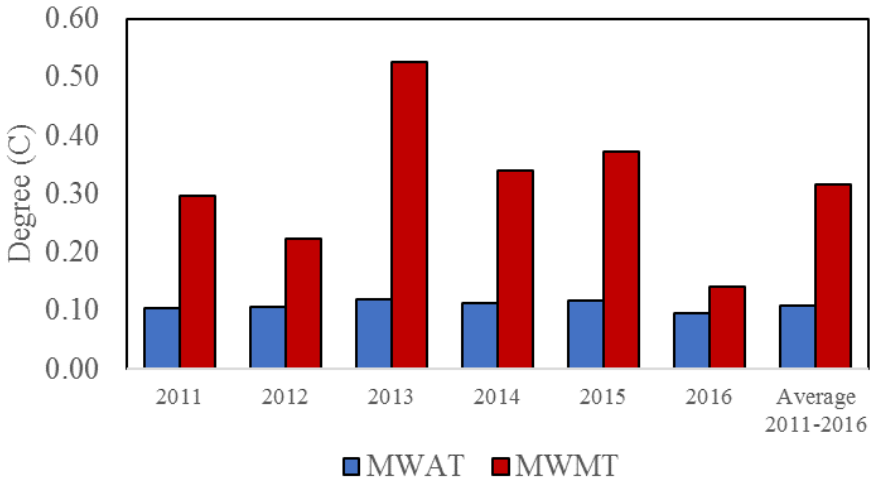

Figure 4.6: **Harvest Scenario.** Temperature (°C) differences between pre and post harvest conditions for MWAT and MWMT values.

4.3.3 Riparian Vegetation Conversion

When clearing of riparian vegetation along the 300-m segment was simulated, RBM predicted an increase in stream temperature of 0.72°C for MWAT and 1.88°C for MWMT. Further down the stream network at Reach 2, RBM predicted similar increases in MWAT and MWMT when riparian clearing occurred, 0.86°C and 2.87°C, respectively. However, for this reach (Reach 2) when no vegetation change occurred RBM predicted a slight increase in water temperature. Whereas, RBM predicted a slightly lower stream temperature at Reach 1. Figure 4.7 depicts the difference between simulated temperatures directly above and at the bottom of each stream reach using initial riparian conditions and simulating clearing.

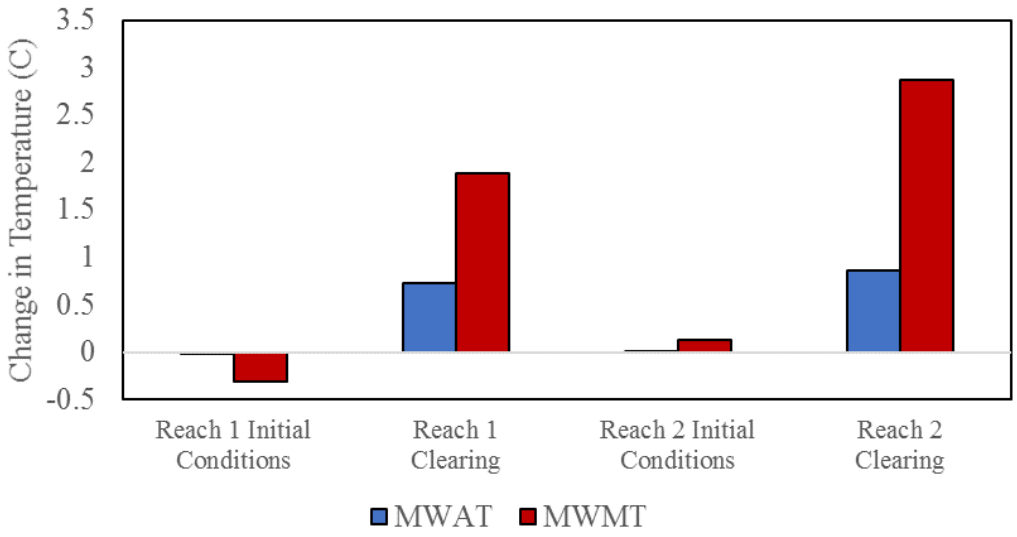

Figure 4.7: **Riparian Vegetation Conversion.** Temperature (°C) difference when clearing stream reaches to simulate converting alder dominated to conifer dominated riparian zones.

4.4 Sensitivity Analysis

The first sensitivity analysis completed evaluates the impact that each of the modifiable RBM vegetation characteristics has on stream temperature at the QUE station. For each graph in Figure 4.8 the specified characteristic is either increased or decreased, depending on what was appropriate for the variable. Bars that are solid represent MWAT results, while bars that are the same color, but with strips, represent the MWMT results for that same reduction or increase value.

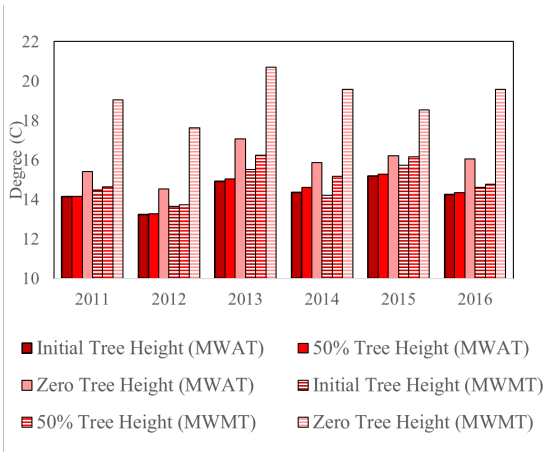

(a) Tree Height

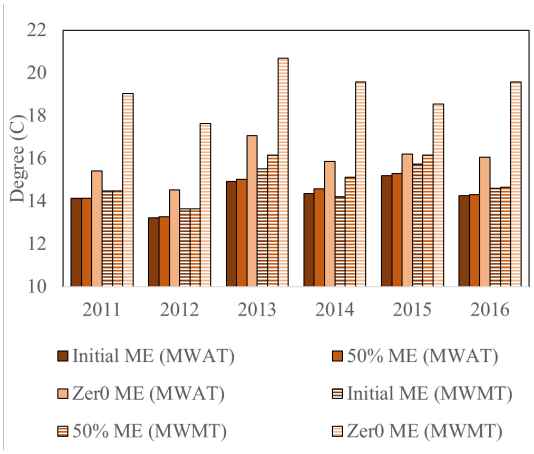

(b) Monthly Extinction Coefficient

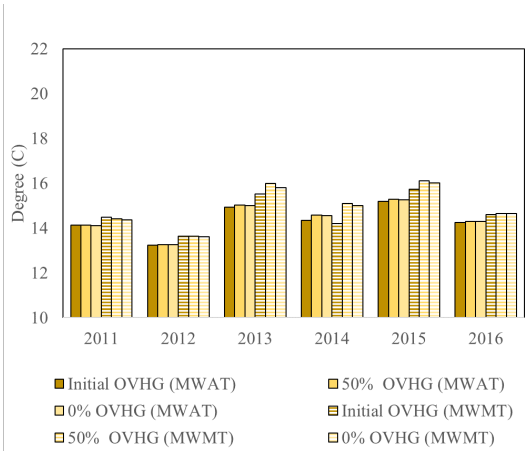

(c) Overhang Coefficient

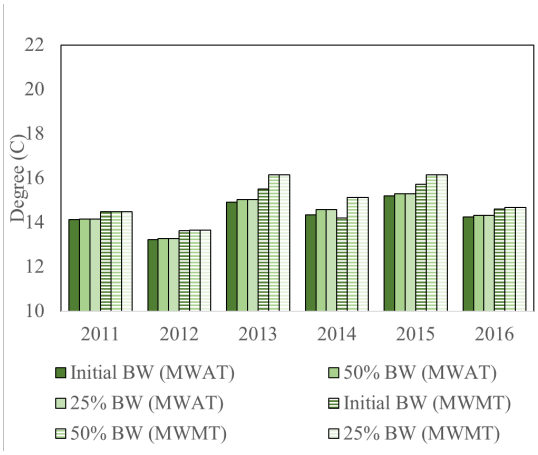

(d) Buffer Width

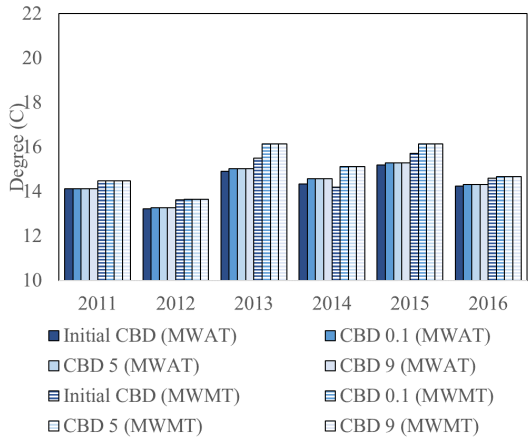

(e) Canopy Bank Distance

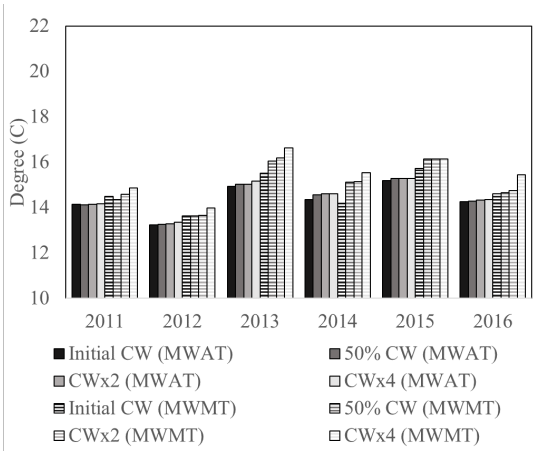

(f) Channel Width

Figure 4.8: **Sensitivity Analysis - Riparian Vegetation Characteristics.** Sensitivity Analysis of adjustable riparian characteristics used in RBM. Bars that are solid represent MWAT results, while bars that are the same color but with strips, represent the MWMT results for that same reduction or increase value.

Reducing tree height or monthly extinction coefficient to zero had the same effect for this watershed, with an average increase of 1.51°C for MWAT and 4.48°C for MWMT across the years. Oddly, RBM predicted slightly lower MWAT and MWMT values when the overhang coefficient was reduced to 50% of initial conditions, compared to when it was reduced to 0% of initial conditions. However, these differences were only on average 0.01°C different for MWAT values and 0.07°C different for MWMT values. Varying the buffer width, canopy bank distance and channel width only produced small differences in MWAT and MWMT results.

The second sensitivity analysis examined RBMs sensitivity to air temperature and relative humidity inputs using values from Blithe, CA CIMIS station (Figure 3.11). Air temperatures and relative humidity estimates between May and September averaged 13.9°C and 78.7%, respectively at SFC. Whereas Blithe air temperature averaged 29.3°C and 49.2% relative humidity. Riparian vegetation was reduced along all stream class segments. Results for MWAT and MWMT predictions are shown in Figures 4.9a and 4.9b, respectively. For both figures, solids lines use South Fork Caspar collected values and dashed lines use Blithe values. On average, the Blithe data increased MWAT values by 3.61°C (range: 2.72-4.96°C) and MWMT values by 3.95°C (range: 3.02-5.61°C) compared to SFC. Year to year variation was low for the Blithe data.

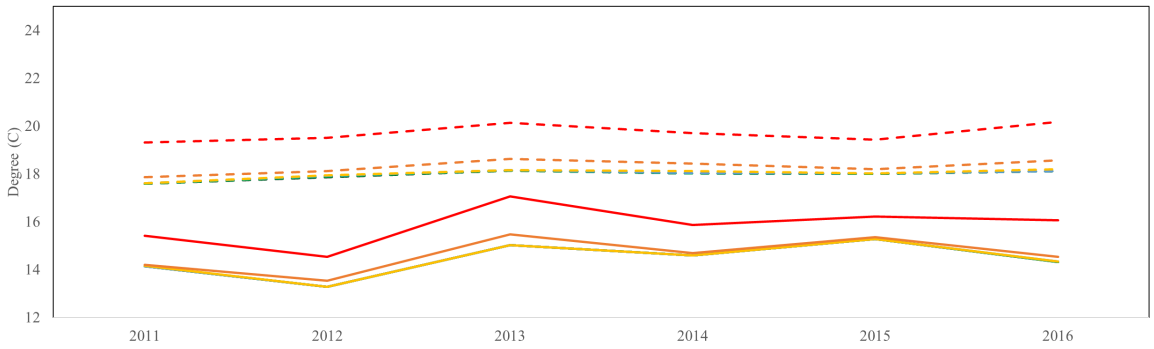

(a) MWAT

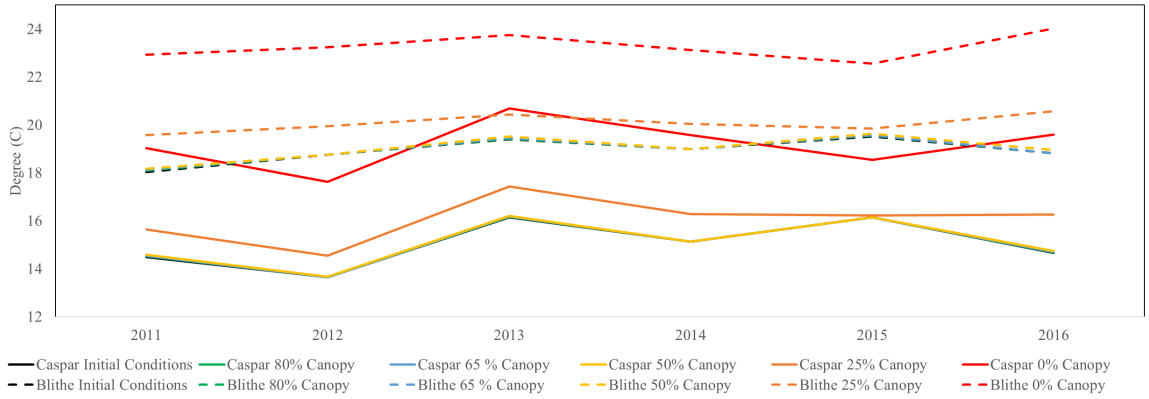

(b) MWMT

Figure 4.9: **Sensitivity Analysis - Air Temperature and Relative Humidity.** Simulated (a) MWAT and (b) MWMT temperatures using SFC or Blithe, CA CIMIS air temperature and relative humidity values. Solid lines use Caspar collected values, while dashed lines use Blithe, CA collected values.

The third sensitivity analysis evaluates RBMs ability to predict temperatures at upstream locations along the South Fork of Caspar Creek. For this, measured temperature readings from the CDFW stations (2A, 4B, 6C and 8D, Figure 3.1) are compared to simulated estimations at the closest corresponding RBM segment. MWAT values are displayed in Figure 4.10a and MWMT values in Figure 4.10b. Solid lines represent measured values, while dashed lines of the same color correspond to the RBM segment closest to that temperature station.

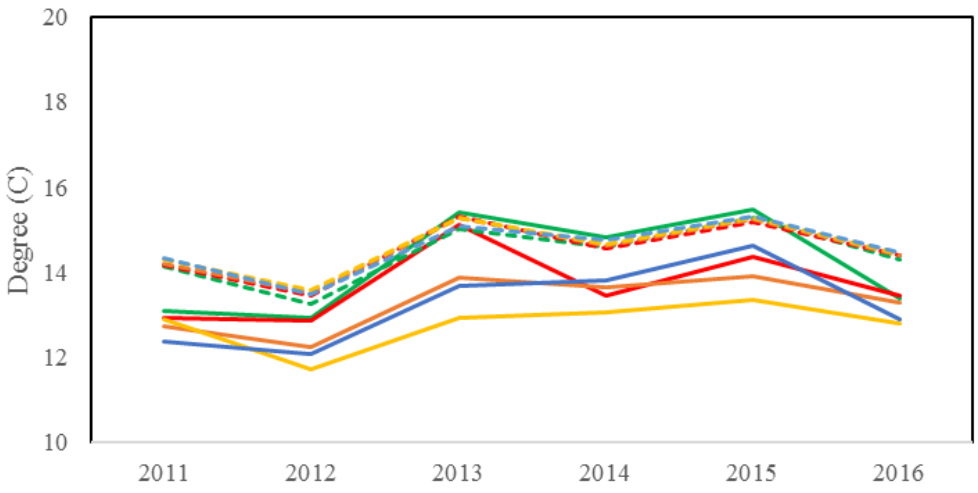

(a) MWAT

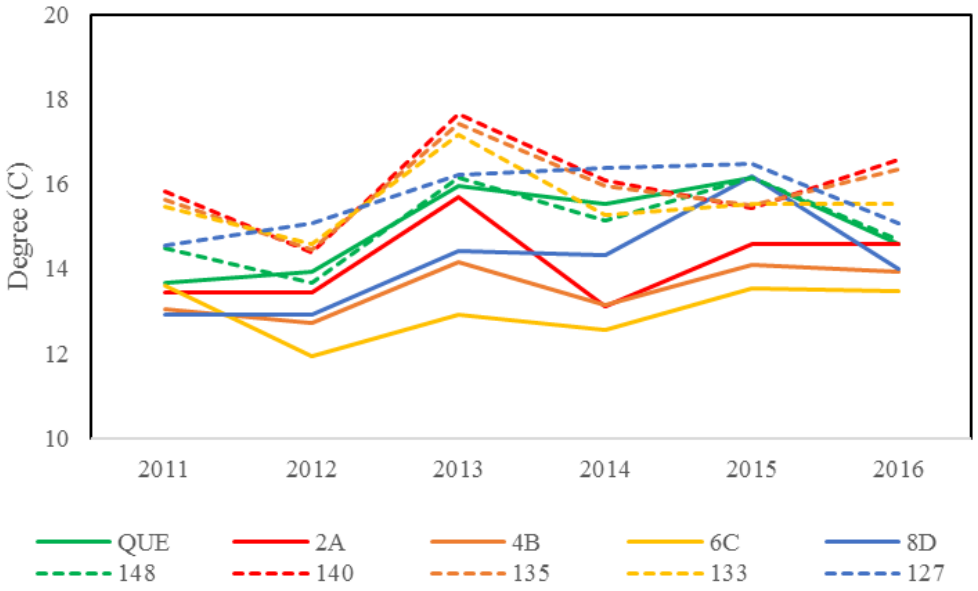

(b) MWMT

Figure 4.10: **Sensitivity Analysis - Upstream Stations.** Simulated and measured (a) MWAT and (b) MWMT temperatures for various stream temperature stations located throughout the SFC stream network (Figure 3.9 and 3.10).

From this, we can see that RBM does not accurately capture the expected decreasing trend in MWAT water temperature seen in measured temperature stations going up the stream network. Instead, RBM predicts consistent MWAT temperatures

along the stream network. For MWMT results, RBM appears to over estimate upstream temperatures, but somewhat captures the decreasing trend measured between stations 2A, 4B and 6C, although not nearly as much as as in measured temperatures.

Chapter 5

Discussion

Because water temperature is the primary focus of this report, a discussion for the DHSVM calibration results is not included.

5.1 RBM Calibration

Calibration results for SFC are in line with those of other studies using RBM. Brennan (2015) obtained a combined NSE value of 0.721 using VIC-RBM for the Connecticut River. Truitt (2018) found NSE values of 0.89, 0.86, and 0.64, respectively, for the South, North and Middle forks of the Nooksack River Basin in Washington State. Sun et al. (2015) calibrated RBM to an NSE of 0.90 for the lowest streamflow quartile and also estimated the largest differences between measured and simulated temperatures during winter (overestimating measured readings). RMSE for Perry et al. (2011) work evaluating potential dam removal had RMSE values between 0.8 and 1.5°C for the calibraiton period and 0.8 to 1.4°C for the verification period. Lastly, RMSE values for twelve basins modeled by Cao et al. (2016) ranged between 0.63 and 1.92°C, with similarly lower model performance in the verification period

compared to the calibration period. Therefore, although SFC calibration results are on the lower spectrum, it suggests that RBM estimations are within a reasonable range.

Most of the works above attribute inaccuracies to estimations of the amount and timing of meltwater inputs. For SFC, it is hypothesized that groundwater inputs and soil pipe flow are largely contributing to the discrepancies between measured and simulated values for both streamflow and stream temperatures. Additionally, discrepancies may be a result of uncertainty in the meteorological forcing files; coefficients used to estimate river hydraulic properties (Leopold coefficients); the use of simulated flows (DHSVM); that riparian vegetation is assumed to be uniform on both sides of the stream network and have no effect on streamflow; that turbidity influences on solar gain and fog drip known to occur at Caspar Creek (Henry, 1998) are not taken into account; and the potential effect of microclimate differences throughout the watershed. Furthermore, estimating water temperature in a system with a measurement device, such as a thermistor, is impossible to do without some degree of uncertainty. This arises from inherent error in the measurement device, sampling error or mapping of point observations to block (areal or volume) predictions (Yearsley, 2009). Data collection errors for both input and comparison data may also be adding to differences between model simulations and measured readings.

Furthermore, Arismendi et al. (2014) concluded the Mohseni model does not accurately predict stream temperatures over long periods of time or work well to extrapolate future predictions due to the non-stationary relationship between air and stream temperatures over time. Our need to significantly reduce the Mohseni variables are similar to studies who observed a better fit using variables calculated from headwater segments, rather than those on the main stem or at lower elevation tributaries Truitt (2018). For these reasons, the Mohseni variables may also be contributing to the discrepancies between model simulations and measured recordings.

5.2 Modeling Scenarios

5.2.1 Canopy Reduction

Sun et al. (2015) compared urban riparian vegetation to 1883 forested vegetation in the Mercer Creek watershed in Washington state, which was similar to those used in our third-growth, initial conditions. They found that average annual peak stream temperatures generally decreased by about 4°C, when using the 1883 vegetation, for the basin outlet. Similarly, Cao et al. (2016) modeled 1883 and 2002 vegetation covers for both basin-wide and riparian only modifications in the Puget Sound Basin of Washington. For the basin wide scenario, they noted changes in summer temperature at various basin outlets ranging between -0.12 and 0.19 °C. However, for the riparian vegetation only scenarios, the changes in summer temperatures ranged from 0.19 to 1.75°C. These are similar to the differences in MWAT and MWMT values for the initial-third growth riparian conditions, versus the 25% and 0% canopy cover reduction scenarios, as well as the old growth scenario. This corroborates the conclusion of the importance of riparian vegetation in moderating stream temperatures.

Hines and Ambrose (2000) studied six coastal watersheds in the northwestern portion of Mendocino County, to determine stream temperature thresholds for juvenile Coho salmon rearing. He concluded that the best single threshold to predict Coho salmon presence and absence is an MWAT of 17.6°C. A second study conducted on the Mattole River, just north of Caspar Creek, found that tributaries with juvenile coho salmon presence was limited to MWAT and MWMT values less than 16.7°C and 18.0°C (Welsh et al., 2004). The RBM simulations for SFC show only one year, with 0% canopy retention, that exceeded the MWAT thresholds. However, all but one of the MWMT estimates exceeded 18.0°C at the 0% retention level. Additionally, Hines and Ambrose (2000) strongly caution against the use of a single value to predict such complex phenomenons as salmonid presence.

Moore et al. (2005) observed an approximately 5°C increase in daily maximum temperatures downstream of a clear-cut harvest in a coastal headwater stream in British Columbia. For Johnson and Jones (2000) a 7°C increase in daily maximum stream temperatures in the western Cascades of Oregon was seen. The high change was attributed to influence from conductive heat transfer from a dark bedrock substrate. RBM did not predict as high of an increase for Caspar Creek. However, at the 0% canopy retention level increases were on average 4.14°C above baseline conditions. Under state law incoming waters cannot raise receiving water temperature by more than 5°F (2.78°C), meaning the scenario would exceed this limit.

Clearcutting the entire watershed was simulated to produced less of an increase in MWAT and MWMT values, than reducing just the riparian area to 0% canopy retention. It likely is attributed to the decrease in ET and subsequent increase in water yield following the basin-wide clearcut, which is consistent with globally recognized effects of harvesting (Buttle, 2011).

5.2.2 SFC Phase Three Harvest Scenario

The removal of riparian vegetation has been recognized to increase solar radiation, wind speed and exposure to advected energy from nearby harvested areas, thus increasing water temperatures (Moore et al., 2005). However harvesting can also increase the discharge of groundwater. Increases in groundwater discharge may lessen impacts to stream temperatures, depending on the influence the harvest has to potentially warming shallow groundwater or the hyporheic exchange of surface and subsurface waters (Buttle, 2011). Average MWAT increases of 0.11°C and 0.32°C for MWMT were estimated following the harvest simulation. Both of these values are under the maximum 2.78°C increase in cold water systems allowed under state law. Additionally, the average MWAT and MWMT estimates (14.5°C and 15.4°C, re-

spectively) were below thresholds for Coho and Steelhead species (Eaton et al., 1995; McCullough et al., 2001; Sloat and Osterback, 2013; Welsh et al., 2004).

The average 0.11°C change in MWAT and 0.32°C change in MWMT values, are similar to those of Cao et al. (2016) who used DHSVM-RBM in the Puget Sound area. For that study, it was found that basin-wide land cover changes affected stream temperature less than 0.2°C in both summer and winter seasons. This is similar to the harvest and clearcut scenario in this report, which suggest that increases in baseflow volume following a loss of ET help to mitigate the impacts of a decrease in riparian cover. However, the temperature changes were lower for the harvest scenario, compared to the $\leq$ 50% canopy retention, we can assume that the FPR WLPZ requirements mitigated impacts to stream temperature.

Overall, model results suggests there will be a slight increase in MWAT and MWMT stream temperatures following the actual SFC harvest. Stream temperature was not collected after selective harvesting occurred in SFC in the early 1970s. However, summer maximum and average daily high temperatures in an uncut tributary basin for the North Fork were 2.8°C lower than those in the clearcut mainstem that used buffer strips on both sides (Cafferata, 1990). But further down the mainstem of the North Fork, summer maximums were found to only be 15.6°C, suggesting that waters were diluted with cooler water from three uncut tributaries below the clearcut. These findings suggest that because of the location of QUE at the end of the mainstem, as well as the mix of harvest rates, RBM is within a somewhat expected range for what may occur following harvest in the South Fork. However, these estimations should be validated and/or disputed using measured stream temperatures in the future.

5.2.3 Riparian Vegetation Conversion

In 1967, following road building at SFC, researchers recorded increases of 1.7 to 2.2°C in areas "where water flowed from shaded to open areas" two years after the road was built (Cafferata, 1990). However, it was not noted how long these distances were, making it difficult to compare to our riparian vegetation conversion scenario. Overall, the conversion scenario suggest approximately 0.5°C increase in MWAT values and a 2.5°C increase in MWMT values, moving from the top to the bottom of the cleared 300-yard reach. However, these results are in question for two reasons.

The sensitivity analysis evaluating RBMs ability to predict upstream temperatures using CDFW stream temperature stations suggest that RBM did not accurately predict temperatures in upstream segments for SFC. Temperatures for the stream segment immediately following the clearing were back to identical readings of those directly above the clearing. RBM may be doing little to track water particles downstream and instead is predicting temperatures directly based on riparian conditions.

5.3 Sensitivity Analysis

Each adjustable riparian variable for RBM was reduced and/or increased to assess their sensitivity in the South Fork model. Overall, tree height and monthly extinction coefficient were shown to be the most influential. These results agree with those of DeWalle (2010), who also found buffer height and extinction coefficient to be crucial to stream shading using a model developed to predict the transmission of potential solar beam radiation (PSBR). He suggests that to increase maximize stream shading, emphasis should be placed on promoting dense, tall riparian areas, as opposed to focusing on wider buffer widths. Additionally, he found that for E-W streams (Caspar's

orientation), buffer widths above 6-7 m did not provide any additional shading due to shifts in solar beam pathway from the sides to the tops of the buffers. Both of these findings can be generally supported by the findings using RBM in the South Fork of Caspar Creek.

Consistency between the increases in MWAT and MWMT values, when substituting in Blithe, CA air temperature and relative humidity values, support that stream temperature changes are largely attributed to the modifications of downward solar radiation through topography and riparian vegetation. They also show that on a year to year basis, Caspar Creek has much more variable meteorology than other parts of California- cautioning that these results only be applied to similar maritime environments. Lastly, although this substitution was done to evaluate the aforementioned reasons, and additional analyses would need to be completed to better estimate a likely increase, the roughly 3.5 - 4.0°C increase in stream temperatures using Blithe air temperatures that were on average 15.4°C above those measured at Caspar, suggest climate change may affect stream temperature. With initial riparian conditions the Blithe results go over observed MWAT and MWMT thresholds for juvenile Coho salmon presence (16.7°C, 18.0°C) (Welsh et al., 2004). However, the Intergovernmental Panel on Climate Change estimates global warming is likely to reach 1.5°C between 2030 and 2052 if it continues to increase at the current rate (IPCC, 2018). Therefore, current riparian shade levels may be enough to moderate for fish presence.

Finally, RBM did not accurately predict upstream temperatures in the South Fork of Caspar Creek. However, preliminary results from another study currently being done in the South Fork suggest that summer stream temperatures are positively related to elevation, while winter temperatures are negatively related. This reveals that RBM may in fact be doing a reasonable job at predicting the trend in upstream temperatures during the summer period, but that further work would need to be done to assess the affects on winter periods alone. This also supports the hypothesis that

the South Fork is highly influenced by groundwater inputs, which vary with the wet season.

5.4 Limitations and Future Work

The primary limitation to this study was the inability to differentiate between inner, outer and core riparin zones. This required simplification of the true design of buffer area protection zones used in California FPRs; therefore limiting RBMs ability to truly analyze California's modern FPRs. Conjointly, the inaccuracies in predicting daily extremes (i.e. diurnal fluctuations) limit the ability to know the results of extreme warmer and cooler temperatures that are crucial to very sensitive species.

As mentioned, future work should be to compare expected increases in summer stream temperatures following the harvest to those measured in the field. Additionally, researching the trend in segments going up the main stem during winter periods, could better assess if RBM is able to accurately predict stream temperatures for various points along the stream network. DHSVM-RBM has been used to run numerous climate change scenarios in other parts of the United States (Sun et al., 2015; Cao et al., 2016; Brennan, 2015; Truitt, 2018), evaluating this potential effect to maritime dominated areas, where snow melt does not occur, would aid at understanding how these findings may potentially differ with climate change. Additional modeling suggestions include calibrating RBM to warmer environments, evaluate the response to streams of N-S orientation with similar watershed characteristics and assessing the impact of watershed size.

Chapter 6

Conclusion

Intensive datasets collected at the Caspar Creek Paired Experimental Watershed Study allowed for the application of a highly detailed, distributed hydrology-stream temperature model. DHSVM-RBM was calibrated to historical readings to reasonably predict Maximum Weekly Average Temperatures (MWATs) and Maximum Weekly Maximum Temperatures (MWMTs) at the outlet of the South Fork of Caspar Creek. MWAT estimates resulted in NSE values of 0.69 and 0.65 for the verification and calibration periods, respectively. MWMT estimates resulted in NSE values of 0.73 and 0.34 for the calibration and verification periods, respectively. These values are in line with those of other modeling studies (Sun et al., 2015; Perry et al., 2011; Cao et al., 2016; Brennan, 2015; Truitt, 2018), but differences in model fit between calibration and verification periods demonstrate some uncertainty in model precision. Model discrepancies are hypothesized to be primarily a result of inaccuracies estimating groundwater inputs and soil pipe flow, uncertainty in the meteorological forcing files and coefficients used to estimate hydraulic properties and initial headwater temperatures.

The three scenarios addressed were (1) varying the degree of riparian canopy cover, (2) the 2018-2019 SFC forest harvest and (3) an experimental design simulating

a conversion of stream reaches from one dominating vegetative species to another. RBM did not predict substantial changes in stream temperature until reducing buffer canopy to 25% and 0% retention levels, with all but one year for MWMT estimates rising above recommended temperature thresholds for juvenile Coho salmon (Welsh et al., 2004) and state laws requiring increases for incoming waters remain below 2.78°C. RBM estimates that if clearcutting the entire watershed occurs, significant enough decreases in ET and increase in water yield could mitigate increases in MWAT and MWMT values. Overall, these findings support the work of other modeling efforts regarding the importance of riparin vegetation in moderating stream temperatures.

Current 2019 FPR guidelines for WLPZ areas were shown to adequately maintain pre-harvest steam temperatures following the 2018-2019 harvest. However, limitations in modeling the core, inner and outer zones required by California FPRs in areas with anadromous fish highlight a degree of uncertainty. For this scenario, an increase of 0.11°C in MWAT and 0.32°C in MWMT values were estimated, both of which are under the maximum allowable increase in coldwater systems under state law (2.78°C). Additionally, the average MWAT and MWMT estimates (14.5°C and 15.4°C, respectively) are under advised thresholds for Coho and Steelhead species (Eaton et al., 1995; McCullough et al., 2001; Sloat and Osterback, 2013; Welsh et al., 2004). These findings are recommended to be validated and/or disputed with future measured data.

At this time, we cannot say with certainty that DHSVM-RBM accurately predicts upstream temperatures in the SFC, using a calibration set for the outlet of the mainstem. Inaccuracies regarding estimations are again hypothesized to primarily be due to groundwater inputs, soil pipe flow and varying microclimates. Preliminary findings of another study in Caspar Creek show a potentially negative trend between winter stream temperatures and elevation, suggesting future modeling work be done to evaluate winter time periods.

Sensitivity analyses support other modeling efforts in suggesting management officials concentrate on maintaining tall, dense buffers, as opposed to focusing on buffer widths. Buffer width has been shown to be closely related to the orientation of the stream (N-S vs E-W), which may be playing a significant role in these findings and should also be further evaluated. Substitution of considerably warmer air temperature and lower relative humidity values warn of potentially large impacts to stream temperatures in SFC with climate change.

Bibliography

Adriance, A. (2018). *Optimizing the Distributed Hydrology Soil Vegetation Model for Uncertainty Assessment with Serial, Multicore and Distributed Accelerations (MSc thesis)*. California Polytechnic State Unviersity, San Luis Obispo.

Ahlgren, G. (1987). Temperature functions in biology and their application to algal growth constants. *Oikos*, 49(2):177–190.

Allen, P. M., Arnold, J. C., and Byars, B. W. (1994). Downstream channel geometry for use in planning-level models. *Journal of the American Water Resources Association*, 30(4):663–671.

Ames, D. P., Rafn, E. B., Van Kirk, R., and Crosby, B. (2009). Estimation of stream channel geometry in Idaho using GIS-derived watershed characteristics. *Environmental Modelling and Software*, 24(3):444–448.

Arismendi, I., Safeeq, M., Dunham, J. B., and Johnson, S. L. (2014). Can air temperature be used to project influences of climate change on stream temperature? *Environmental Research Letters*, 9(8).

Armour, C. L. (1991). Guidance for evaluating and recommending temperature regimes to protect fish. U.S. Fish and Wildlife Service. Technical Report 22, U.S. Department of the Interior Fish and wildlife Service.

Arvola, T. F. (1976). Regulation of logging in California: 1945-1975.

Beck, M. B. (1987). Water quality modeling: A review of the analysis of uncertainty. *Water Resources Research*, 23(8):1393–1442.

Benyahya, L., Caissie, D., St-Hilaire, A., Ouarda, T. B. M. J., and Bobee, B. (2007). A review of statistical water temperature models. *Canadian Water Resources Journal*, 32(3):179–192.

Berrill, J.-P. and O'Hara, K. L. (2007). Patterns of leaf area and growing space efficiency in young even-aged and multiaged coast redwood stands. *Canadian Journal of Forest Research*, 37(3):617–626.

Beschta, R., Bilby, R., Brown, G., Holtby, L. B., and Hostra, T. D. (1987). Stream temperature and aquatic habitat: fisheries and forestry interactions. In *Streamside managment: forestry and fishery interactions*, pages 191–232. College of Forest Resources, University of Washington.

Beyene, T., Lettenmaier, D. P., and Kabat, P. (2010). Hydrologic impacts of climate change on the Nile River Basin: Implications of the 2007 IPCC scenarios. *Climatic Change*.

Bigley, R. and Deisenhofer, F. (2006). *Implementation procedures for the habitat conservation plan riparian forest restoration strategy*. DNR Scientific Support Section, Olympia, Washington.

Bowling, L. and Lettenmaier, D. (2001). The effects of forest roads and harvest on catchment hydrololgy in a mountainous maritime environment. In Wigmosta, M. S. and Burges, S. J., editors, *Land Use and Watersheds: Human Influence on Hydrology and Geomorphology in Urban and Forest Areas, Volume 2*. American Geophysical Union.

Bowling, L., Storck, P., and Lettenmaier, D. P. (2000). Hydrologic effects of logging in Western Washington, United States. *Water Resources Research*, 36(11):3223–3240.

Brandow, C. A. and Cafferata, P. H. (2014). Forest Practice Rules Implementation and Effectiveness Monitoring (FORPRIEM) Program: monitoring results from 2003 thorugh 2013. Technical report, Monitoring Study Group California Board of Forestry and Fire Protection, Sacramento, CA.

Brennan, L. (2015). *Stream temperature modeling : a modeling comparison for resource managers and climate change analysis (MSc thesis)*. University of Massachusetts Amherst.

Brown, G. W. and Krygier, J. T. (1970). Effects of clear cutting on stream temperature. *Water Resources Research*, 6(4):1133–1139.

Buttle, J. M. (2011). The effects of forest harvesting on forest hydrology and biogeochemistry. In Levia, D. F., Carlyle-Moses, D., and Tanaka, T., editors, *Forest Hydrology and Biogeochemisty, Synthesis of Past Research and Future Directions*, pages 659–678. Springer, ecological edition.

Cafferata, P. (1990). Temperature regimes of small stremas along the Mendocino coast.

Cafferata, P. H. and Reid, L. M. (2013). Applications of long-term watershed research to forest management in California : 50 years of learning from the Caspar Creek Experimental Watersheds. Technical Report 5, California Department of Forestry & Fire Protection.

Caissie, D. (2006). The thermal regime of rivers: A review.

California Department of Fish and Wildlife (2006). Stream inventory report: South Fork Caspar Creek. Technical report, The Pacific States Marine Fisheries Commission (PSMFC).

California Department of Forestry and Fire Protection (2019). California Forest Practice Rules.

California Department of Water Resources (2019). California Irrigation Managment Information System (CIMIS).

Cao, Q., Sun, N., Yearsley, J., Nijssen, B., and Lettenmaier, D. P. (2016). Climate and land cover effects on the temperature of Puget Sound streams. *Hydrological Processes*, 30(13):2286–2304.

Carr, A. E., Loague, K., and Vanderkwaak, J. E. (2014). Hydrologic-response simulations for the north fork of caspar creek: Second-growth, clear-cut, new-growth, and cumulative watershed effect scenarios. *Hydrological Processes*, 28(3):1476–1494.

Carroll, G. D., Schoenholtz, S. H., Young, B. W., and Dibble, E. D. (2004). Effectiveness of forestry streamside managment zones in the sand-clay hills of Mississippi: early indications. *Water, Air, and Soil Pollution: Focus*, 4(1):275–296.

Cayan, D. R., Das, T., Pierce, D. W., Barnett, T. P., Tyree, M., and Gershunov, A. (2010). Future dryness in the southwest US and the hydrology of the early 21st century drought. *Proceedings of the National Academy of Sciences of the United States of America*, 107(50):21271–21276.

Chapra, S. C. (1997). *Surface water-quality modeling*. McGraw-Hill Companies, Inc., New York.

Cheng, S.-T. and Wiley, M. J. (2016). A reduced parameter stream temperature model (RPSTM) for basin-wide simulations. *Environmental Modelling and Software*, 82:295–307.

Christensen, N. S., Wood, A. W., Voisin, N., Lettenmaier, D. P., and Palmer, R. N.

(2004). The effects of climate change on the hydrology and water resources of the Colorado River Basin. *Climate Change*, 62(1-3):337–363.

Clar, C. R. (1957). *Brief history of the California Division of Forestry*. State Board of Forestry, Sacramento.

Clar, C. R. (1959). *California Government and Forestry: from Spanish Days until the creation of the Department of National Resources in 1927*. Division of Forestry, Department of Natural Resources, State of California, Sacramento.

Clar, C. R. (1969). *California Government and Forestry II: During the Young and Rolph Administrations*. Division of Forestry, Department of Conservation, State of California, Sacramento.

Cole, E. and Newton, M. (2013). Influence of streamside buffers on stream temperature response following clear-cut harvesting in western Oregon. *Canadian Journal of Forest Research*, 43(11):993–1005.

Cuo, L., Lettenmaier, D., Mattheussen, B., Stork, P., and Wiley, M. (2008). Hydrologic prediction for urban watersheds with the Distributed Hydrology-Soil-Vegetation Model. *Hydrological Processes*, 22(21):4205–4213.

Das, T., Dettinger, M. D., Cayan, D. R., and Hidalgo, H. G. (2011). Potential increase in floods in California's Sierra Nevada under future climate projections. *Climatic Change*.

DeWalle, D. R. (2010). Modeling stream shade: Riparian buffer height and density as important as buffer width. *Journal of the American Water Resources Association*, 46(2):323–333.

Donato, M. M. (2002). A statistical model for estimating stream temperatures in

the Salmon and Clearwater River basins, central Idaho. Technical report, U. S. Geological Survey, Boise, ID.

Duan, Z. (2017). CreateStreamNetwork_PythonV.

Dugdale, S. J., Hannah, D. M., and Malcolm, I. A. (2017). River temperature modelling: A review of process-based approaches and future directions. *Earth-Science Reviews*, 175(January):97–113.

Dwarakish, G. and Ganasri, B. (2015). Impact of land use change on hydrological systems: A review of current modeling approaches. *Cogent Geoscience*, 1(1).

Dymond, S. F. (2016). Caspar Creek Experimental Watersheds Experiment Three Study Plan: The influence of forest stand density reduction on watershed processes in the South Fork. Technical report, USDA Forest Service Pacific Southwest Research Station.

Eaton, J. G., McCormick, J. H., Goodno, B. E., O'Brien, D. G., Stefany, H. G., Hondzo, M., and Scheller, R. M. (1995). A field information-based system for estimating fish temperature tolerances. *Fisheries*.

Eliason, E. J., Clark, T. D., Hague, M. J., Hanson, L. M., Gallagher, Z. S., Jeffries, K. M., Gale, M. K., Patterson, D. A., Hinch, S. G., and Farrell, A. P. (2011). Differences in thermal tolerance among Sockeye salmon populations. *Science*, 332:109–112.

Elliot, J. M. (1981). Some aspects of thermal stress on freshwater teleosts. *Stress and Fish*, pages 209–245.

Elsner, M. M., Cuo, L., Voisin, N., Deems, J. S., Hamlet, A. F., Vano, J. A., Mickelson, K. E., Lee, S. Y., and Lettenmaier, D. P. (2010). Implications of 21st century climate change for the hydrology of Washington State. *Climatic Change*.

Emmingham, B., Chan, S., Mikowski, D., Owston, P., and Bishaw, B. (2000). Silviculuture Practices for Riparian Forests in the Oregon Coast Range. Technical report, Forest Research Laboratory, Corvallis, Oregon.

Ferreira, V. and Chauvet, E. (2011). Future increase in temperature more than decrease in litter quality can affect microbial litter decomposition in streams. *Oecologia*, 167(1):279–291.

Ficklin, D. L. and Barnhart, B. L. (2014). SWAT hydrologic model parameter uncertainty and its implications for hydroclimatic projections in snowmelt-dependent watersheds. *Journal of Hydrology*.

Ficklin, D. L., Luo, Y., Stewart, I. T., and Maurer, E. P. (2012). Development and application of a hydroclimatological stream temperature model within the Soil and Water Assessment Tool. *Water Resources Research*.

Flerchinger, G. N., Xaio, W., Marks, D., Sauer, T. J., and Yu, Q. (2009). Comparison of algorithms for incoming atmospheric long-wave radiation. *Water Resources Research*.

Foreman, M. G., Lee, D. K., Morrison, J., Macdonald, S., Barnes, D., and Williams, I. V. (2001). Simulations and retrospective analyses of fraser watershed flows and temperatures. *Atmosphere - Ocean*, 39(2):89–105.

Gentry, G. Y. (2016). Forest Management Regulation in California.

Gomi, T., Moore, R. D., and Dhakal, A. S. (2006). Headwater stream temperature response to clear-cut harvesting with different riparian treatments, coastal British Columbia, Canada. *Water Resources Research*, 42(8):1–11.

Hannah, D. M. and Garner, G. (2015). River water temperature in the United King-

dom: Changes over the 20th century and possible changes over the 21st century. *Progress in Physical Geography*, 39(1):68–92.

Henry, N. (1998). Overview of the Caspar Creek Watershed Study. In *Proceedings of the Conference on Coastal Watersheds: The Caspar Creek Story*, pages 1–9. Pacific Southwest Research Station, Ukiah, CA.

Hester, E. T. and Doyle, M. W. (2011). Human impacts to river temperature and their effects on biological processes: A quantitative synthesis. *Journal of the American Water Resources Association*.

Hines, D. and Ambrose, J. (2000). Evaluation of stream temperatures based on observations of juvenile coho salmon in northern California streams. Technical report, Campbell Timberladn Management, Inc. and National Marine Fisheries Service.

Hoegh-Guldber, O., Jacob, D., Tayor, M., Binid, M., Brown, S., Camilloni, I., Diedhious, A., Djalante, R., Ebi, K., Engelbrecht, F., Guiot, J., Hijioka, Y., Mehrotra, S., Payne, A., Seneviratne, S. I., Thomas, A., Warren, R., and Zhou, G. (2018). Impacts of 1.5 °C global warming on natural and human systems. In *Global warming of 1.5 °C. An IPCC Special Report on the impacts of global warming of 1.5 °C above pre-industrial levels and related global greenhouse gas emission pathways, in the context of strengthening the global response to the threat of climate chang*, pages 175–311. The International Panel on Climate Change.

Hogg, I. D. and Williams, D. D. (1996). Response of stream invertebrates to a global-warming thermal regime: an ecosystem-level manipulation. *Ecology*, 77(2):395–407.

Humboldt Watersheds Independent Scientific Review Pannel (2003). Phase II report: independent scientific review panel on sediment impairment and effects on beneficial

uses of the Elk River and Stitz , Bear , Jordan and Freshwater creeks. Technical report, Humboldt Watersheds Independent Scientific Review.

Iberle, B. G. (2016). *Ninetry-two years of tree growth and death in a second-growth coast redwood forest (MSc thesis)*. Humboldt State University.

Iowa Environmental Mesonet (IEM) (2019). McGuires Raws (MCGC1) Meterological Station.

IPCC (2018). Summary for Policymakers. In *Global warming of 1.5 °C. An IPCC Special Report on the impacts of global warming of 1.5 °C above pre-industrial levels and related global greenhouse gas emission pathways, in the context of strengthening the global response to the threat of climate chang*, pages 1–21.

Johnson, S. L. and Jones, J. A. (2000). Stream temperature responses to forest harvest and debris flows in western Cascades, Oregon. *Canadian Journal of Fisheries and Aquatic Sciences*, 57(S2):30–39.

Jones, B. E., Krupa, M., and Tate, K. W. (2013). Aquatic ecosystem response to timber harvesting for the purpose of restoring aspen. *PLOS ONE*, 8(12):1–29.

Kaushal, S. S., Likens, G. E., Jaworski, N. A., Pace, M. L., Sides, A. M., Seekell, D., Belt, K. T., Secor, D. H., and Wingate, R. L. (2010). Rising stream and river temperatures in the United States. *Frontiers in Ecology and the Environment*, 8(9):461–466.

Keepeler, E. (2019). Personal communication on soil auger holes for sub surface wells May 9, 2019.

Keppeler, E. T. and Ziemer, R. R. (1990). Logging effects on streamflow, water yield and summer low flows at Caspar Creek in northwestern California. *Water Resources Bulletin*, 26(7):1669–1679.

Kersten, E. (2002). Timber harvesting and water quality: Forest Practice Rules fail to adequately address water quality and endangered species. Technical report, California Senate Office of Research, Sacramento, CA.

Klein, R. D., Lewis, J., and Buffleben, M. S. (2012). Logging and turbidity in the coastal watersheds of northern California. *Geomorphology*, 139-140:136–144.

Krause, P., Boyle, D. P., and Bäse, F. (2005). Comparison of different efficiency criteria for hydrological model assessment. *Advances in Geosciences*, 5:89–97.

Kundzewicz, W. Z., Mata, L., Arnell, N., Doell, P., Kabat, P., Jiménez, B., Miller, K., Oki, T., Şen, Z., and Shiklomanov, I. (2007). Freshwater resources and thier managment. In *Climate Change 2007: Impacts, Adaptation and Vulnerability. Contribution of Working Group II to the Fourth Assessment Report of the Intergovernmental Panel on Climate Change*, chapter 3, pages 173–210. Cambridge University Press.

Kura, P. K., Alila, Y., and Weiler, M. (2012). Forest harvesting effects on the magnitude and frequency of peak flows can increase with return period. *Water Resources Research*, 48(1):1–20.

La Marche, J. L. and Lettenmaier, D. P. (2001). Effects of forest roads on flood flows in the Deschutes River, Washington. *Earth Surface Processes and Landforms*, 26(2):115–134.

Larson, L. L. and Larson, S. L. (1996). Riparian shade and stream temperature: a perspective. *Society for Range Managment*, 18(4):149–152.

Leopold, L. B. and Maddock, T. J. (1953). The hydraulic geometry of stream channels and some physiographic implications.

Liang, X., Lettenmaier, D. P., Wood, E. F., and Burges, S. J. (1994). A simple hydrologically based model of land surface water and energy fluxes for general circulation models. *Journal of Geophysical Research*.

Ligon, F., Rich, A., Rynearson, G., Thornburgh, D., and Trush, W. (1999). Report of the scientific review panel on California Forest Practice Rules and salmonid habitat. Technical report, The Resources Agency of California and the National Marine Fisheries Service, Sacramento, CA.

Lynch, J. A. and Corbett, E. S. (1990). Evaluation of Best Management Practices for controlling nonpoint pollution from silvicultural operations. *Journal of the American Water Resources Association*, 26(1):41–52.

Maas-Hebner, K. G., Emmingham, W. H., Larson, D. J., and Chan, S. S. (2005). Establishment and growth of native hardwood and conifer seedlings underplanted in thinned Douglas-fir stands. *Forest Ecology and Management*, 208(1-3):331–345.

Manson, J. R., Wallis, S. G., and Hope, D. (2001). A conservative semi-Lagrangian transport model for rivers with transient storage zones. *Water Resources Research*, 37(12):3321–3329.

Mantua, N., Tohver, I., and Hamlet, A. (2010). Climate change impacts on streamflow extremes and summertime stream temperature and their possible consequences for freshwater salmon habitat in Washington State. *Climatic Change*.

McCullough, D., Spalding, S., Sturdevant, D., and Hicks, M. (2001). Summary of technical literature examining the physiological effects of temperature on salmonids. *US Environmental Protection Agency*, pages 1–119.

Meyer, J. L., Slae, M. J., Mulholland, P. J., and Poff, N. L. (1999). Impacts of climate change on aquatic ecosystems functioning and health. *Journal of the American Water Resources Association*, 35(9):1373–1386.

Mohseni, O., Stefan, H. G., and Erickson, T. R. (1998). A nonlinear regression model for weekly stream temperatures. *Water Resources Research*, 34(10):2685–2692.

Moore, R. D., Spittlehouse, D. L., and Story, A. (2005). Riparian microclimate and stream temperature response to forest harvesting: A review. In *Journal of the American Water Resources Association*.

Morgan, T. A., Brandt, J. P., Songster, K. E., Keegan, C. E., and Christensen, G. A. (2012). California's Forest Products Industry and Timber Harvest, 2006. Technical report, USDA Forest Service Pacific Northwest Research Station.

Morrison, J., Quick, M. C., and Foreman, M. G. (2002). Climate change in the Fraser River watershed: flow and temperature projections. *Journal of Hydrology*, 263:230–244.

Mote, P. W., Hamlet, A. F., Clark, M. P., and Lettenmaier, D. P. (2005). Declining mountain snowpack in western North America. *American Meteorological Society*, 86(1):39–49.

Mount, J. F. (1995). *California rivers and streams: the conflict between fluvial process and land use*. University of California Press, Berkeley and Los Angeles, CA, first edition.

Nakamoto, R. J. (1998). Effects of timber harvest on aquatic vertebrates and habitat in the North Fork Caspar Creek. *Changes*, pages 87–95.

Napolitano, M., Jackson, F., and Cafferata, P. (1989). A history of logging in the Caspar Creek basin.

National Centers for Environmental Information (2018). Arcata Eureka Airport, CA Data USAF 725945.

Naz, B. S., Frans, C. D., Clarke, G. K., Burns, P., and Lettenmaier, D. P. (2014). Modeling the effect of glacier recession on streamflow response using a coupled glacio-hydrological model. *Hydrology and Earth System Sciences*, 18(2):787–802.

Neitsch, S. L., Arnold, J. G., Kiniry, J. R., and Williams, J. R. (2011). Soil and water assessment tool theoretical documentation version 2009. Technical report, Texas Water Resource Institute, College Station, TX.

Niemeyer, R. J., Cheng, Y., Mao, Y., Yearsley, J. R., and Nijssen, B. (2018). A thermally-stratified reservoir module for large-scale distributed stream temperature models with application in the Tennessee River Basin. *Water Resources Research*, pages 8103–8119.

Nijssen, B. and Lettenmaier, D. P. (1999). A simplified approach for predicting shortwave radiation transfer through boreal forest canopies. *J. Geophys. Res.*, 104(D22):27859–27868.

North Coast Regional Water Quality Control Board (2011). Water Quality Control Plan for the North Coast Region. Technical report, State water Resources Control Board, Santa Rosa, CA.

Parkyn, S. M., Davies-Colley, R. J., Halliday, N. J., Costley, K. J., and Croker, G. F. (2003). Planted riparian buffer zones in New Zealand: Do they live up to expectations? *Restoration Ecology*, 11(4):436–447.

Patric, J. (1980). Effects of wood products harvest on forest soil and water relations. *Journal of Environmental Quality*, 9(1):73.

Perry, R., Risley, J., and Brewer, S. (2011). Simulating daily water temperatures of the Klamath River under dam removal and climate change scenarios. *US Geological Survey Open-File Report*, 2011-1243.

Prata, A. J. (1996). A new long-wave formula for estimating downward clear-sky radiation at the surface. *Quarterly Journal of the Royal Meteorological Society*.

Quinn, J. M., Steele, G. L., Hickey, C. W., and Vickers, M. L. (1994). Upper thermal tolerances of twelve New Zealand stream invertebrate species. *New Zealand Journal of Marine and Freshwater Research*, 28(4):391–397.

Rajwa-Kuligiewicz, A., Bialik, R. J., and Rowiński, P. M. (2015). Dissolved oxygen and water temperature dynamics in lowland rivers over various timescales. *Journal of Hydrology and Hydromechanics*, 63(4):353–363.

Raptis, C. E. and Pfister, S. (2016). Global freshwater thermal emissions from steam-electric power plants with once-through cooling systems. *Energy*, 97:46–57.

Raptis, C. E., Van Vliet, M. T., and Pfister, S. (2016). Global thermal pollution of rivers from thermoelectric power plants. *Environmental Research Letters*, 11(10).

Rice, R. M., Tilley, F. B., and Datzman, P. A. (1979). A watershed's response to logging and roads: South Fork of Caspar Creek, California 1967-1976. Technical report, Pacific Southwest Forest and Range Experiment Station, Berkeley, CA.

Risley, J. C., Roehl, E. A., and Conrads, P. A. (2003). Estimating water temperatures in small streams in western Oregon using neural network models. Technical report, U.S. Geological Survey, Portland, OR.

Roth, T. R., Westhodd, M. C., Huwald, H., Huff, J. A., Rubin, J. F., Barrenetxea, G., Vetterli, M., Parriaux, A., Selker, J. S., and Parlange, M. B. (2010). Stream temperature response to three riparian vegetation scenarios by use of a distributed temperature validated model. *Environmental Science & Technology*, 44:2072–2078.

Rutherford, J. C., Scarsbrook, M. R., and Broekhuizen, N. (2000). Grazer control of

stream algae: modeling temperature and flood effects. *Journal of Environmental Engineering*, 126(4):331–339.

Schweppe, F. (1973). *Uncertain Dynamic Systems*. Prentice Hall, Englewood Cliffs, N. J.

Sinokrot, B. A. and Stefan, H. G. (1994). Stream water-temperature sensitivity to weather and bed parameters. *Journal of Hydraulic Engineering*.

Sloat, M. R. and Osterback, A.-M. K. (2013). Maximum stream temperature and the occurrence, abundance, and behavior of steelhead trout (Oncorhynchus mykiss) in a southern California stream. *Canadian Journal of Fisheries and Aquatic Sciences*, 70(1):64–73.

Smith, K. (1972). River water temperatures- an environmental review. *Geographical Magazine*, 88(3):211–220.

Staff, S. S. (2019). Web soil survey.

Stednick, J. D. (1996). Monitoring the effects of timber harvest on annual water yield. *Journal of Hydrology*, 176(1-4):79–95.

Stefan, H. G. and Preud'homme, E. B. (1993). Stream temperature estimation from air temperatures. *JAWRA Journal of the American Water Resources Association*, 29(1):27–45.

Stonesifer, C. S. (2007). Modeling the cumulative effects of forest fire on watershed hydrology: a pos-fire application of the distributed hydrology-soil-vegetation model (DHSVM). *J. Hydrol.*, 10:282–290.

Storck, P., Bowling, L., Wetherbee, P., and Lettenmaier, D. (1998). Application of a GIS-based distributed hydrology model for prediction of forest harvest effects on peak stream flow in the Pacific Northwest. *Hydrological Processes*, 12(6):889–904.

Storck, P., Lettenmaier, D., Connelly, B., and Cundy, T. (1995). Implications of forest practices on downstream flooding, phase II final report. Technical report, University of Washington, Seattle.

Story, A., Moore, R. D., and Macdonald, J. S. (2003). Stream temperatures in two shaded reaches below cutblocks and logging roads: downstream cooling linked to subsurface hydrology. *Canadian Journal of Forest Research*, 33(8):1383–1396.

Strzepek, K., Fant, C., Gebretsadik, Y., Lickley, M., Boehlert, B., Chapra, S., Adams, E., Strzepek, A., and Schlosser, C. A. (2015). Water body temperature model for assessing climate change impacts on thermal cooling. Technical report, MIT Joint Program on the Science and Policy of Global Change, Cambridge, MA.

Sullenberger, M. (1980). *Dogholes and donkey engines: a historical resources study of six state park system units on the Mendocino Coast*. State of California, Resources Agency, Dept. of Parks and Recreation, Sacramento, CA.

Sun, N., Yearsley, J., Voisin, N., and Lettenmaier, D. P. (2015). A spatially distributed model for the assessment of land use impacts on stream temperature in small urban watersheds. *Hydrological Processes*, 29(10):2331–2345.

Surfleet, C. G., Dietterick, B., and Skaugset, A. (2014). Change detection of storm runoff and sediment yield using hydrologic models following wildfire in a coastal redwood forest, California. *Canadian Journal of Forest Research*, 44(6):572–581.

Surfleet, C. G., Skaugset, A. E., and Meadows, M. W. (2011). Road runoff and sediment sampling for determining road sediment yield at the watershed scale. *Canadian Journal of Forest Research*, 41(10):1970–1980.

Surfleet, C. G., Tullos, D., Chang, H., and Jung, I.-W. (2012). Selection of hydrologic modeling approaches for climate change assessment: A comparison of model scale and structure. *Journal of Hydrology*, 464-465:233–248.

Sweeney, B. W. and Newbold, J. D. (2014). Streamside forest buffer width needed to protect stream water quality, habitat, and organisms: A literature review. *Journal of the American Water Resources Association*, 50(3):560–584.

The Univeristy of California Committee on Cumulative Watershed Effects (2001). A scientific basis for the prediction of cumulative watershed effects. Technical report, University of California Wildland Resource Center.

Thomas, S. C. and Winner, W. E. (2011). Leaf area index of an old-growth Douglas-fir forest estimated from direct structural measurements in the canopy. *Canadian Journal of Forest Research*, 30(12):1922–1930.

Thompson, R. P. and Dicus, C. A. (2005). The impact of California's changing environmental regulations on timber harvest planning costs. Technical report, The California Institute for the Study of Specialty Crops and The Forest Foundation.

Thyer, M., Beckers, J., Spittlehouse, D., Alila, Y., and Winkler, R. (2004). Diagnosing a distributed hydrologic model for two high-elevation forested catchments based on detailed stand- and basin-scale data. *Water Resources Research*, 40(1).

Tobin, I., Greuell, W., Jerez, S., Ludwig, F., Vautard, R., Van Vliet, M. T., and Breón, F. M. (2018). Vulnerabilities and resilience of European power generation to 1.5 °c, 2 °c and 3 °c warming. *Environmental Research Letters*, 13(4).

Truitt, S. E. (2018). *Modeling the effects of climate change projections on streamflow in the Nooksack River Basin, Northwest Washington (MSc thesis).* Western Washington University.

Unsworth, M. H. and Monteith, J. . (1975). Long-wave radiation at the ground. *Q. J. R. Meteorol. Soc.*, 101:25–34.

Van Vliet, M. T., Donnelly, C., Strömbäck, L., Capell, R., and Ludwig, F. (2015). European scale climate information services for water use sectors. *Journal of Hydrology*, 528:503–513.

Van Vliet, M. T., Ludwig, F., Zwolsman, J. J., Weedon, G. P., and Kabat, P. (2011). Global river temperatures and sensitivity to atmospheric warming and changes in river flow. *Water Resources Research*.

Van Vliet, M. T., Sheffield, J., Wiberg, D., and Wood, E. F. (2016). Impacts of recent drought and warm years on water resources and electricity supply worldwide. *Environmental Research Letters*, 11(12).

Van Vliet, M. T., Yearsley, J. R., Franssen, W. H., Ludwig, F., Haddeland, I., Lettenmaier, D. P., and Kabat, P. (2012a). Coupled daily streamflow and water temperature modelling in large river basins. *Hydrology and Earth System Sciences*, 16(11):4303–4321.

Van Vliet, M. T. H. (2012). *Global Rivers Warming Up: Impacts on Cooling Water Use in the Energy Sector and Freshwater Ecosystems*. PhD thesis, Wageningen Unviersity, Wageningen, NL.

Van Vliet, M. T. H., Franssen, W. H. P., Yearsley, J. R., Ludwig, F., Haddeland, I., Lettenmaier, D. P., and Kabat, P. (2013). Global river discharge and water temperature under climate change. *Global Environmental Change*, 23(2):450–464.

Van Vliet, M. T. H., Yearsley, J. R., Ludwig, F., Vögele, S., Lettenmaier, D. P., and Kabat, P. (2012b). Vulnerability of US and European electricity supply to climate change. *Nature Climate Change*, 2(9):676–681.

Vliet, M. T. H. V., Ludwig, F., and Kabat, P. (2013). Cross-sectoral conflicts for water under climate change: the need to include water quality impacts. In *International Conference on Climate Change Effects*, pages 1–7.

Wagenbrenner, J. (2018). Addendum to Caspar Creek Experimental Watersheds Experiment Three Study Plan: The influence of forest stand density reduction on watershed processes in the South Fork. Technical report, USDA Forest Service Pacific Southwest Research Station.

Walker, J. H. and Lawson, J. D. (1977). Natural stream temperature variations in a catchment. *Water Research*, 11(4):373–377.

Ward, J. (1985). Thermal characteristics of running waters. *Hydrobiologia*, 125(1):31–46.

Waterloo, M. J., Schellekens, J., Bruijnzeel, L. A., and Rawaqa, T. T. (2007). Changes in catchment runoff after harvesting and burning of a Pinus caribaea plantation in Viti Levu, Fiji. *Forest Ecology and Management*, 251(1-2):31–44.

Webb, B. W., Hannah, D. M., Moore, R. D., Brown, L. E., and Nobilis, F. (2008). Recent advances in stream and river temperature research. *Hydrological Processes*, 22:902–918.

Webb, B. W. and Nobilis, F. (1995). Long term water temperature trends in Austrian rivers. *Hydrological Sciences Journal*, 40(1):83–96.

Webb, B. W. and Nobilis, F. (2007). Long-term changes in river temperature and the influence of climatic and hydrological factors. *Hydrological Sciences Journal*, 52(1):74–85.

Webb, L. (2019). Unpublished forest stand data from Jackson Demonstration State Forest.

Welsh, H. H., Hodgson, G. R., Harvey, B. C., and Roche, M. F. (2004). Distribution of juvenile Coho salmon in relation to water temperatures in tributaries of the Mattole

River, California. *North American Journal of Fisheries Management*, 21(3):464–470.

Wenger, S. J., Luce, C. H., Hamlet, A. F., Isaak, D. J., and Neville, H. M. (2010). Macroscale hydrologic modeling of ecologically relevant flow metrics. *Water Resources Research*, 46(9).

Whitaker, A., Alila, Y., Beckers, J., and Toews, D. (2003). Application of the Distributed Hydrology Soil Vegetation Model to Redfish Creek, British Columbia: Model evaluation using internal catchment data. *Hydrological Processes*, 17(2):199–224.

Wigmosta, M. and Perkins, W. (2001). Simulating the effects of forest roads on watershed hydrology. In Wigmosta, M. S. and Perkins, W. A., editors, *Land Use and Watersheds: Human Influence on Hydrology and Geomorphology in Urban and Forest Areas, Volume 2*, pages 127–143. American Geophysical Union.

Wigmosta, M. S., Vail, L. W., and Lettenmaier, D. P. (1994). A distributed hydrology-vegetation model for complex terrain. *Water Resources Research*, 30(6):1665–1679.

Wilkerson, E., Hagan, J. M., Siegel, D., and Whitman, A. A. (2006). Effectiveness of different buffer widths for protecting headwater stream temperature in Maine. *Forest Science*, 52(3):221–231.

Wu, H., Zhang, X., Liang, S., Yang, H., and Zhou, G. (2012). Estimation of clear-sky land surface longwave radiation from MODIS data products by merging multiple models. *Journal of Geophysical Research Atmospheres*.

Wurm, T. (1986). *Mallets on the Mendocino Coast: Caspar Lumber Company, railroads and steamships*. Trans-Anglo Books, glendale, edition.

Yearsley, J. (2001). Application of a 1-D heat budget model to the Columbia River system. Technical report, EPA.

Yearsley, J. (2012). A grid-based approach for simulating stream temperature. *Water Resources Research*, 48(3):1–15.

Yearsley, J. R. (2009). A semi-Lagrangian water temperature model for advection-dominated river systems. *Water Resources Research*, 45(12):1–19.

Ziemer, R. R. and Alright, J. S. (1987). Subsurface pipeflow dynamics of north-coastal California swale system. In *Corvallis Symposium*, number 165, pages 71–80. IAHS Publ. no. 165.

Ziemer, R. R. T. C. (1998). Proceedings of the Conference on Coastal of Agriculture Watersheds: The Caspar Creek Story. Technical report, USDA Forest Service, Pacific Southwest Research Station ch Station, Ukiah, CA.

APPENDIX: FINDINGS FROM CASPAR CREEK STUDIES I & II

The following summarizes a compilation of findings by Cafferata and Reid (2013) from the first and second studies at the Caspar Creek Experimental Watershed.

PEAK FLOWS

• The largest percentage increase in peak flows following forest harvesting occurs for small storms in the fall, when the largest difference in soil moisture levels occur.

• Increases in peak flow following harvesting during winter are attributed to reduced interception loss and transpiration.

• Increases in peak flow were greater with increasing proportion of the basin logged and smaller with increasing antecedent wetness, storm size and time since logging.

• Peak flow responses decreased to pre-treatment levels approximately 10 years after logging, but increased again after pre-commercial thinning.

SUMMER LOW FLOWS & ANNUAL WATER YIELD

• Low flows were higher than expected for 7 years after selective harvesting in the SFC and then started to decline below expected values for the following 20 years.

• Late-summer flows doubled after clearcutting in the NFC, but returned to pre-treatment levels after 16 years.

• Annual water yields increased for 8-11 years following logging in both SFC and NFC.

HILLSLOPE HYDROLOGY

• Pipeflow plays an important role in delivery of water from hillslopes in the area.

• Peak piezometric levels, soil moisture content and subsurface pipeflow rates increased following clearcut logging in the NFC.

• Pore pressure response increased at and above a road constructed across a headwater swale and clearcutting occurred above and below the road.

FOG DRIP

• Fog drip rates were greatest along ridge-top sites and considerably lower at midslope and valley-bottom sites.

• Fog drip rates were similar in clearcut areas to those within forest stands.

• Reduced rainfall interception and transpiration exceeded the rate of decreased fog drip.

SEDIMENT YIELDS

• Year to year variation of suspended sediment load is high and reflects the size of storms and watershed treatments applied.

• 6 years after tractor logging, suspended sediment yield in the SFC more than quadrupled expected rates.

• Deterioration of road systems two decades after logging showed a second increase in sediment production.

• Improvements in road network design decreased suspended sediment levels.

• Post logging increasing suspended sediment loads were strongly correlated with increases in stormflow volumes.

• Sediment loads recovered within 10 years of logging, until pre-commercial thinning began.

SURFACE EROSION, CHANNEL EROSION, GULLIES & LANDSLIDES

• Post logging in-channel erosion was thought to be the major sediment source during periods without landslides.

• Drainage density is believed to have increased after logging because of increased runoff, even where roads were not present.

• Clearcut logging is thought to have influenced landsliding and destabilization of slopes adjacent to roads.

• The largest landslides occurred 9 to 14 years after logging and shortly after pre-commercial thinning, when root strength is believed to be low and hydrologic changes begin to occur again.

• Rocked road segments resulted in less sediment production.

STREAM TEMPERATURE

• SFC road building in 1967 reduced shading and increases of as much as 11°C in maximum summer temperatures were reported at some sites after road construction.

• Following road construction maximum summer temperatures rose to near 21°C, with the highest being 25.3°C.

• In the NFC maximum summer temperatures only increased a little and remained within the range to be tolerable for Coho salmon in a similar watershed.

NUTRIENT CYCLING

• Nitrate concentrations were higher in streams draining clearcut sub-watersheds, but fluxes were relatively low compared to other studies in forest ecosystems.

• Nitrate concentration increases decreased substantially by the time flow reached downstream sampling points.

• Immobilization of nutrients by the rapid regrowth of stump sprouts suggest redwood forests may be relatively resistant to nutrient losses from leaching following timber harvesting.

• There is concern of nitrogen, phosphorous and sulfur losses for this type of forested ecosystem.

LARGE WOODY DEBRIS

• Following clearing in the NFC, selection-logged buffer strips on inner gorge slopes had higher windthrow rates during large storms than similar unlogged second-growth stands not adjacent to clearcuts.

• Douglas-fir, grand fir and alder trees decay more rapidly than redwood species.

• Trees within one tree height of the channel account for the majority of the wood inputs from fallen trees in WLPZs, but 30% of these falls were triggered by falls further upslope.

• Primary input mechanisms for large wood volume in the NFC are windthrow and bank erosion.

• Post logging inputs provide sediment storage and pool volume in the short term, but decreased wood recruitment and subsequent channel impacts are expected in the long term.

BIOLOGICAL CHANGES

• Salmonid populations decreased immediately after road construction in the SFC, but recovered to only 20% lower than before disturbances by the second spring.

• Salmonid densities recorded before logging were lower in variance for autumn compared to three years after road construction, and showed a shift to single-species dominated communities.

• Riparian insect drop increased after the riparian SFC road was built.

• Logging in the NFC did not create significant changes to Steelhead trout, Coho salmon or Pacific giant salamander communities.

• Macroinvertebrate and stream algae density and diversity, increased after NFC logging- presumably due to light, nutrient and temperature increases.

• Increased sediment loads in the NFC showed little effect to macroinvertebrates, leaf decay rates and algae.

CUMULATIVE WATERSHED EFFECTS

• Changes to peak and storm flow vary with the proportion of each sub-watershed logged, regardless of watershed size, suggesting changes are additive.

• Correlations between sediment load and flow increases following logging.

• Sediment yields had greater variety of response than flow.

• Impacts caused differing channel responses in different parts of the channel (first order grew headwater, low order incised and widened, higher order aggraded).

• Post-logging landslides were largest right after pre-commercial thinning.

• Legacy sediment sources from old-growth logging continue to remain influential.

• Old growth logging caused lasting effects, including incision, channel form simplification, reduction in sediment storage capacity and decreasing wood loading rates.

• Long term responses may be as important as short-term response, but are difficult to predict.